EFFECT OF MICROSTRUCTURE ON THE STRESS CORROSION CRACKING AND ANODIC POLARIZATION OF PRESTRESSING STEEL WIRES

By

ASHOK KUMAR

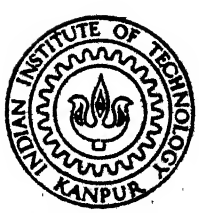

DEPARTMENT OF METALLURGICAL ENGINEERING
INDIAN INSTITUTE OF TECHNOLOGY KANPUR

AUGUST, 1983

EFFECT OF MICROSTRUCTURE ON THE STRESS CORROSION CRACKING AND ANODIC POLARIZATION OF PRESTRESSING STEEL WIRES

A Thesis Submitted
In Partial Fulfilment of the Requirements
for the Degree of
MASTER OF TECHNOLOGY

By

ASHOK KUMAR

to the
DEPARTMENT OF METALLURGICAL ENGINEERING
INDIAN INSTITUTE OF TECHNOLOGY KANPUR
AUGUST, 1983

C E R T I F I C A T E

This is to certify that this work "Effect of Microstructure on the Stress Corrosion Cracking and Anodic Polarization of Prestressing Steel Wires" by Ashok Kumar has been carried out under our supervision and the same has not been submitted elsewhere for a degree.

(RAJ NARAYAN)
Assistant Professor

(K.P. SINGH)
Professor

Department of Metallurgical Engineering
Indian Institute of Technology,
Kanpur-208016

"DEDICATED TO MY GRAND MOTHER"

A C K N O W L E D G E M E N T S

It gives me a great pleasure to express my profound gratitude and sincere thanks to Dr. K.P. Singh and Dr. Raj Narayan for their able guidance, useful discussions and suggestions during the course of this work.

I am indebted to Dr. D.C. Agarwal and Dr. S.P. Gupta for their invaluable discussions on various topics related to the work embodied in this thesis.

I wish to express my sincere thanks to Mr. M.N. Mungole for his ever-ready help and constant inspiration at every stages of this work.

Special thanks towards Mr. K.P. Mukherjee of Physical Metallurgy, Mr. V.P. Sharma of SEM and Mr. B.K. Jain of Material Testing Laboratory for their assistance in various stages of this work. I would like to express my humble thanks to Mr. Rakesh Kumar and friends those who have rendered help at all stages to this work.

Grateful acknowledgement is due to CSIR for providing me financial assistance for this project.

Mr. N.P. Singh is to be congratulated and thanked for this excellent typing. Mr. V.P. Gupta is also thanked for his help in preparing the drawings.

I am grateful to M/s Steel Private Ltd., E-37 Chikalthana Industrial Area, Aurangabad, for providing the prestressed steels for this experiment.

Ashok Kumar

CONTENTS

LIST OF FIGURES

LIST OF TABLES

A B S T R A C T

Susceptibility of prestressing steel wires in As Received, Annealed, Isothermally Transformed and Quenched & Tempered conditions to Stress Corrosion Cracking in Saturated H_2S at room temperature, 50% $Ca(NO_3)_2$ + 5% NH_4NO_3 at 100°C and 20 to 80% $Ca(NO_3)_2$ solutions has been studied.

Potentiodynamic anodic polarization studies on prestressing steel wires in different conditions of heat treatment in the above solutions has also been carried out.

It has been observed that prestressing steel wires were susceptible to stress corrosion cracking in all conditions of heat treatment in the environments studied. Quenched and tempered wires in general are more susceptible than annealed and isothermally transformed wires. As received Wire had intermediate susceptibility.

Anodic polarization behaviour of prestressing steel wires was effected by the nature of the heat treatment given to it. However, the change was not very systematic.

There was not much correlation between the anodic polarization behaviour of prestressing steel wire and its susceptibility to stress corrosion cracking except that in some case a change in slope in time to failure curves was associated with minimum difference in $E_{corr.}$ in unstressed and stressed conditions.

CHAPTER-I

INTRODUCTION

During the last two decades prestressed concrete structures have replaced with increasing frequency conventional reinforced concrete where lighter and thinner structural members are required to sustain the applied load.

Prestressed concrete structures, reinforced with high strength steel wires or cables stressed up to 70% of the U.T.S., are produced by two methods :

(i) by pre-tensioning, in which the reinforcing wires are stressed before the concrete has set and

(ii) by post-tensioning, in which the wires are threaded through preformed ducts in concrete and stressed after the concrete has set. Usually, the post-tensioning duct is pumped full of cement grout to protect the wire from corrosion and to form a link for transferring the tensile force, imposed by loading the steel, to concrete.

The following types of steels are mainly used for this purpose.

- the patented and cold drawn wires which are heated to 800°-900°C, at the end of their fabrication process, and cooled rapidly to about 500°C. After keeping the wires at this temperature for some time, they are then cold drawn to the final diameter to give the desired strength level.

- the quenched and tempered wires which after getting the final diameter are also heated to 800°-900°C, and are quenched to room temperature. Afterwards they are tempered at 400°-500°C to give the desired strength level.
- less commonly isothermally transformed wires @ IT 400 or so.

Although the stress corrosion hazard to prestressing steels has been proved by experience to be low, several service failures have been reported. These have often stimulated researchers to investigate the cause of such failures.

An extensive literature review revealed that very little work has been carried out specially in India. The present investigation was,therefore,undertaken to study the stress corrosion cracking behaviour and polarization characteristics of prestressing steels of Indian origin in nitrate and hydrogen sulphide solutions in as received and heat treated conditions.

CHAPTER-II

REVIEW OF LITERATURE

2.1. FAILURES ENCOUNTERED IN INDUSTRY

Although the stress corrosion hazard to prestressing steels has beenproved by experience to be low, several service failures have been reported. It will be worthwhile to describe briefly some of the more notable of these failures.

In 1952,extensive stress corrosion failure of circumferential prestressing wire was observed[1,2] in a five mile section of prestressed concrete pipe at Regina, Canada. These pipes were made by winding 0.142 in. diameter prestressing wire around the ordinary Portland cement-concrete core. The wire spiral was covered with a sulphate resisting cement applied pneumatically. Calcium chloride was used as an accelerator both in core and cover mixes. The covering shell was found to be cracking away from the core in about 5 months. The following factors were supposed to be responsible for causing cracking[4].

(a) the use of Portland and sulphate resisting cements with the wire sandwiched between them may have contributed to an electrolytic couple.

(b) the use of high concentration of calcium chloride in the mix.

(c) the concentration of sulphate content of the recirculated hot water used during curing.

(d) the spaces between wire and concrete containing an unidentified salt.

Gilchrist[5] showed that partly pearlitic and partly particulate carbide structure of steel might had an important additive factor to those mentioned earlier leading to crack formation along with corrosion.

Failure of prestressed concrete pressure pipes carrying water from a dam occurred in France[6]. These were made by winding a helical loop of steel wire under tension on a core made with rapid hardening Portland cement. This was then covered with 2-3 cm. of fine concrete. After six months of storage in a field, in contact with grass and exposed to the atmosphere, the pipes were found to contain broken wires. This was attributed[7] to differential concentration and aeration cells set up by two types of cement and the possible release of sulphides from the small amount of calcium sulphide in the slag.

Failures of a German heat treated wire in Holland was explained[8] by the Dutch as being mainly due to defective steel and by the suppliers to careless storage in a marine atmosphere. No details were given about the nature of the defect in the steel.

Two failures of similar nature, one in Austria[9] and other in Germany[10] involved the failure of German wire. Post tensioned wires snapped within few hours or days after stressing and before being grouted in. Presumably corrosion had occurred during storage resulting in absorption of hydrogen which caused fracture when the wires were stressed.

Prestressed concrete flooring units made with high alumina cement incorporating blast furnace slag of a foundry in Germany failed after 3 years of use[11]. Whereas similar units containing ordinary Portland cement were intact. Observation of the corrosion product revealed[7] the existence of iron sulphide. Presence of H_2S, produced from the action of calcium sulphide (in slag) with condensed acid vapours entering concrete, probably caused failure.

Failure of quenched and tempered prestressing wire used in the roof beams of a cowshed occurred in Germany[12]. Cement made from a high alumina blast furnace type slag, which is specially prepared for the purpose, was used in their construction due to the fact that it gives very rapid setting concrete. The cement is prone to carbonation which is accompanied by loss of density and consequent increase in porosity and accessibility to gases. There will be plenty of CO_2, H_2O, H_2S and NH_3 in cowsheds. Slag has fairly high sulphur content too. Failure almost certainly was due to H_2S but the pH of $CaCO_3$ environment is believed to be 8.5. Gilchrist and Narayan[13] have shown that SCC of patented and cold drawn in sat. H_2S solutions can occur between pH 5 and pH 10.5.

Stress corrosion failure of galvanised prestressing wire, after stress had been applied for some time, occurred inthe foundations of an Australian construction project. Several strands of the wire cable had fractured over that portion of the vertical

grout-lined duct which was filled with water from a nearby river. Hydrogen embrittlement caused by the absorption of hydrogen produced at the zinc coated steel surface probably caused the failure[7].

Failure of isothermally transformed wire from cables used to strengthen a cassion of prestressed concrete has been described by Hache & Libert[14]. No explanation is given for the cause of this failure.

After several years of successful service, one of the sewage treatment tanks collapsed completely at Owls Head, New York[5]. Infiltration of the liquors from the tank down between the concrete wall and gunnite cover was the apparent reason for stress corrosion cracking. Better design or execution would, presumably, have postponed this failure indefinitely. A similar failure occurred at Stockport[5], although the failure in this case was discovered before the collapse of any sewage treatment tank.

Hard drawn wire failed at a hospital site in Edinburgh[5]. At most of the places the wire had suffered heavy corrosion and only at one place it appeared to have failed without any loss of cross-section which was not explained properly in any way. However the wire would have failed in any case by general corrosion.

Although much detailed information about most of these failures is not available because of the fact that in the majority of the cases these were not examined by corrosion experts at early stages, the following general conclusions can be drawn.

- corrosion was involved in all cases. This could be either general or localised due to concentration cell etc.
- in some cases corrosion occurred before any stresses were applied and probably caused absorption of hydrogen by steel which failed on subsequent application of stresses.
- in other cases corrosion of the stressed wires occurred. This either reduced the cross-section to such an extent that the failure of the wire occurred or caused stress corrosion cracking.
- other factors e.g. presence of certain substance like chlorides, sulphides etc. and potentials developed due to concentration cells etc. might have increased the cracking tendency of the steel in some cases.

It could be seen that in most of these cases the failure of prestressing wires could have been prevented if proper care was taken to avoid the corrosive conditions during handling and using of the wire.

2.2. EFFECT OF HEAT TREATMENT & MICROSTRUCTURE

Very little work has been done on the effect of heat treatment and microstructure on stress corrosion cracking behaviour of prestressing steel. Everling[15] showed that cold drawn prestressing steel wire was superior to quenched and tempered wire in all of the solutions tested. Although he gave no explanation for this difference this view is now generally accepted. Libert & Hatche[16] observed that under cathodic charging conditions in H_2SO_4 patented prestressing steel wire fractured more rapidly at high stress level but had a critical stress level, i.e. stress below which failure will not occur, higher than quenched and tempered steels. No explanation was given for this difference in resistances to cracking.

Gilchrist[5] showed that cold drawn wire did not fail in any of the tested solutions whereas oil quenching and tempering below 500°C or isothermal transformation below 350°C made the wire susceptible to cracking. The susceptibility to cracking was associated with a structure containing fine cementite particles or platelets and was independent of how this structure was produced. Structures entirely pearlitic or coarsely spheroidal cementite were not susceptible to cracking, but cracks once formed would proceed through such structures. Pearlite offered greater resistance to crack propagation than the spheroidised structures. These conclusions were mainly based on tests in boiling solutions of calcium nitrate + ammonium nitrate and did not show the range

of environmental conditions under which these will be effective. Uhlig[3] has confirmed that a severly cold worked steel containing about 0.8% carbon was not readily susceptible to stress corrosion cracking in boiling calcium-ammonium nitrate solution and was similarly resistant if cooled through the transformation range so as to produce a pearlitic structure.

The fact that patented and cold drawn prestressing steel wires are in general more resistant to cracking as compared to quenched and tempered wires has been confirmed by many investigators.

2.3. TENSILE STRESS LEVEL

As the magnitude of tensile stress increases the time to failure, in general, decreases. Failure has never been observed with compressive stresses. Libert & Hache[16] studied the effect of applied stress on failure time of quenched and tempered and patented prestressing steel wires in H_2SO_4 solution at 20°C during cathodic polarization at a current density of 200 mA/cm^2. Their results, (Fig. 2.1) showed that the time of failure decreased with increasing applied stress and there was a threshold or limiting stress below which stress corrosion cracking did not occur. However, Gilchrist & Narayan[13] observed no clear threshold stress for prestressing steels in 5% $FeCl_3$ solution (Fig. 2.2) and in saturated H_2S solution (Fig. 2.3).

2.4. TORSIONAL STRESSES

During the production process the wire may be subjected to plastic torsional strain due to slight misorientation of the jaws pulling it. As torsional prestressing of a steel specimen has been shown[17] to be very effective in initiating brittle fracture by reducing its ductility, it may also affect the stress corrosion susceptibility of prestressing steel.

This view is also supported by the observations[12] on the cold drawn and patented prestressing wire failed at Regina and Owl's Head. Cracks in wire from Regina failure were shallow spiral and longitudinal suggesting that some element of torsional stressing was involved. Samples of this wire could be cracked in the laboratory only when it was twisted and stressed and not when in pure tension. The cracks in the wire from Owl's Head failure also followed a spiral path.

Apart from the work of Kazfasz & Czernak[18] very little information is available on this aspect of the problem. They have shown that the initial torsional stressing of the prestressing steel wires reduced their time to failure in 5N NH_4NO_3 solution. Assuming the life time of the non twisted wires to be unity, the corresponding values for twisted wires were approximately equal to 0.70 for 2 x 180°/meter twist and 0.33 for 3 x 180°/meter twist.

Thus it may be concluded that torsional stresses, in general, increase the susceptibility of prestressing steel wires. However, more work is required before drawing any definite conclusions.

2.5. SURFACE CONDITION

Surface condition of the specimen plays an important part in its behaviour towards embrittlement. However, little information is available on this subject.

Herzog[19] observed that electropolishing increased the time to failure of a steel (0.335% C, 1.76% Si, 0.014% P, 0.008% S, 0.13% Mo) as compared to As Recd. wire in 1% NaCl solution containing H_2S.

Hache & Libert[14] showed that surface treatments which suppressed all geometric defects increased the specimen life remarkably (Table 2.1).

TABLE 2.1 EFFECTS OF SURFACE TREATMENTS ON TIME TO FAILURE OF COLD DRAWN PRESTRESSING STEEL WIRE AT 80% $E_{0.2}$ AND 2.5 mA/cm^2 CATHODIC IN N/10 H_2SO_4

SURFACE CONDITION	TIME TO FAILURE (Minutes)
As Received	10
Pickled	10
As Recd. and swaged	50
Pickled and swaged	400
Phosphated	880
Sand blasted	2100
Shot peened	3500
Shot peened and electropolished	4600
Pickled and electropolished	3000

Davis[20] also observed that surface finishes produced by chemical milling, electropolishing and grinding increased the resistance of the steel specimens towards stress corrosion cracking.

2.6. SOLUTION pH

Libert & Hache[16] showed (Fig. 2.4) that prestressing steel containing 0.7% C and 0.58% Mn oil quenched and tempered $E_{0.2}$ = 143 Kg/mm^2 (1402.34 MPa) and stressed to 1.5 Kg/mm^2 (14.710 MPa) in N/10 - N/1000 H_2SO_4 solution failed below pH 3.3 only on cathodic polarization (20-100 mA). The time of failure decreased with decrease in pH.

Herzog[20] reported that prestressing steel containing 0.7% C and 0.7% Mn, oil quenched and tempered at 200°C strained to $E_{0.2}$ in $CaSO_4$ solution at pH 3 failed within 20-40 minutes whereas at pH of 7.4 it took about 10-20 days to fail.

In prestressing wires isothermally transformed at 276°C, the following effects of pH have been observed[5,12].

- boiling solution of 20% Na_2SO_3 at pH 9.3 produced cracking. when pH was adjusted to 6.4 only corrosion occurred without any cracking, whereas a pH 11.5 neither corrosion nor cracking occurred[7].
- cracking occurred rapidly in cold aqueous solution of H_2S, whereas no failure occurred in CaS solution[7].
- 5% Na_2SO_4 solution at pH 6.5 produced cracks whereas at pH 11.8, adjusted by adding excess lime, no cracking occurred.

- the nature of cracks changed as the pH of saturated H_2S solution was changed. In acidic conditions the cracks were filled with FeS but in alkaline solution steel was embrittled without any apparent chemical attack.
- nitrates produced cracking in acidic and weakly basic solutions only. In highly alkaline solution no cracking was observed.
- chlorides produced cracking only when the solutions were strongly alkaline.

McGuinn & Griffiths[22] showed that stress corrosion cracking of prestressing steels in saturated $Ca(OH)_2$ solution took place only when pH was below 12.3.

Thus it may be seen that stress corrosion cracking in high strength steels is, in general, accelerated in acidic solution whereas alkalinity tends to inhibit it, except in the case of alkaline chlorides for prestressing steels.

2.7. SCC IN CHLORIDE SOLUTIONS

Godfrey[23] showed that stress corrosion cracking in prestressing steel wires was caused due to the presence of chlorides in concrete mixer used. His tests indicated that prestressed concrete beams without calcium chloride in the mix were in a satisfactory condition after a 3-year exposure to the industrial atmosphere. While steel strands in the beams, with calcium chloride[22 to 25] in the mix, were badly corroded.

As a result it was suggested that calcium chloride should not be used in prestressed concrete.When chlorides[22] are present the hydroxyl-ion concentration has to be raised to prevent cracking. A higher pH is necessary to prevent film rupture and consequent loss of passivity.

The behaviour of cold-drawn prestressed steel wire was examined in concrete containing $CaCl_2$ admixtures and alkaline chloride solutions[26]. The wire was stressed to 70-80% of its UTS before the test. The degree of corrosion depended on the quality of chloride added and the quality of the concrete.

Jorg Eickemeyer[27], studied the effect of Cl^- additions to sat. $Ca(OH)_2$ solution on stress corrosion cracking of prestressing steel wires using fatigue precracked notched cantilever beam specimens. He showed that very small amounts of chloride ions were sufficient to inducue stress corrosion susceptibility in these wires as shown by a sharp decrease in time to failure (Fig. 2.4). On further increase in chloride ion concentration the time to failure showed at maximum at about 6×10^{-2} mol/l chloride ion concentration (Fig. 2.4). This effect was observed at two different intial stress intencities. If the time to failure was divided into initial time (time from the beginning of the test upto the start of crack growth) and the time for stable crack growth it was shown that the maximum in the time to failure unambiguously resulted from the initial time. The time of stable crack growth (average crack growth rate) was

independent of Cl^- ion concentration. It was, therefore, argued that the Cl^- ions effected the crack initiation whereas crack propagation was adsorption or diffusion of hydrogen site produced by the chemical reaction between iron and water, to the critical side.

Slow strain rate stress corrosion tests on notched or precracked specimens of prestressing steel immersed in $Ca(OH)_2$ solutions, to which HCl was added to adjust the pH, showed[28] that enhanced cracking occured at potentials below about -900 mV, irrespective of pH, and that there was a further regime of environment sensitive fracture at higher potentials, with an intermediate regime in which cracking was absent or less severe than at other potentials. The lower potential regime of cracking appeared to be related to the ingress of hydrogen into the steel, whereas at higher potentials occured when the pitting potential was exceeded and appeared to be dissolution related[29].

2.8. SCC IN NITRATE SOLUTIONS

Stress Corrosion Cracking (SCC) if prestressed steel wires occurs in solutions of calcium nitrate, amonium nitrate and by their mixtures. Their mixtures being most corrosive. The susceptibity of steel to SCC in nitrate solution is influenced by the concentration and temperature[29]. In calcium nitrate solution, rapid cracking occured at concentration of 200-500[30] Kg/m^3 in mixed solution of ammonium nitrate and calcium nitrate,

the rate of cracking reached a maximum at a 60-90% concentration of these counpounds[31]. An increase in temperature of solution containing calcium nitrate and ammonium nitrate, from 30 to 80, 90 and 110°C decreased the time of failure by factors of 6.6, 80 and 330 respectively. Consequently an increase in the solution temperature and solution concentration increased the rate of SCC of prestressing steel wires in nitrate solutions[32]. The rate of SCC also depended on the purity of nitrate solutions.

Parkins[33] presented evidence that the susceptibility of steel to SCC in boiling calcium-ammonium nitrate solutions was related to the presence of carbide particles within the crystal boundaries. Pollard[34] produced cracking of bridge wires by immersion in 0.01 normal solutions of ammonium or sodium nitrate.

2.9. SCC IN SULPHIDE SOLUTIONS

Several investigators[35 to 39] have observed that prestressing steel wire are highly susceptible to stress corrosion cracking (SCC) in saturated H_2S solution at RT (room temperature). No cracking was observed in distilled water, 3.5% NaCl, HCl and occured only when the these solutions were saturated with H_2S. Stress corrosion cracking took place only in moist H_2S, this proves that both H ions and sulphide produce cracking.

Unlike in nitrate solutions, where numerous cracks are formed but failure takes place only along one of them, hydrogen sulphide solutions produce only one cracking which leads to fracture of metal[40].

Fractographic studies using SEM were made on fractured surface and the cracking was found to be intergranular. Stress corrosion test under potentiostatic control showed that the failure at open circuit potential in Sat. H_2S solution was due to hydrogen embrittlement[36].

2.10. MECHANISM OF FAILURE

Failure of high strength steels, including prestressing steels, can occur due to either hydrogen embrittlement of active path corrosion cracking. Very little work seems to have been done on the mechanism of failure of prestressing steel wires in various environments.

Gilchrist & Narayan[13] showed that failure of prestressing steel wires isothermally transformed at 275°C in cold 5% $FeCl_3$ and saturated H_2S solutions was due to hydrogen embrittlement, whereas in boiling solution of IM ammonium nitrate solution it was due to active path corrosion cracking.

Parkins et. al.[28] have shown cracking of patented and cold drawn prestressing steel wires in $Ca(OH)_2$ solutions containing HCl for pH adjustment was due to two different mechanisms operating in different potential regions. Below about -900 mV (SCE) failure was hydrogen embrittlement whereas at higher potentials, above about -600 mV (SCE) failure was due to active path corrosion.

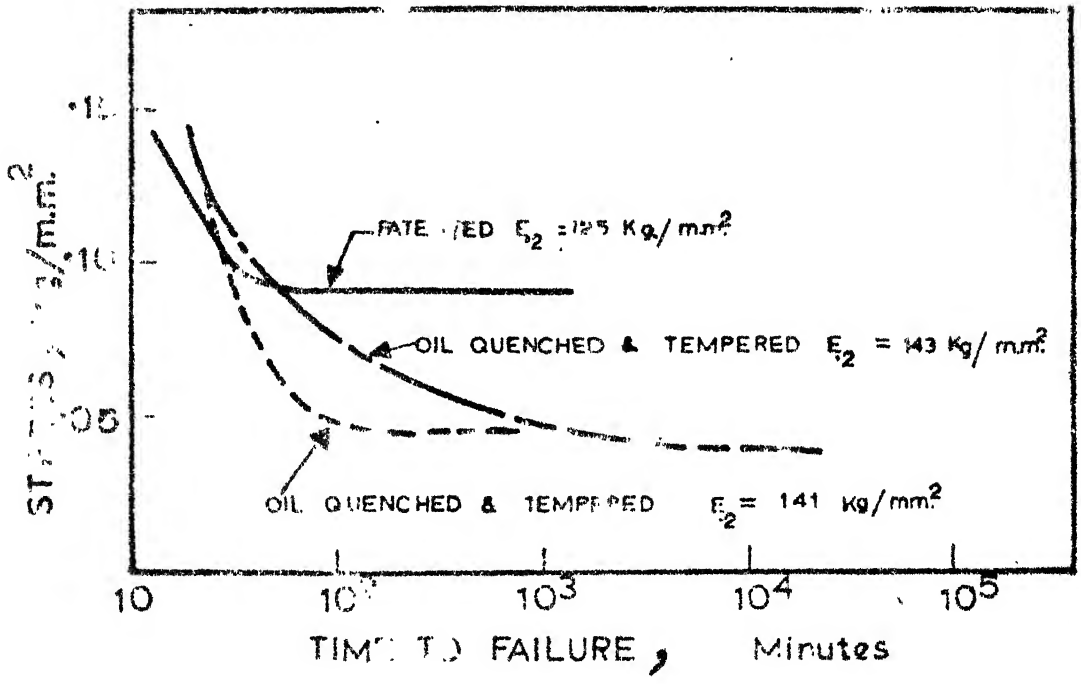

FIG. 2.1 EFFECT OF APPLIED STRESS ON TIME TO FAILURE OF THREE PRESTRESSING STEELS
(Replotted data of Libert & Hache[16])

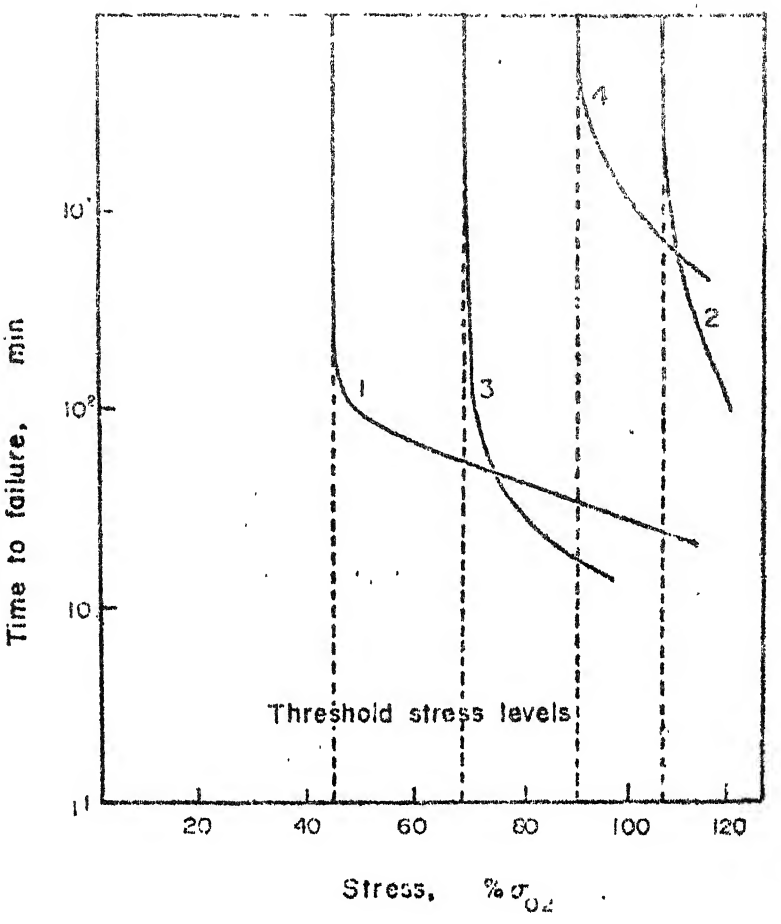

FIG. 2.2 The effect of stress as a proportion of $\sigma_{0.2}$ on the time to failure of various wires in cold 5% ferric sulphate solution.
(1) IT 325 cathodically polarized,* (2) IT 325 without polarization, (3) IT 275 without polarization, (4) CD† cathodically polarized.*
*about 0·5 V galvanostatically. †CD wire did not fail under $\sigma_{0.2}$ without polarization.
(Replotted data of Gilchrist & Narayan[13])

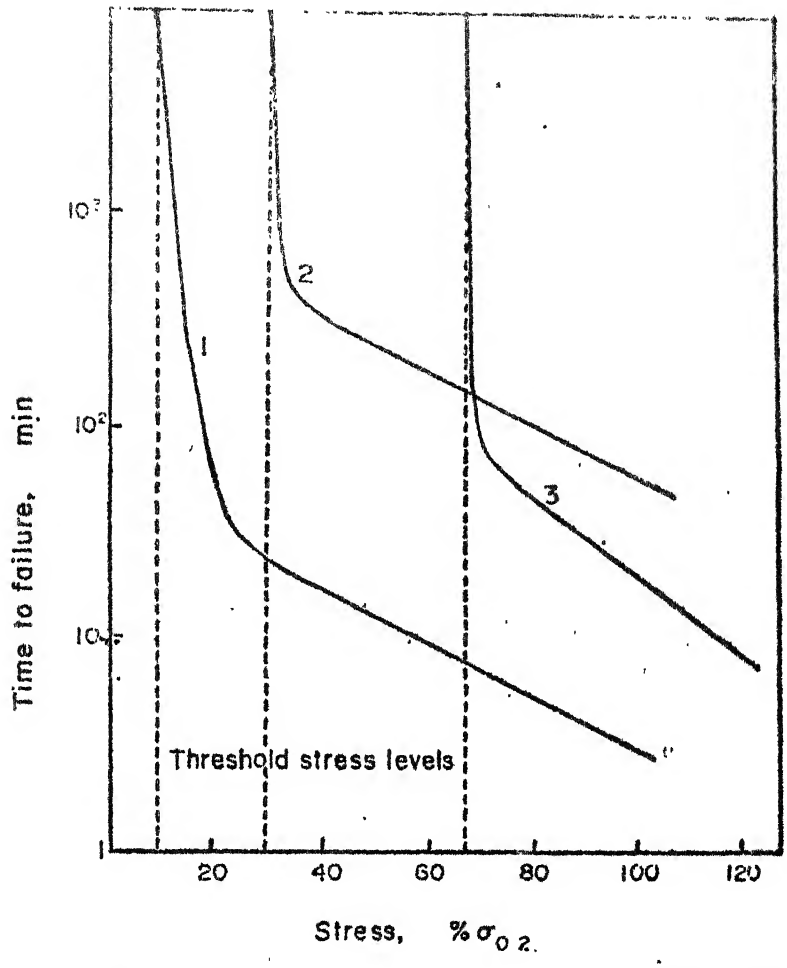

FIG. 2.3 The effect of stress as a proportion of $\sigma_{0.2}$ on the time to failure of various wires in saturated H_2S solution buffered to pH 5·3 and all at room temperature. (1) IT 275 without polarization, (2) CD without polarization and (3) IT 400 cathodically polarized to about 0·4 V.
(Gilchrist & Narayan[13])

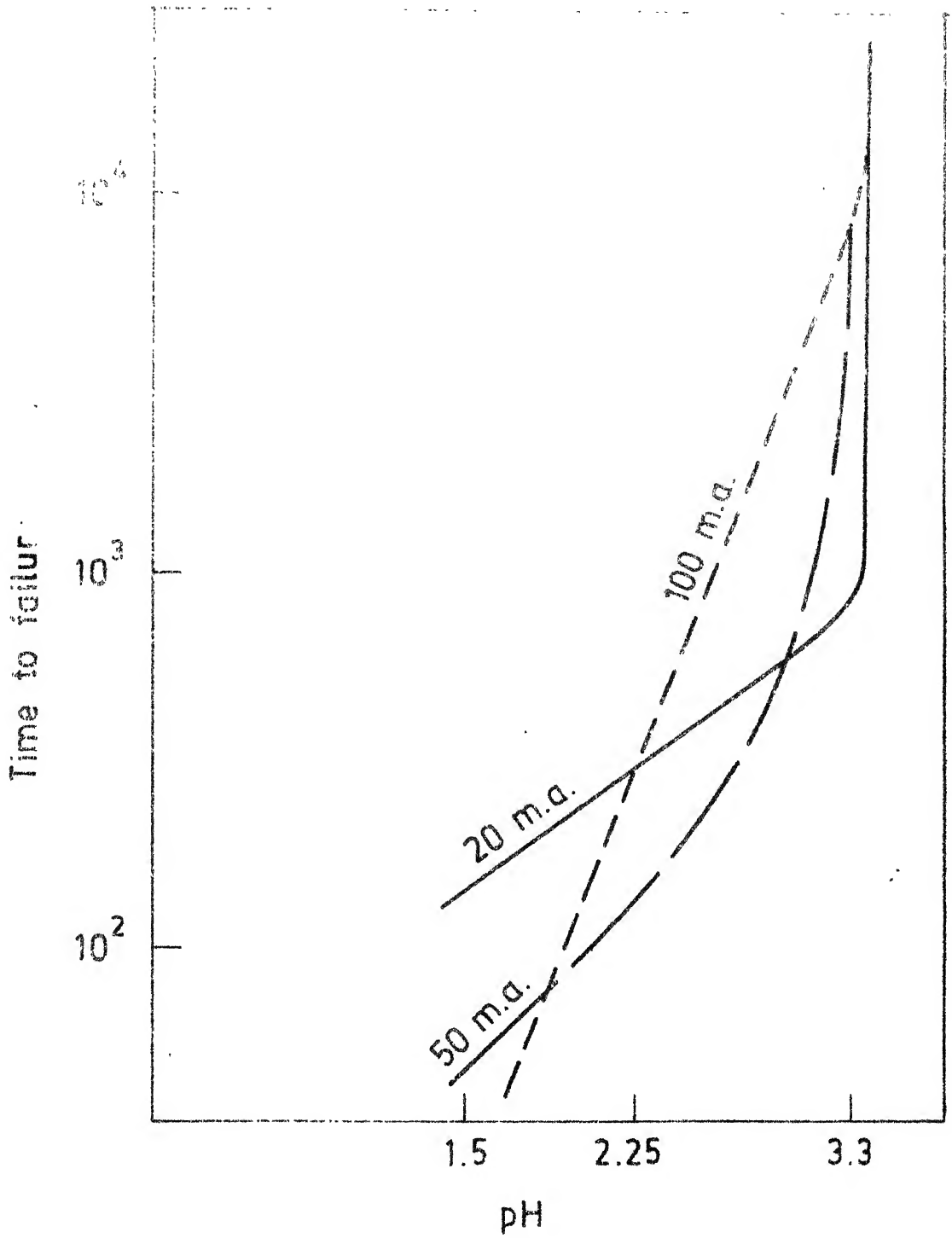

Fig. 2.4. Effect of pH on time to failure of prestressing steel in dil. H_2SO_4 solution with cathodic polarization at 3 currents (Libert & Hache[16]).

CHAPTER-III

EXPERIMENTAL TECHNIQUES

3.1. HEAT TREATMENT OF SAMPLES

This basically included two different types of treatments.

(i) Isothermal Transformation, and

(ii) Quenching & Tempering.

The purpose of the former treatment (i.e. isothermal transformation) was to attain different structure of pearlite, banite and ferrite by carrying out austenite to pearlite and/or banitic and ferritic transformation at different temperatures. Whereas in the later case the idea was to affect the morphology of iron carbide formed in tempering stage by carrying out tempering at different temperatures and time.

Heat treatment of samples was carried out using a vaccum (10^{-3} to 10^{-4} Torr) furnace, lead or salt bath depending upon the temperature of treatment involved. The purpose of using salt/lead bath in same treatment was

(i) to prevent the oxidation of samples

(ii) better temperature control in low temperature range, and

(iii) less time required for stabilisation of temperature, temperature control in limit $\pm$ 2°C was obtained.

The composition of salt baths are given in table 3.1. Various steps involved in the two types of treatments are described below.

1. Annealing of As Received wire in high vaccum (10^{-3} to 10^{-4} Torr) furnace at temperature 800°C for 2 hours. This was done to homogenise the samples.
2. Threading and cutting etc. of the samples.
3. Heating of the above samples at 780°C for 10 minutes.
4. (a) for isothermal transformation, samples (after heating at 780°C for 10 minutes), were cooled to different temperature in lead bath maintained at temperatures 350, 425, 500, 575 & 670°C. Samples were allowed to remain at bath temperature for 15, 5, 1/2, 1 & 10 minutes respectively and then quenched in brine solution to prevent any further transformation.
   (b) in the other category of treatment, samples heated to 780°C for 10 minutes were quenched in brine solution to obtain martensitic structure. Samples thus obtained were tempered at different temperatures (200, 300, 400, 500 & 600°C) for 1 and 4 hours respectively.

3.2. MECHANICAL TESTING

Two types of mechanical tests were done (1) Hardness testing and (2) Tensile testing.

3.2.1. HARDNESS TESTING

Indentation hardness is resistance offered by metals to indentation. Physically speaking this is measurement of plasticity and density of metals. These measurements on

As Received and heat treated samples were done using a Rockwell Hardness Tester (Model-WILSON-3JR, U.S.A.). Hardness values were read on c-scale. Other details are given below.

Penetrator - Brale

Primary loading - 10 kg

Secondary loading - 150 kg

Dial figure - Black

Hardness was taken at four different points and their average reported.

3.2.2 Tensile Testing

Tensile testing for As Received and heat treated samples was done on Universal Testing Machine (Model-INSTRON-1195). Sample used for testing was a 3.00 mm diameter wire of length 150 mm and Gauge length was 100 mm. Load vs. elongation plot obtained after tensile test was used to calculate proof stress, ultimate tensile strength, fracture stress and % elongation. Percent reduction in area was also measured.

3.3. METALLOGRAPHIC STUDIES

As Received and heat treated wires were mounted in a polythene tube using araldite. They were polished on a wheel using alumina (1 μm) suspension. The polished surface of the sample was then etched with 2% picral for 10 to 15 seconds and examined under the SEM or optical microscope.

3.4. CORROSION STUDIES

Corrosion studies mainly include polarization and stress corrosion cracking studies. Polarization studies on as received and heat treated wires in different environments namely mixture of calcium nitrate and ammonium nitrate and saturated H_2S were done in different stress conditions. Also time to failure and nature of fractured surface were studied for samples subjected to 70% of 0.2% Proof stress and aforementioned environments.

3.4.1 Description of Stress Corrosion Testing Machine & Its Operation

Stress corrosion testing machine was fabricated in I.I.T., Kanpur. The schematic diagram of the machine is shown in Fig. 3.1. It essentially consists of following parts.

(i) Samples grips and tensile loading system (Fig. 3.2). The specimen prepared, as per specification, is fitted in grips the cell, which is then fitted in the specimen of the specimen. The specimen is loaded through a double lever system. Accuracy of loading is ensured by a spirit level placed on the outer lever. A small rubber buffer on the base plate below this lever absorbs the shock when the specimen fractures. The specimen is held between top and bottom grips, the lower being connected to the lever loading system and the upper to an adjusting nut arrangement; so that the lever can be levelled with the specimen in correct position. The adjusting nut runs on a thrust bearing to reduce friction.

(ii) a cell surrounding the specimen in which desired cell is vented through a water cooled condenser to prevent the change in concentration of the medium and to reduce the escape of fumes. A small electric element in an asbestos cloth mantle, regulated by a temperature controller heats the corrosive liquid. and

(iii) time measuring device (hour meter). The inner lever operates a microswitch inside the machine to cut off the power when the specimen fails and to switch off the red light. An hourmeter automatically records the duration of the test.

3.4.2 Calibration of Stress Corrosion Testing Machine

Calibration was done using load cell fitted to the Instron machine in order to know the load on the specimen. When some known weight was applied on the pan of lower lever after balancing lower lever by spirit level and adjusting tension rod.

For calibration purpose, a suitable attachment had been designed (Fig. 3.3) and stress corrosion testing machine base plate was bolted with a small plate using nut and bolts. The small plate has a bar whose upper part being in the middle of Stress Corrosion Testing Machine base plate and in insertion core of small plate, while Instron machine lower grip has been gripped with a bar. A tensile sample of 8 mm diameter, whose one end was gripped in Stress Corrosion Testing Machine lower

specimen grip and its other end in Instron machine upper grip. A load cell of 5000 kg was used with full scale deflection on the machine and chart representing 2000 kg. When no weights, were kept on the load pan, tensile load was applied on the specimen with the help of Instron so that the load arm of the stress corrosion testing machine, as indicated by the spirit level was horizontal. This load was then noted. After leveling the weight on the load pan was progressive increased and the load on the specimen was read using the load cell attached to the Instron. This calibration was repeated three times. The data is given in Table 3.2. From this data a straight line calibration curve was drawn using the following procedure.

Let the equation for the straight line

$$Y = mx + c$$

where x = applied load on machine, kgs.

Y = load on specimen, kgs.

c = constant

& m = slope of curve

Now we have two values of Y,

where observed value = $y_{obs} = Y_i$

Calculated value = $Y_{cal} = Y_i$

$$\text{Error} = Y_i - y_i$$

$$M = \text{Error}^2 \;\&\; \mathcal{L} = M/N$$

$$\therefore M = \Sigma (Y_i - y_i)^2 \qquad (1)$$

$$\mathcal{L} = \frac{1}{N} \Sigma (Y_i - y_i)^2 \qquad (2)$$

Where N = number of observations

$$y_i = mx_i + c \qquad (3)$$

From equation (2) and (3) we have,

$$\mathcal{L} = \frac{1}{N}\Sigma(Y_i - mx_i - c)^2$$

$$= \frac{1}{N}\Sigma(y_i^2 + m^2x_i^2 + c^2 - 2mY_ix_i - 2cY_i + 2cmx_i)$$

$$= \frac{1}{N}\Sigma Y_i^2 + \frac{m^2}{N}\Sigma x_i^2 + c^2 - \frac{2m}{N}\Sigma x_iY_i - \frac{2c}{N}\Sigma Y_i + \frac{2cm}{N}\Sigma x_i \qquad (4)$$

We have

$$\bar{Y} = \frac{\Sigma Y_i}{N} \qquad (5)$$

and

$$\bar{X} = \frac{\Sigma x_i}{N} \qquad (6)$$

where $\bar{Y}$ and $\bar{X}$ are average values

From equation (4), (5) & (6) we have,

$$\mathcal{L} = \frac{\Sigma Y_i^2}{N} + \frac{m^2}{N}\Sigma x_i^2 + c^2 - \frac{2m}{N}\Sigma x_iy_i - x\bar{Y} + 2cm\bar{X}$$

differentiating with respect to m

$$\frac{d\mathcal{L}}{dm} = \frac{2m}{N}\Sigma x_i^2 - \frac{2}{N}\Sigma x_iY_i + 2c\bar{X} \qquad (7)$$

Putting $\frac{d\mathcal{L}}{dm} = 0$, then we have,

$$\frac{2m}{N}\Sigma x_i^2 - \frac{2}{N}\Sigma x_iY_i + 2c\bar{X} = 0$$

$$m\ \Sigma x_i^2 - \Sigma x_iY_i + cN\bar{X} = 0$$

$$m\ \Sigma x_i^2 - \Sigma x_iY_i + c\ \Sigma x_i = 0 \qquad (8)$$

Now we have

$$\Sigma(\ Y_i - y_i\ ) = 0 \qquad (9)$$

From equation (9) and (3) we have,

$$\Sigma (Y_i - mx_i - c) = 0$$

$$\Sigma Y_i - m \Sigma x_i - c = 0$$

$$c = (\bar{Y} - m\bar{X}) \qquad (10)$$

Putting the value of c from equation (10) to equation (8) then we have,

$$m \Sigma x_i^2 - \Sigma x_i Y_i + \Sigma x_i(\bar{Y} - m\bar{X}) = 0$$

$$m \Sigma x_i^2 - \Sigma x_i Y_i + \Sigma x_i \bar{Y} - m\bar{X} \Sigma y_i = 0$$

$$m \Sigma x_i^2 - \frac{(\Sigma x_i)^2}{N} = \Sigma x_i Y_i - \frac{\Sigma x_i \Sigma y_i}{N}$$

$$\therefore m = \frac{\Sigma x_i Y_i - \frac{(\Sigma x_i)(\Sigma y_i)}{N}}{\Sigma x_i^2 - \frac{(\Sigma x_i)^2}{N}} \qquad (11)$$

From equation (10) we have,

$$c = \bar{Y} - m\bar{X}$$

$$\therefore c = \frac{1}{N} (\Sigma Y_i) - m\left(\frac{\Sigma x_i}{N}\right) \qquad (12)$$

COMPUTER PROGRAMMING FOR DETERMINATION OF m & c

```
      DIMENSION X(144), Y(144)
      REAL  M
      N = 144
      READ*, (X(I), Y(I), I = 1, 144)
      DO 110 I = 1, 144
```

```
110     TYPE*, X(I), Y(I)
        SUM X=0.; SUM Y=0.; SUM XY=0.; SUM SQ=0.
        DO 100 I=1, 144
        SUM X = SUM X + X(I)
        SUM Y = SUM Y + Y(I)
        SUM XY = SUM XY + X(I)* Y(I)
        SUM SQ = SUM SQ + X(I)* X(I)
100     CONTINUE
        A = SUM XY - SUM X* SUM Y/N
        B = SUM SQ - SUM X* SUM X/N
        M = A/B
        C = (SUM Y - M* SUM X)/N
        TYPE 10, M, C
 10     FORMAT (100X, 'GRADIENT=', 2X, E15.7, 10X, 'C=',2X, E15.7)
        STOP; END
```

After observed valuesof slope of curve (m) and constant (c) from computer then putting these values on the straight line equation $Y = mx + c$ choosing any value of x i.e., x=1, x=20 & x=40 and calculating Simultaneous Value of Y. A plot between these values is shown in Fig. 3.4.

where $m = 25.02$ & $c = 31.47$

Standard error = 28.38

Root mean square of error = 340.60

3.4.3 Stress Corrosion Cracking Studies

These studies on as received and heat treated wires were carried out in stress corrosion testing machine. The wires were subjected to a tensile stress equivalent to 70% of 0.2% Proof stress (as found out in tensile testing). The behaviour of as received wire was studied in following environments.

(i) Solutions of calcium nitrate having following concentration 20, 40, 60 & 80% (by weight). Temperature of solution was maintained at 100°C.

(ii) Solution of 50% Calcium Nitrate and 5% Ammonium Nitrate (by weight) at 100°C. and

(iii) H_2S saturated water at room temperature.

Behaviour of heat treated samples was studied in above mentioned (ii) and (iii) environments.

Time require for failure of a wire was read on the hour meter. Fractured surface of wires were studied with or without polishing. Fracture surface was seen in SEM without polishing while polished etched fracture surface was seen in Optical microscope, picral was used as the etchant.

3.5. POLARIZATION STUDIES

For automatically recording polarization curves following instruments were used.

(a) Wenking Model HP-72, High Power Potentiostat

(b) Wenking Model SMP-72, Scanning Potentiometer

(c) PEC-LM, Logarithemic Current Converter

(d) Series 2000, X-Y Recorder

(e) Corrosion Cell

(f) Passive Modulator and assorted cable.

Connections of instruments are given in Fig. 3.5.

High Power Potentiostat and Scanning Potentiometer

High power potentiostat used for a controlled potential supply which alters its potential slowly enough so that the current can reached to a stationary value in following potential change. For slow potential scanning during automatic recording with potentiostatic controlled can be done by using Scanning Potentiometer SMP-72, whose output voltage changed in small steps at intervals of time that can be adjusted with wide limits. The output voltage of the SMP-72 superimposed on a starting voltage set up the control voltage supply inside the potentiostat. The potential scan and the scanning rate (45 mV/min) was set on the Scanning Potentiometer, Model SMP-72.

Potential was recorded on the Y-axis of the X-Y recorder using a sensitivity of 125 mV/cm.

PEC-LM Logarithmic Current Converter

The PEC-LM log current converter permits direct, convenient and accurate interpretations of current between micro-amperes and 1.0 ampere without requiring a range change. The input may thus ride at potentials of 25 volts above or below the output. While producing an accurate log of current output. The output is expressed as a change of 1 volt per decade, with more positive values being larger and zero volts equaling 10 micro-amperes. Representive outputs would be 5V=1A, 2V=1mA and -2V=0.1 μA.

Current was recorded on the X-axis of the X-Y recorder using a sensitivity of 500 mV/cm.

Corrosion Cell

A schematic diagram of corrosion cell and it connections are shown in (Fig. 3.5 to 3.6). Details can be found in the manual of High Power Potentiostat Model HP-72.

3.6. FRACTORGRAPHY

The fracture surface of wires were examined in the scanning electron microscope. A brass sample holder with a slit to accommodate the sample and a screw to hold it intact was made. The whole fracture surface was examined and the notable features photographed.

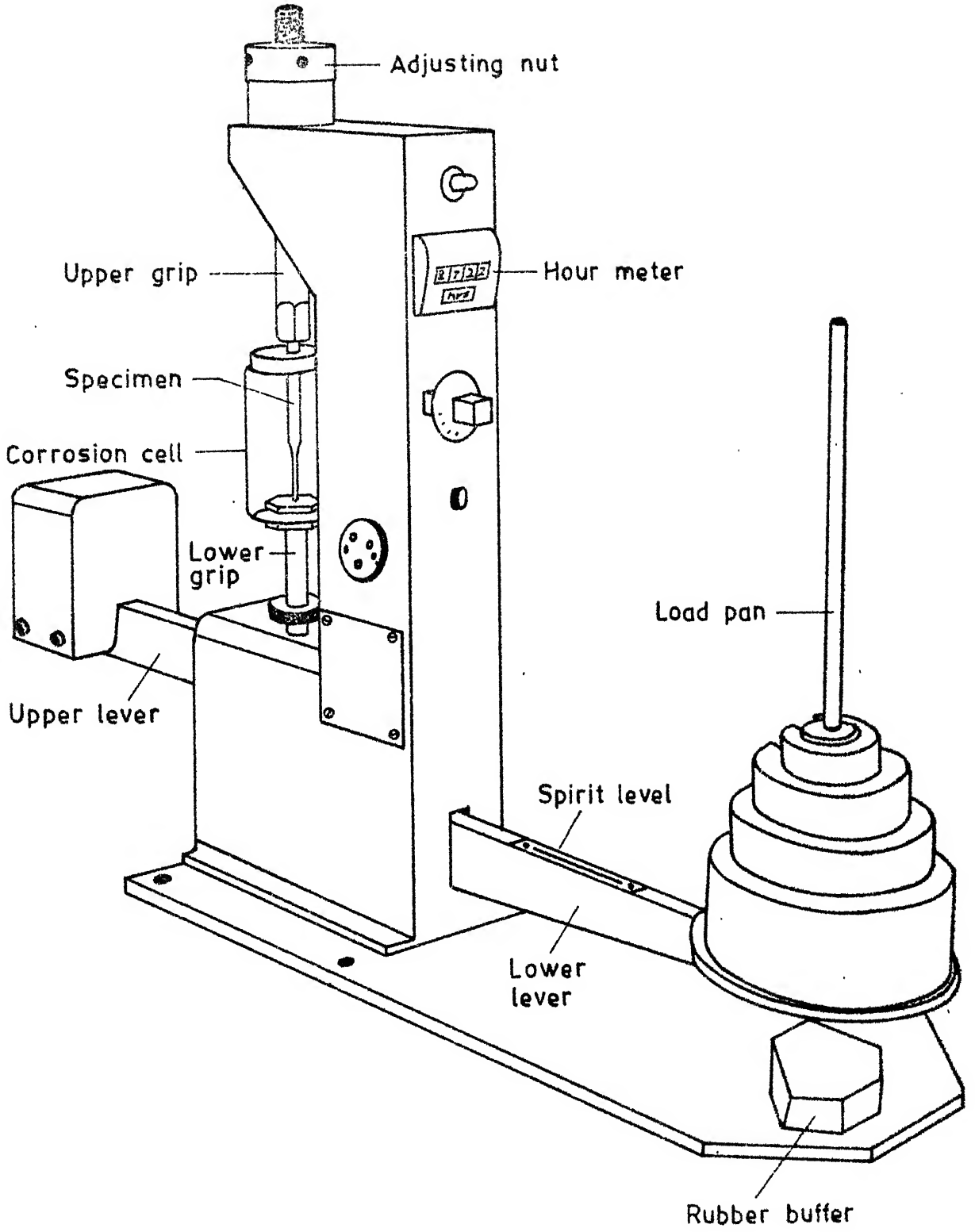

Fig. 3.1. Stress corrosion testing machine (schematic).

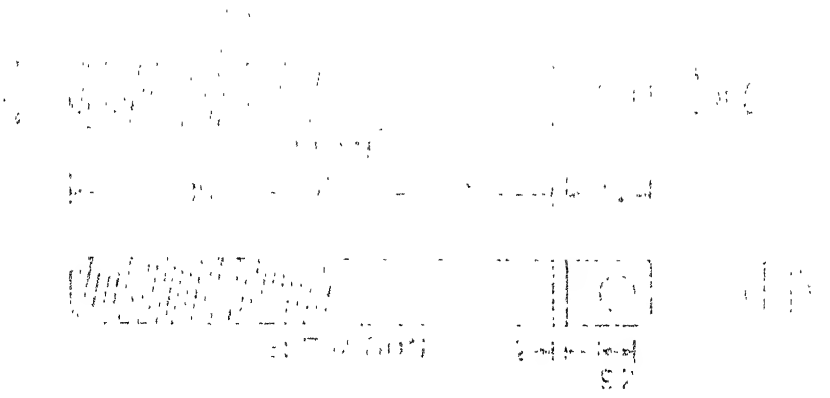

(a) Adjusting tension rod

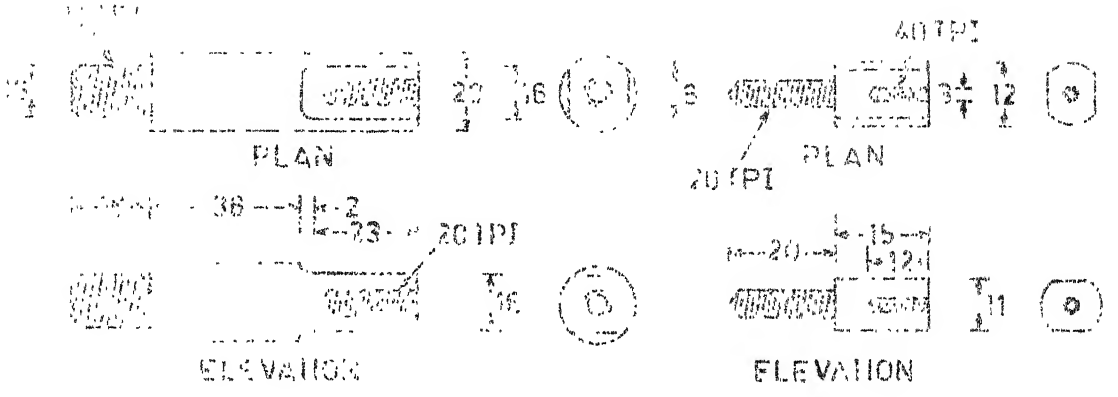

(b) Lower Specimen Grip (c) Adapter

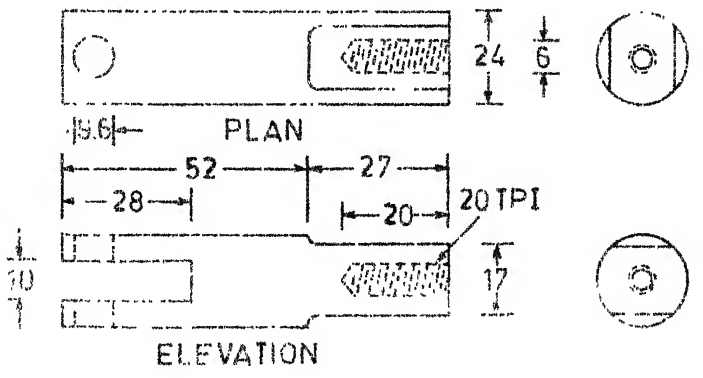

All dimensions in mm

(d) Upper Specimen Grip

Fig. 3.2. Lower and upper specimen grips, their adapters and adjusting tension rod.

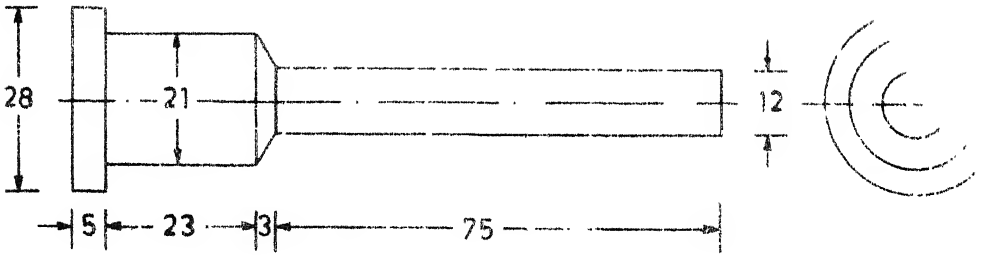

(a) Rod

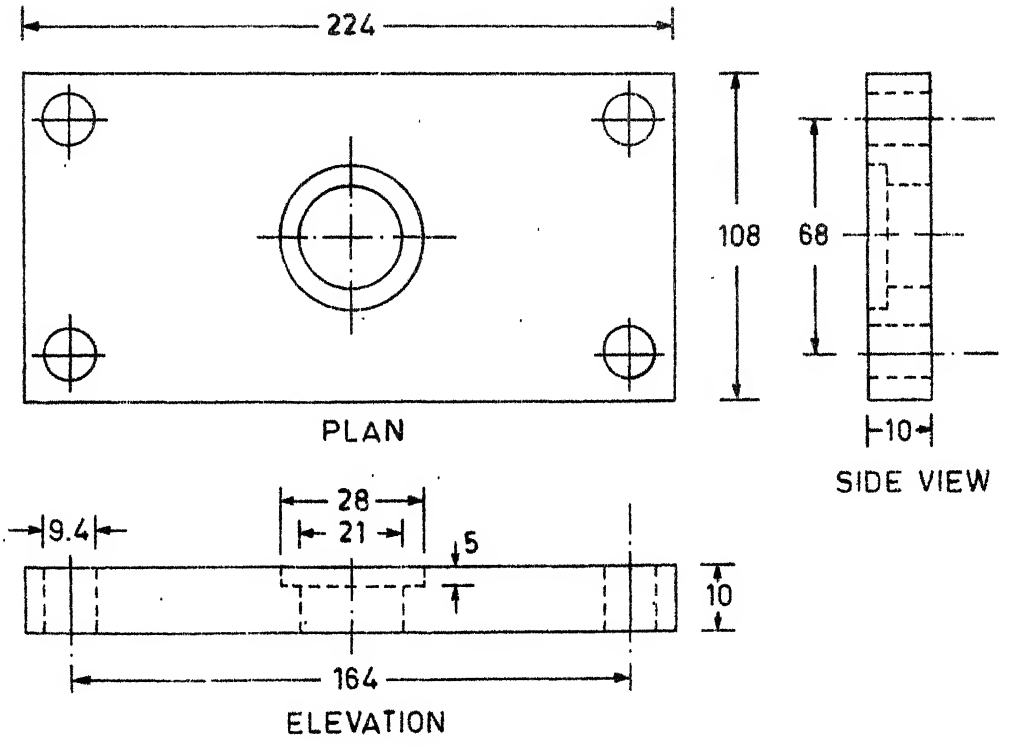

(b) Plate

Fig. 3.3. Calibration attachment for stress corrosion testing machine.

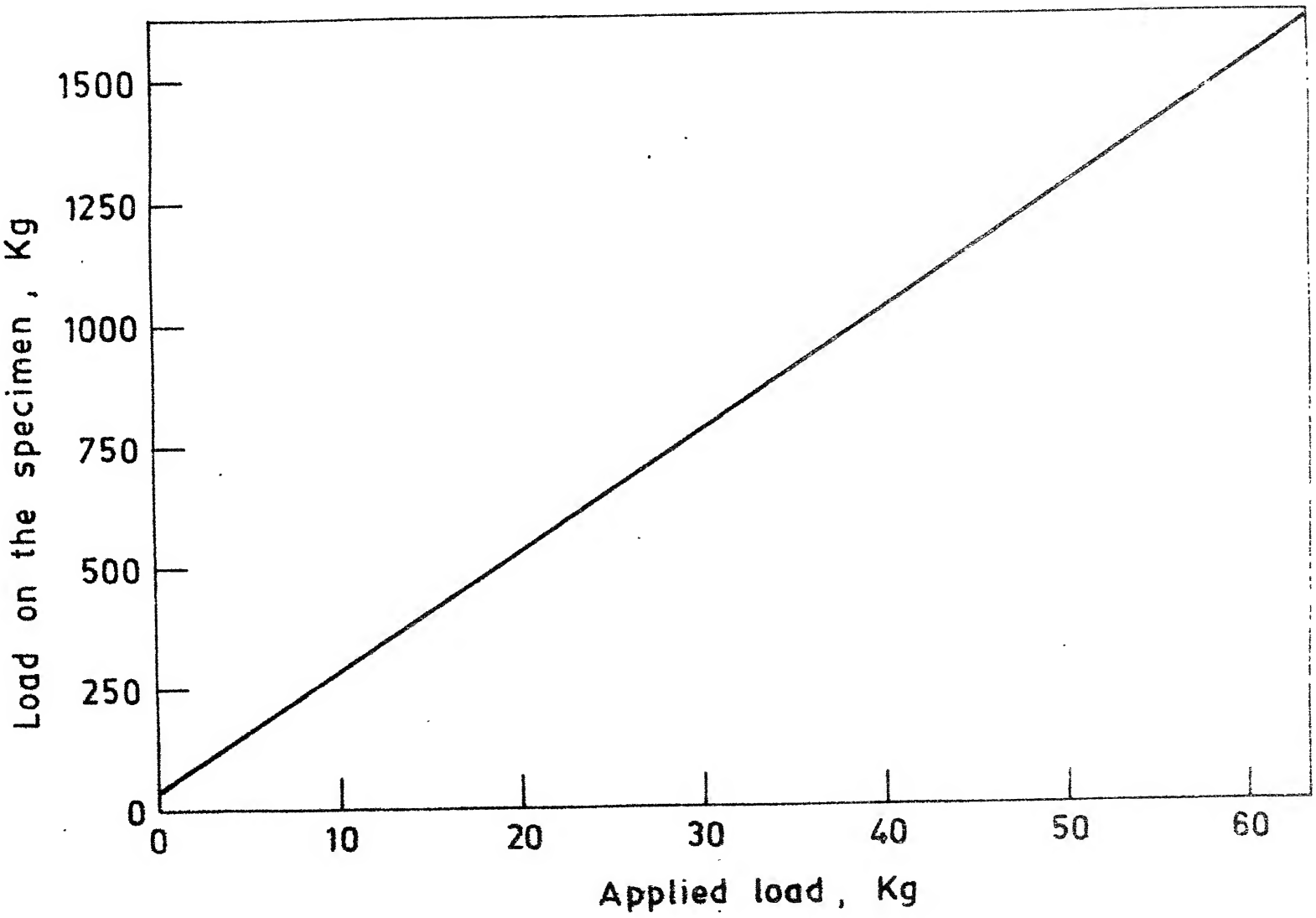

Fig. 3.4. Calibration curve for stress corrosion testing machine.

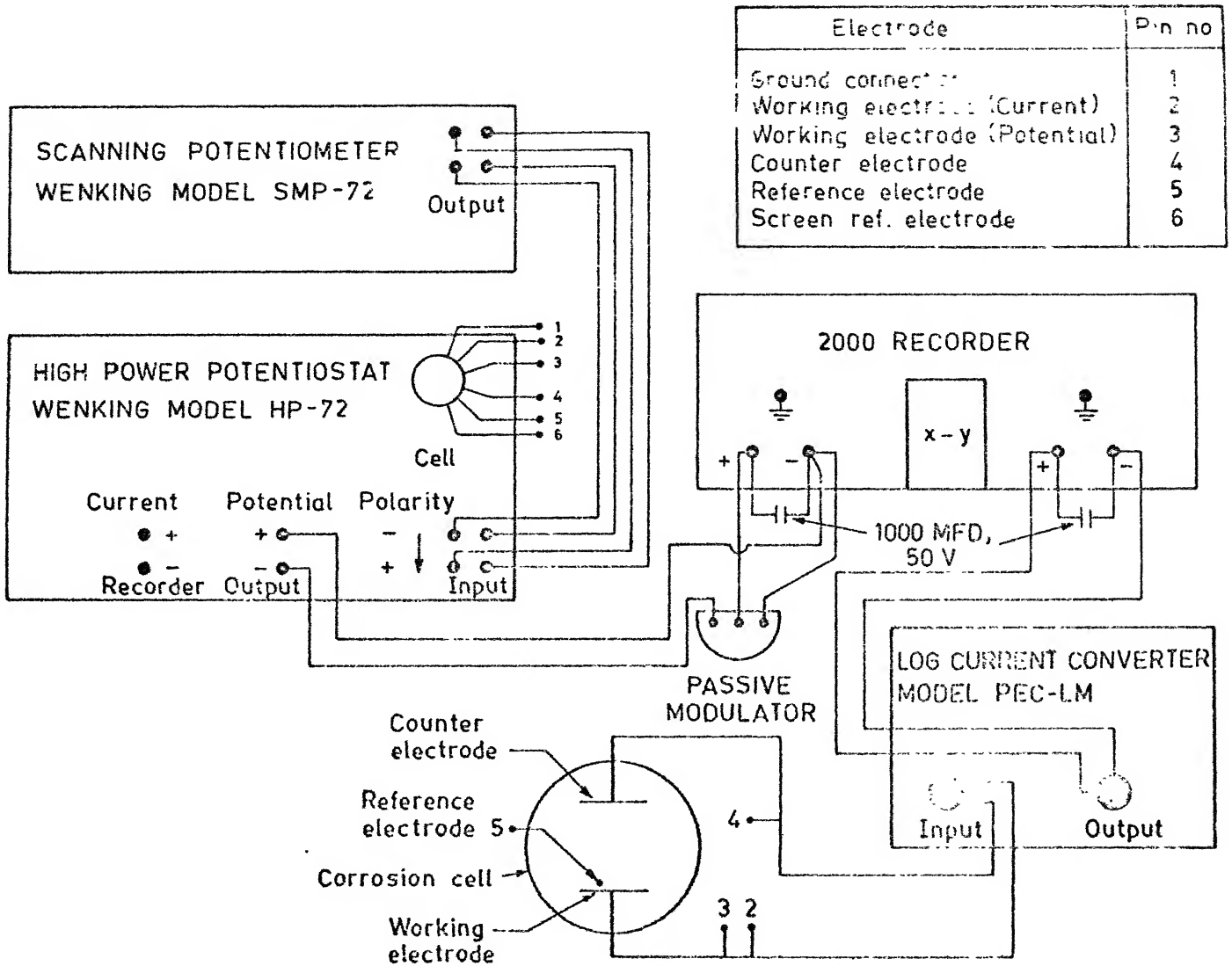

Fig. 3.5. Set-up for polarization studies (schematic).

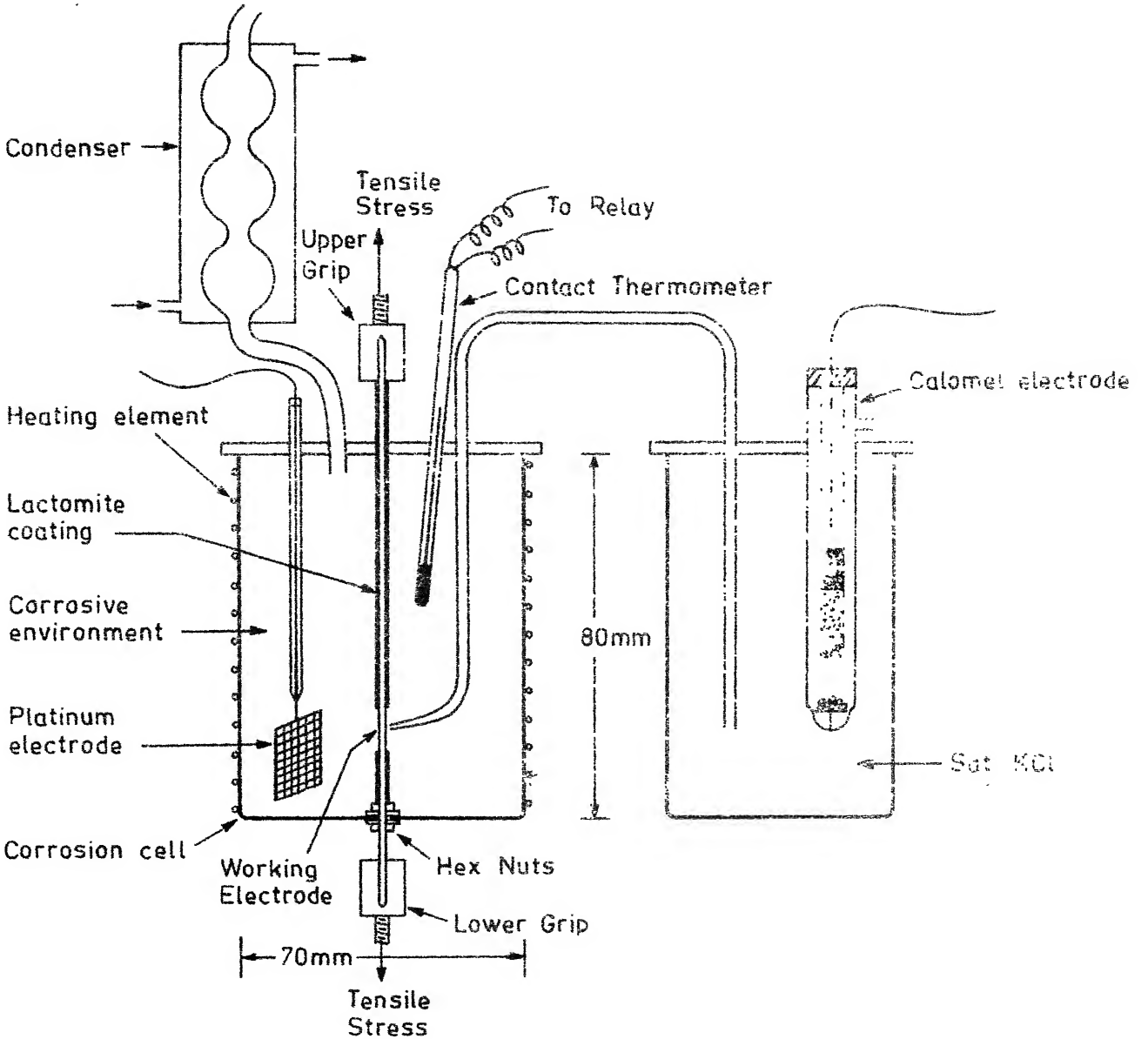

Fig. 3.6. Corrosion cell for polarization studies on stressed specimen.

TABLE 3.1

Nominal composition of salts for heat treatment.

Weight percentage					Approximately mp		Recommended heating range	
NaCl	KCl	$BaCl_2$	KNO_3	$NaNO_2$	°F	°C	°F	°C
15-20	20-30	50-60	-	-	1100	593	1250-1700	675-925
10-20	-	80-90	-	-	1400	760	1500-2000	815-1093
-	-	-	50-60	40-50	290	143	325-1200	162-648

TABLE 3.2

Applied load vs. load on the specimen for stress corrosion testing machine.

Sl. No.	Load applied on stress corrosion testing m/c, kg	Load on the specimen, kg						Mean load, kg
		1st set		2nd set		3rd set		
		Loading	Unloading	Loading	Unloading	Loading	Unloading	
1.	0	33	34	34	34	34	34	33.83
2.	0.475	44	46	46	45	45	47	45.50
3.	1.455	67	70	70	70	69	70	69.33
4.	3.140	107	104	110	114	118	111	110.66
5.	4.260	131	140	134	141	134	139	136.50
6.	5.070	150	160	154	159	152	158	155.50
7.	5.870	170	178	174	175	174	175	174.33
8.	6.660	192	192	191	191	191	191	191.33
9.	12.485	325	360	360	360	360	360	354.16
10.	15.995	405	450	430	455	430	450	436.66
11.	19.480	487	540	510	550	510	550	524.50
12.	22.890	570	630	590	630	590	620	605.00
13.	26.465	665	720	720	720	740	670	720.00
14.	29.985	745	820	750	820	760	820	785.83
15.	33.445	830	890	840	890	840	900	865.00
16.	37.090	925	960	950	960	930	960	947.50
17.	40.580	1020	1020	1020	1020	1020	1020	1020.00
18.	43.005	1100	1190	1170	1200	1080	1150	1148.33
19.	46.465	1180	1290	1230	1300	1170	1265	1239.16
20.	49.950	1260	1350	1290	1260	1250	1335	1290.83
21.	53.360	1360	1420	1370	1400	1335	1390	1379.16
22.	56.870	1460	1460	1455	1455	1430	1430	1448.33
23.	59.495	1540	1440	1555	1555	1555	1555	1533.33
24.	62.905	1600	1600	1600	1600	1600	1600	1600.00

CHAPTER-IV

RESULTS AND DISCUSSIONS

4.1 MECHANICAL PROPERTIES

Mechanical properties of the prestressing steel wires containing 0.8% C, 0.73% Mn, 0.25% Si, 0.024% S and 0.021% P in As Received, Annealed, Quenched and Tempered (QT) and Isothermally Transformed (IT) conditions were determined (Fig. 4.1 to 4.3; Table 4.1). Annealing was done at 800°C for 2 hours. Annealed wires were austenitized at 780°C for 10 minutes followed by brine quenching. The quenched wires were tempered for 1 hour and 4 hours respectively at 200, 300, 400, 500 & 600°C. Annealed wires were also austenitized at 780°C for 10 minutes followed by Isothermal Transformation at 350°C (15 minutes), 425°C (5 minutes), 500°C (30 seconds), 575°C (1 minute) and 670°C (10 minutes). The samples were brine quenched after the completion of isothermal transformation.

Tensile strength as measured by fracture stress, UTS and 0.2% proof. stress and hardness of quenched and tempered wires decreased whereas the ductility as measured by % reduction in area and % elongation increased with increasing tempering temperatures for 1 hour tempering (Fig. 4.1; Table 4.1). Similar trend was observed when tempering time was increased to 4 hrs. (Fig. 4.2; Table 4.1). Mechanical properties of isothermally transformed wires also showed a similar trend except that a minimum in case of % reduction in area was observed at 500°C (Fig. 4.3; Table 4.1).

4.2 CORROSION BEHAVIOUR IN SATURATED H_2S SOLUTION

As Received wire failed in 70 hours in saturated H_2S solution when it was stressed to 70% of 0.2% proof strength. It corrosion potential versus saturated calomel electrode in unstressed and stressed condition was - 0.710V and - 0.684V respectively (Table 4.2).

Annealed wire failed due to stress corrosion cracking in saturated H_2S solution at room temperature in 110 hours. Its corrosion potential versus saturated calomel electrode in unstressed and stressed conditions was - 0.750V and - 0.680V respectively (Table 4.2).

Time to failure and corrosion potential ($E_{corr.}$) in stressed condition increased whereas corrosion potential in Unstressed condition decreased with increasing isothermal transformation temperature (Fig. 4.4; Table 4.2).

Time to failure of quenched and tempered wires increased with increasing tempering temperature for both 1 hour and 4 hours tempering (Fig. 4.5; Table 4.2). Corrosion potential in stressed and unstressed conditions showed a peak at about 300°C for 1 hour tempering. For 4 hours tempering the trend in $E_{corr.}$ in stressed condition was similar to that obtained for 1 hour tempering. However, in Unstressed Condition it showed a completely different behaviour and a minimum being observed at about 500°C.

Potentiodynamic anodic polarization curves for As Received, annealed,isothermally transformed and quenched and tempered conditions were determined both in unstressed and stress (70% of 0.2% proof stress) conditions (Fig. 4.6 to 4.22). In all conditions of heat treatment, corrosion potential ($E_{corr.}$) observed at the end of reverse scan was always more noble than that observed during forward scan. In no case the prestressing steel wires showed passive behaviour, the samples remained active in all conditions of heat treatment. A limiting current density observed in unstressed and stressed conditions were with-in 3 mA/cm^2. However,for IT 350, IT 425, IT 500, IT 670 & QT 600 (1 hr.) specimens the limiting current density in stressed condition was much higher (approximately equal to 10 mA/cm^2).

In unstressed condition the anodic polarization curve during reverse scan was on the left of the forward scan curve except for As Received, QT 400 (1 hr.), QT 300 (4 hrs.) and QT 600 (4 hrs.) wires. In stressed condition the anodic polarization curve during reverse scan was also on the left of the curve observed during forward scan in all cases except for IT 350, IT 500, IT 575 and IT 670 wires.

4.3 CORROSION BEHAVIOUR IN 50% $Ca(NO_3)_2$ + 5% NH_4NO_3 SOLUTION AT 100°C

In 50% $Ca(NO_3)_2$ + 5% NH_4NO_3 solution at 100°C it took 175 hours for As Received wire to fail. The corrosion potential versus saturated calomel electrode in unstressed and stressed conditions was - 0.370V and - 0.434V respectively (Table 4.2).

In 50% $Ca(NO_3)_2$ + 5% NH_4NO_3 solution annealed wire took 290 hours to fail. Its corrosion potential versus saturated calomel electrode unstressed and stressed conditions was - 0.460V and - 0.462V respectively.

Time to failure of isothermally transformed wires increased whereas corrosion potential ($E_{corr.}$) in the unstressed condition decreased with increasing transformation temperature (Fig. 4.23; Table 4.2). Corrosion potential ($E_{corr.}$) in the stress condition showed a irregular behaviour, it first showed a minimum at about 470°C and then a maximum at about 575°C.

Time to failure of quenched and tempered wires increased with increasing tempering temperature for both 1 hour and 4 hours tempering (Fig. 4.24; Table 4.2). Corrosion potential ($E_{corr.}$) for wires tempered for 1 hour in unstressed and stressed conditions first increased, then decreased and then increased again with increasing tempering temperature (Fig. 4.24; Table 4.2). For tempering temperatures below about 450°C, $E_{corr.}$ in unstressed condition was less noble than in stressed condition. At temperatures higher than this the reverse trend was observed (Fig. 4.24).

Corrosion potential ($E_{corr.}$) for wires quenched and tempered for 4 hours in unstressed condition remained constant upto 300°C, thereafter it decreased with increasing tempering temperature (Fig. 4.24; Table 4.2). In stressed condition,it first increased upto about 375°C tempering temperature,thereafter, it decreased upto about 500°C tempering temperature and increased thereafter. For tempering temperature below about 450°C, E_{corr} in unstressed condition was less noble than in stressed condition (Fig. 4.24; Table 4.2).

Potentiodynamic anodic polarization curves for As Received, Annealed, Isothermally Transformed and Quenched and empered wires were determined in unstressed and stressed (70% of 0.2% Proof stress) conditions exposed to a solution of 50% $Ca(NO_3)_2$ + 5% NH_4NO_3 at 100°C (Fig. 4.25 to 4.41; Table 4.3 to 4.4). In all conditions of heat treatment, corrosion potential ($E_{corr.}$) observed at the end of reverse scan was more noble than that observed during forward scan. At the end of the reverse scan corrosion potential for stressed wires was more active than unstressed wires in As Received, IT 350, IT 425, IT 500, IT 575, QT 200 (1 hr.), QT 300 (1 hr.), QT 200 (4 hrs.), QT 300 (4 hrs.), QT 400 (4 hrs.) & QT 500 (4 hrs.). In other cases,the reverse of this was observed.

In all conditions of heat treatment, critical current density for stressed and unstressed wires in reverse scan was higher than in forward scan except for IT 670, QT 400 (4 hrs.) & QT 600 (4 hrs.) wires in stressed conditions.

In all cases, primary passive potential during reverse scan was higher than primary passive potential in the forward scan except for annealed, IT 500, IT 670, QT 600 (1 hr.), QT 500 (4 hrs.) & QT 600 (4 hrs.) wires in stressed conditions.

In all cases current in the passive state during reverse scan was less than during forward scan except for QT 600 (1 hr.), & QT 500 (4 hrs.) wires in unstressed conditions and annealed, IT 500, QT 400 (1 hr.) & QT 600 (4 hrs.) wires in stressed conditions, while for QT 400 (1 hr.) wire in unstressed condition and IT 500, QT 600 (1 hr.), QT 400 (4 hrs.) wires in stressed conditions there was no difference in the current in passive state during forward and reverse scan.

Corrosion current ($i_{corr.}$) for isothermally transformed prestressing wires decreased with increasing isothermal transformation temperature upto 500°C, after that it decreased.

During forward scan, the critical current density (i_{crit}) was higher for stressed wires than unstressed wires, except for Annealed and QT 400 (4 hrs.) wires. This trend was also observed during reverse scan except for IT 670 and QT 600 (4 hrs.) wires. There was no effect of stress on i_{crit} for annealed wires during reverse scan.

The area of the anodic loop for isothermally transformed wires in unstressed condition decreased with increasing transformation temperature, except for IT 570 wire (Fig. 4.42). In stressed condition it first decreased upto 575°C and increased thereafter. The area in stressed condition being always less than the area in unstressed condition except for IT 670 wires.

For quenched and tempered for 1 hour wires, the area of the anodic loop in unstressed condition decreased with increasing temperature upto 500°C thereafter it increased, whereas for stressed condition it first increased upto 400°C and thereafter it decreased. The area in stressed condition was always more than the area in unstressed condition except for QT 600 (1 hr.) wires (Fig. 4.42).

For quenched and tempered for 4 hours wires, the area of the anodic loop in unstressed condition showed a different behaviour than quenched and tempered for 1 hour wires. It first increased upto 300°C, thereafter it decreased upto 500°C and increased again upto 600°C. In stressed condition the area of the anodic loop increased upto 300°C, thereafter it decreased. The decrease being significant when the transformation temperature increases from 300°C to 400°C and not so significant thereafter (Fig. 4.42).

During anodic polarization, reverse scan intersects the forward scan at 3 points in most cases. For isothermally transformed wires potential at which the first intersection took

place became more active with increasing transformation temperature for unstressed and stressed wires except for IT 500 (unstressed) and IT 575 (stressed)wires.

The point of third intersection in unstressed condition was practically unchanged whereas in stressed condition it become more active with increasing transformation temperature except IT 575 wire (Table 4.5). There was not much difference in unstressed and stressed conditions.

For quenched and tempered for 1 hour wires the potential at which the first intersection took place became more active with increasing tempering temperature for unstressed and stressed wires except for QT 300, 1 hr. (unstressed) and QT 500, 1 hr. (stressed) wires. The point of third intersection in unstressed and stressed condition was practically unchanged ,whereas in stressed condition it became more active with increasing tempering temperature except QT 500°C , (Table 4.5). There was not much difference in unstressed and stressed conditions.

For quenched and tempered for 4 hours, wires the potential of first and third intersection became more active with increasing tempering temperature for unstressed and stressed wires except for QT 400 (unstressed and stressed), QT 500 (unstressed) & QT 300 (stressed) wires. The point of third intersection in unstressed and stressed condition was practically unchanged whereas in stressed condition it became more active with increasing tempering temperature except for 500°C wire (Table 4.5).

The current density at the first intersection in stressed condition was higher than in unstressed condition except for IT 670 & QT 600 (4 hrs.) wires, while in annealed wire it was unchanged. Current density at the second intersection showed the same behaviour except for annealed, QT 600 (1 hr.) & QT 400 (4 hrs.) wires. For third intersection,the observed value of current density in stressed condition was higher only for As Received, IT 350, IT 425, IT 500, IT 575, QT 200 (1 hr.), QT 500 (1 hr.), QT 600 (1 hr.) & QT 300 (4 hrs.) wires, while in case QT 200 (4 hrs.) & QT 600 (4 hrs.) wires it was unchanged (Table 4.6).

The current density at the first intersection in unstressed and stressed conditions for isothermal transformed wires were increased with increasing transformation temperature except for IT 500 (unstressed) and IT 670 (stressed), while at third intersection point it showed reverse behaviour except for IT 500 (unstressed) and IT 575 (stressed) wires (Table 4.6).

The current density at the second intersection point for quenched and tempered wires for 1 hour in unstressed condition increased with increasing tempering temperature except for QT 400, while for stressed wires it showed a reverse behaviour except for QT 200°C. At the third intersection the current density continuously decreased with increasing tempering temperature except for QT 300 and QT 400 (stressed) wires. Current density at the first intersection point in stressed

condition continuously increased with increasing tempering temperature, while in unstressed condition their was no systematic change.

The current density at the first intersection for quenched and tempered wires for 4 hours in stressed condition increased with increasing tempering temperature except for QT 600 (4 hrs.) wire. Current density at the third intersection in stressed condition increased with increasing tempering temperature, while for unstressed condition their was no systematic change (Table 4.6).

4.4 CORROSION BEHAVIOUR OF AS RECEIVED WIRE IN CALCIUM NITRATE SOLUTION AT 100°C

Time to failure decreased whereas corrosion potential ($E_{corr.}$) in the unstressed and stressed condition for prestressing wires increased with increasing concentration of calcium nitrate (Fig. 4.43, Table 4.7).

Corrosion potential ($E_{corr.}$) in stressed conditions for different concentration of calcium nitrate was more noble than $E_{corr.}$ in unstressed conditions.

Anodic polarization curves showed that corrosion potential ($E_{corr.}$) at the end of reverse scan was always more noble than that observed during forward scan (Fig. 4.44 to 4.49; Table 4.7). Corrosion potential after the reverse scan increased in noble direction with increasing concentration for unstressed and stressed wires. Critical current density ($i_{crit.}$) in

stressed condition for forward and reverse scans increased with concentration of calcium nitrate, while in unstressed condition it did not show any systematic change.

Current in the passive state during reverse scan continuously decreased with increasing concentration of calcium nitrate. In unstressed condition passive behaviour was observed during forward and reverse scans. Whereas in stressed condition passive behaviour was observed during reverse scan only.

The area of the anodic loop in unstress condition increased with increasing concentration of calcium nitrate. In stressed condition it first increased upto 60% of calcium nitrate solution and then decreased. Area of the loop in unstressed condition was higher than in stressed condition except for 60% of calcium nitrate solution where reverse of this behaviour was observed (Fig. 4.50; Table 4.8).

The potential at the first intersection in stressed condition was more noble than in unstressed condition at all concentrations of calcium nitrate. The point of second intersection showed a similar behaviour. The point of third intersection the behaviour was reversed. In stressed condition potential at the first intersection increased with increasing concentration of calcium nitrate, while in unstressed condition their was no systematic change. Similar behaviour was observed at the point of second intersection. Potential in unstressed and stressed condition at the point of third intersection

increased with increasing concentration of calcium nitrate.

The current density at the first intersection in unstressed condition was higher than in stressed condition. At second intersection it showed a similar behaviour except for 60% $Ca(NO_3)_2$, while in 80% $Ca(NO_3)_2$ it was unchanged. Current density at the third intersection showed a similar behaviour as for first intersection. Current density in unstressed and stressed condition at the first intersection increased with increasing concentration of calcium nitrate solution. Current density in unstressed and stressed condition at the second and third intersections it did not show any systematic change (Table 4.8).

4.5 MICROSTRUCTURE

Longitudinal cross-section of the As Received wire showed that the grains were elongated in axial direction (Fig.4.51). The microstructure also showed pearlite bands. In transverse cross-section the micrograph clearly showed the presence of martensitic needless (Fig. 4.51). Dark etching constituent which could be retained austenite was also observed at prior austenite grain boundaries.

The above observations, specially the presence of martensitic needless, indicate that the As Received wire was perhaps quenched after hot drawing and subsequently finished by cold drawing.

Annealing of the As Received wire at 800°C for 2 hours produced coarse pearlite structure (Fig. 4.52).

Isothermal transformation at 350°C (IT 350°C) for 15 minutes produced bainitic structure (Fig. 4.53). As the temperature for isothermal transformation was increased pearlite started to form, its amount increasing with increasing temperature and isothermal transformation, at 670°C (IT 670°C) for 10 minutes produced coarse pearlitic structure (Fig. 4.54 to 4.56).

Wires quenched from 780°C in brine and subsequently tempered for 1 hour and 4 hours for different temperatures showed tempered martensite. Tempering at 600°C for 1 and 4 hours produced completely spherodized cementite in the microstructure (Fig. 4.57 to 4.65).

4.6 FRACTOGRAPHY

Examination of the fracture surface of the As Received wire tested in air showed the fracture was predominantly intergranular ductile following the prior austenite grain boundaries (Fig. 4.66).

Factrographic examination of the specimen after stress corrosion test showed that in most cases the fracture surface was covered with thick layer of corrosion product and it was not possible to see the fine details.

As Received wire tested in 80% $CaNO_3$ showed that the fracture was intergranular with some evidence of transgranular cracking (Fig. 4.67a). On higher magnification some evidence of ductility on microscopic scale was formed (Fig. 4.67b).

QT 300°C (1 hr.) wire tested in 50% $Ca(NO_3)_2$ + 5% NH_4NO_3 at 100°C showed that stress corrosion cracking was predominantly intergranular with clean grain facets (Fig. 4.68).

Failure of Annealed wire in saturated H_2S solution was predominantly interganular cleavage type (Fig. 4.69).

Fracture surface of QT 500°C (1 hr.) wire tested in saturated H_2S solution that the cracking was intergranular with clean facets (Fig. 4.70).

4.7 GENERAL DISCUSSION

Nature of the potentiodynamic anodic polarization curve depends upon the environment and temperature. Anodic polarization curves for As Received, Annealed, Isothermally transformed and Quenched & Tempered prestressing steel wires in saturated H_2S solution at room temperature showed only active behaviour. During reverse scan the polarization curve almost overlapped the curve obtained during forward scan. There was only little difference in $E_{corr.}$ obtained during forward and reverse scan.

For isothermally transformed wires $E_{corr.}$ in stressed condition was alway more noble than in unstressed condition except for IT 350 wire, the difference between the two increased with increasing transformation temperature. The curve for time to failure versus isothermal transformation temperature appear to consist of two sections of different slopes. The change in slope appears approximately where the difference in $E_{corr.}$ in unstressed and stressed condition was minimum (Fig. 4.4).

For prestressing steel wires quenched and tempered for 1 hour similar behaviour was observed, the change in slope in time to failure versus tempering temperature occuring where the difference in $E_{corr.}$ in unstressed and stressed condition was minimum. However, for wires tempered for 4 hours this correlation was not observed.

$E_{corr.}$ for isothermally transformed wires in stressed condition in 50% $Ca(NO_3)_2$ + 5% NH_4NO_3 solution was different than $E_{corr.}$ in unstressed condition. The time to failure versus isothermal transformation curve showed that it was made-up of three sections of different slopes. The change in slope occured almost where the difference in $E_{corr.}$ in unstressed and stressed condition was either maximum or minimum (Fig. 4.23). This is similar to the correlation observed for isothermally transformed and quenched and tempered for 1 hour wires tested in saturated H_2S solution.

Prestressing steel wire quenched and tempered for 1 hour showed similar correlation. However, for wires tempered for 4 hours no such correlation was observed (Fig. 4.24).

No correlation between the area of the anodic loop (Fig. 4.42) and time to failure in 50% $Ca(NO_3)_2$ + 5% NH_4NO_3 could be observed for isothermally transformed and quenched & tempered wires (Fig. 4.23 & 4.24).

Time to failure versus concentration of $Ca(NO_3)_2$ solution curve was composed of two section of different slopes. The change in slope was, however, not reflected in change in $E_{corr.}$ in unstressed and stressed conditions as had been observed for isothermally transformed and quenched & tempered for 1 hour wires in saturated H_2S and 50% $Ca(NO_3)_2$ + 5% NH_4NO_3 solution (Fig. 4.43).

The difference in the area of the anodic loops in unstressed and stressed condition was minimum at around 60% $Ca(NO_3)_2$ concentration (Fig. 4.50) which almost coincides with the concentration at which a change in slope in time to failure curve was observed (Fig. 4.43).

Resistance of quenched & tempered wires to stress corrosion cracking in saturated H_2S solution was lowest as compared to As Received, annealed and isothermally transformed wires except IT 325 wire (Fig. 4.71). The resistance of As Received wire to stress corrosion cracking, as indicated by time to failure, was much inferior to isothermally transformed and annealed wires.

In 50% $Ca(NO_3)_2$ + 5% NH_4NO_3 solution quenched & tempered and isothermally transformed wires had similar resistance to stress corrosion cracking except for IT 350 & IT 425 wires which were less resistant and IT 670 wires which were more resistant than QT wires of equivalent strength (Fig. 4.72). As Received wire has intermediate strength whereas annealed wire had maximum strength to stress corrosion cracking.

Comparatively poor resistance of As Received,which is generally in cold drawn condition, compared to isothermally transformed wire in saturated H_2S and 50% $Ca(NO_3)_2$ + 5% NH_4NO_3 solution observed in this investigation since several investigators have observed the reverse trend. This may perhaps be attributed to the observed presence of retained austenite and martensite in the microstructure.

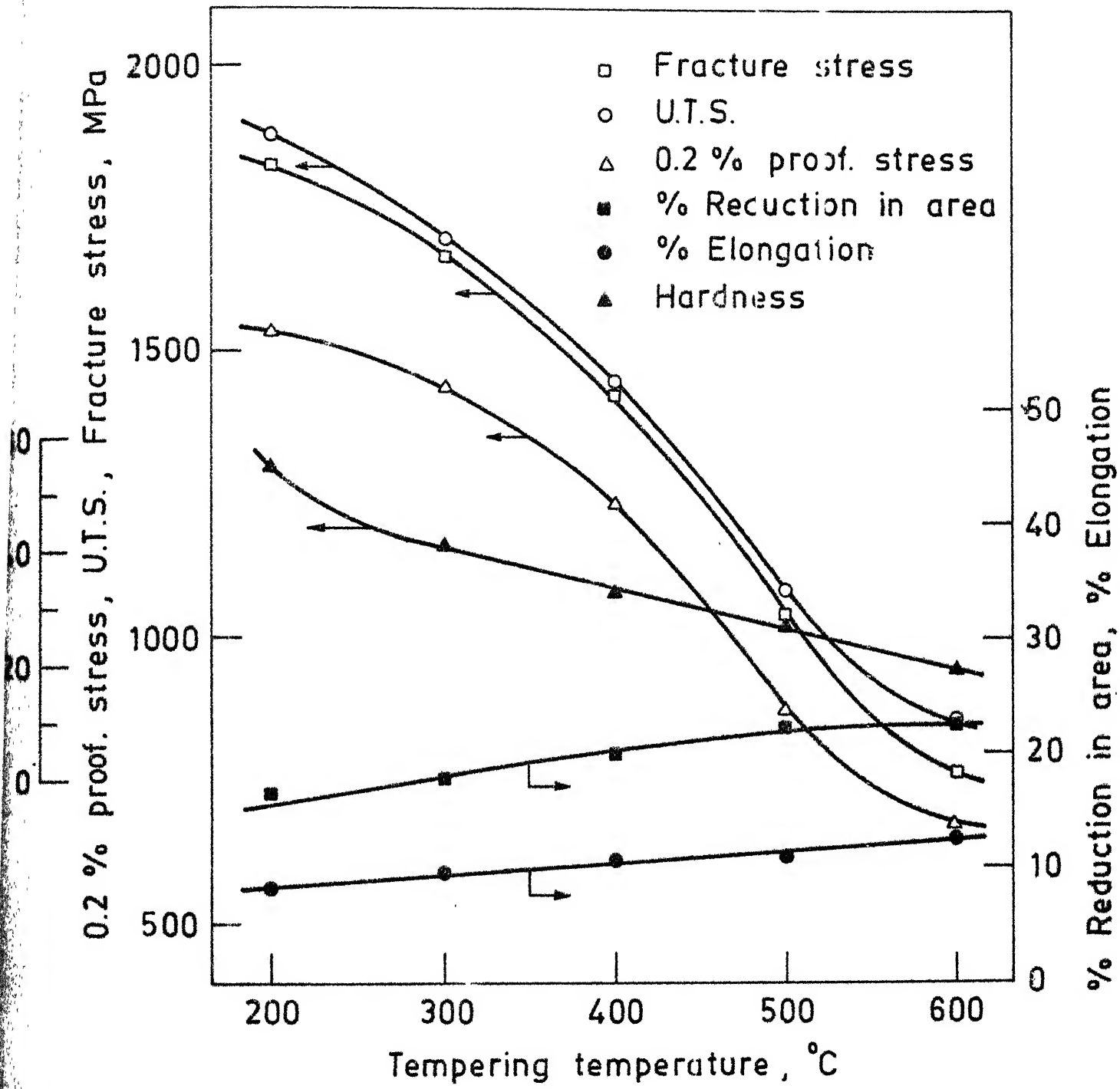

Fig. 4.1. Mechanical properties of prestressing steel wires quenched and tempered for 1 hour at various temperatures.

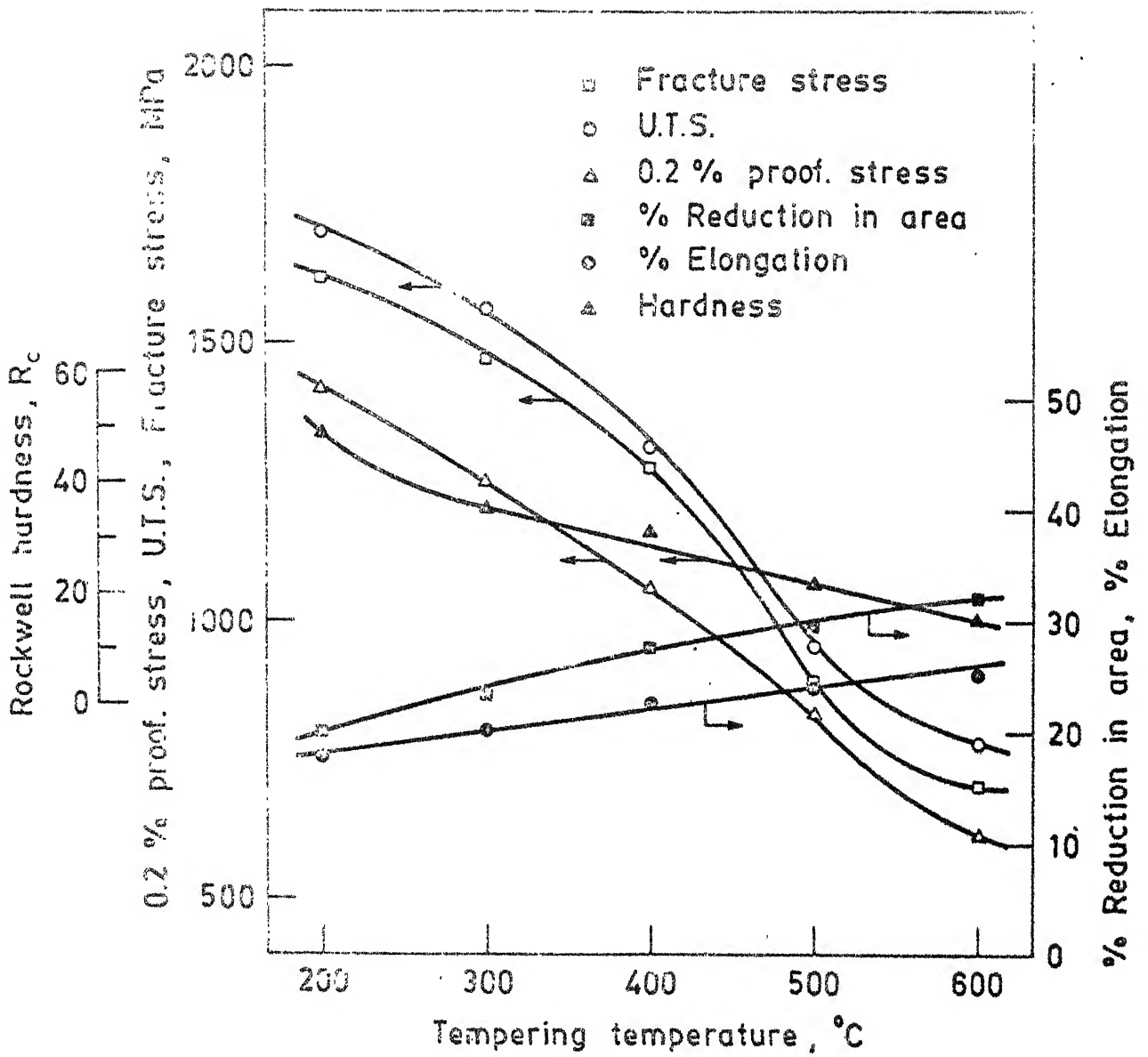

Fig. 4.2 Mechanical properties of prestressing steel wires quenched and tempered for 4 hours at various temperatures.

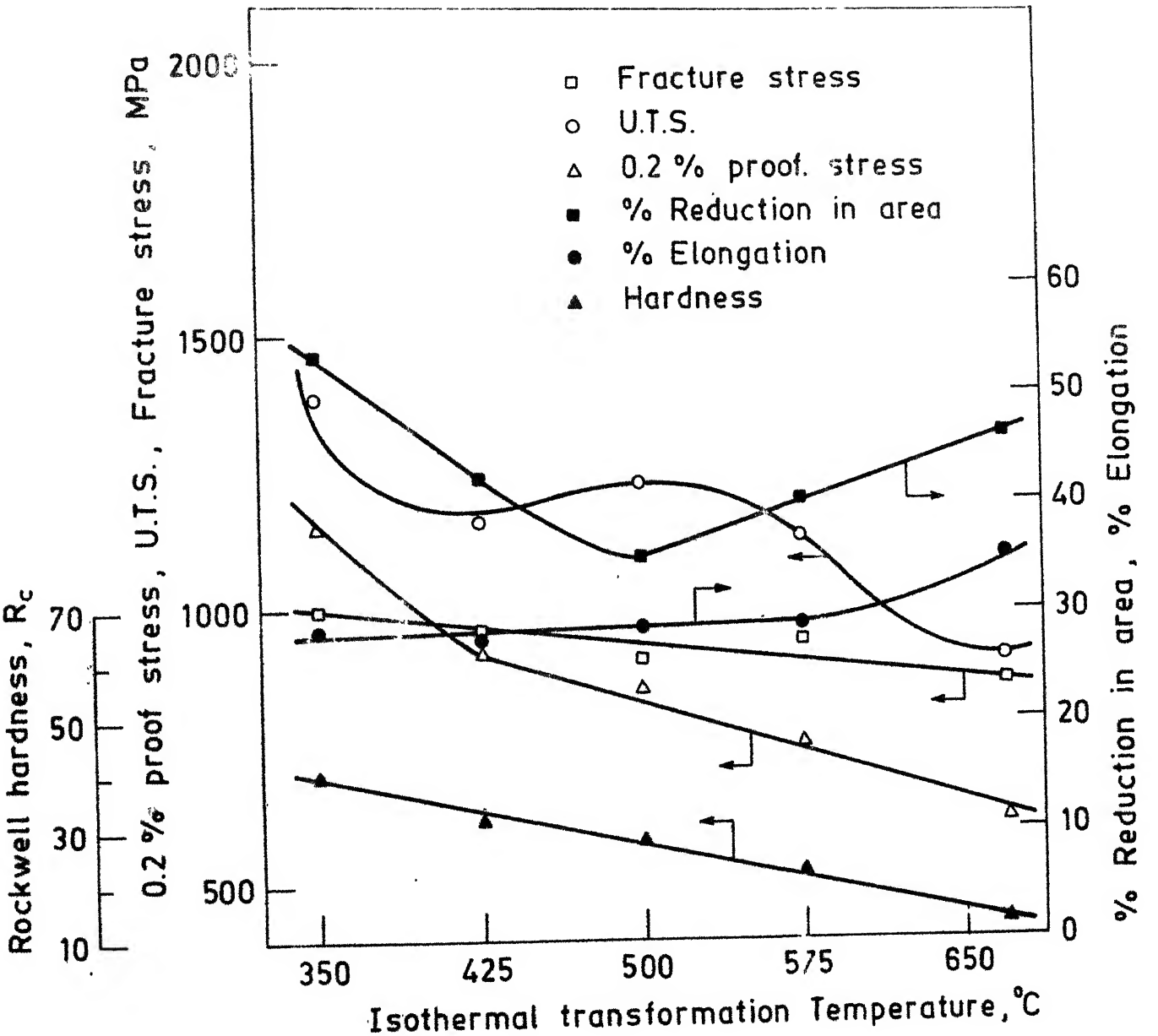

Fig. 4.3. Mechanical properties of prestressing steel wires isothermally transformed at various temperatures.

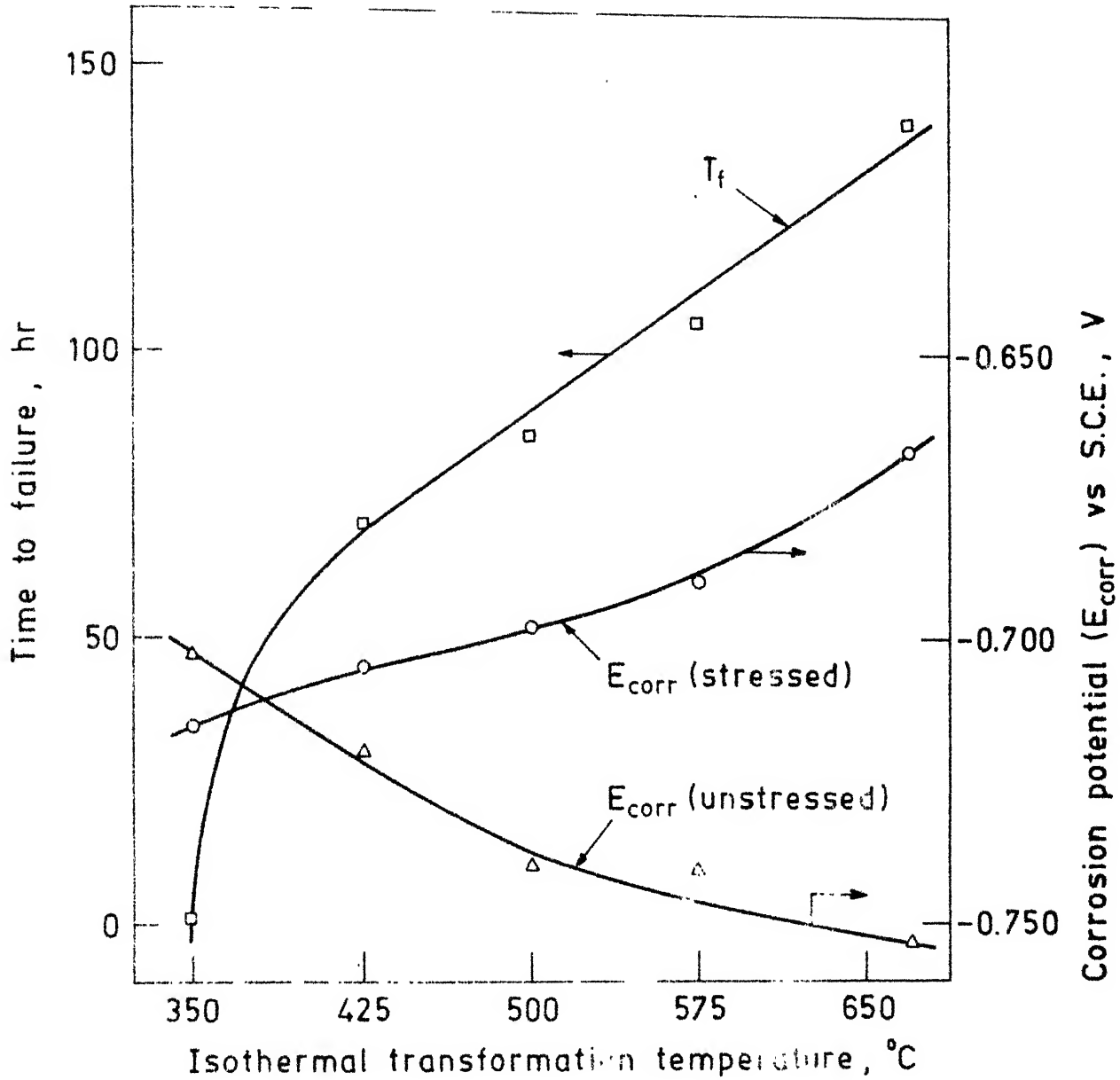

Fig. 44 Effect of isothermal transformation temperature on time to failure (T_f) and corrosion potential (E_{corr}) of unstressed and stressed prestressing steel wires exposed to sat. H_2S solution.

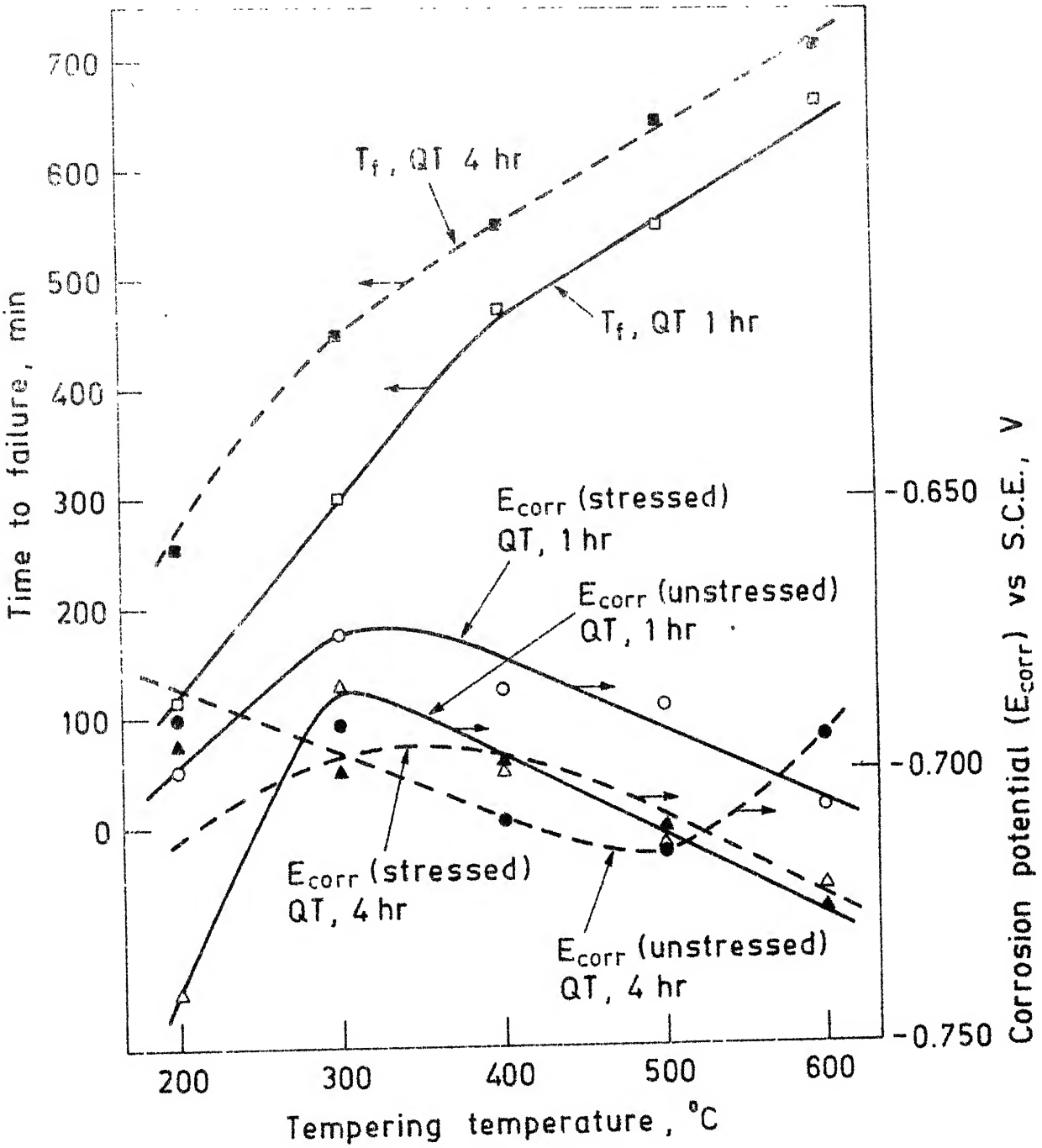

Fig. 4.5. Effect of tempering temperature and time on time to failure (T_f) and corrosion potential (E_{corr}) of unstressed and stressed prestressing steel wires exposed to sat. H_2S solution.

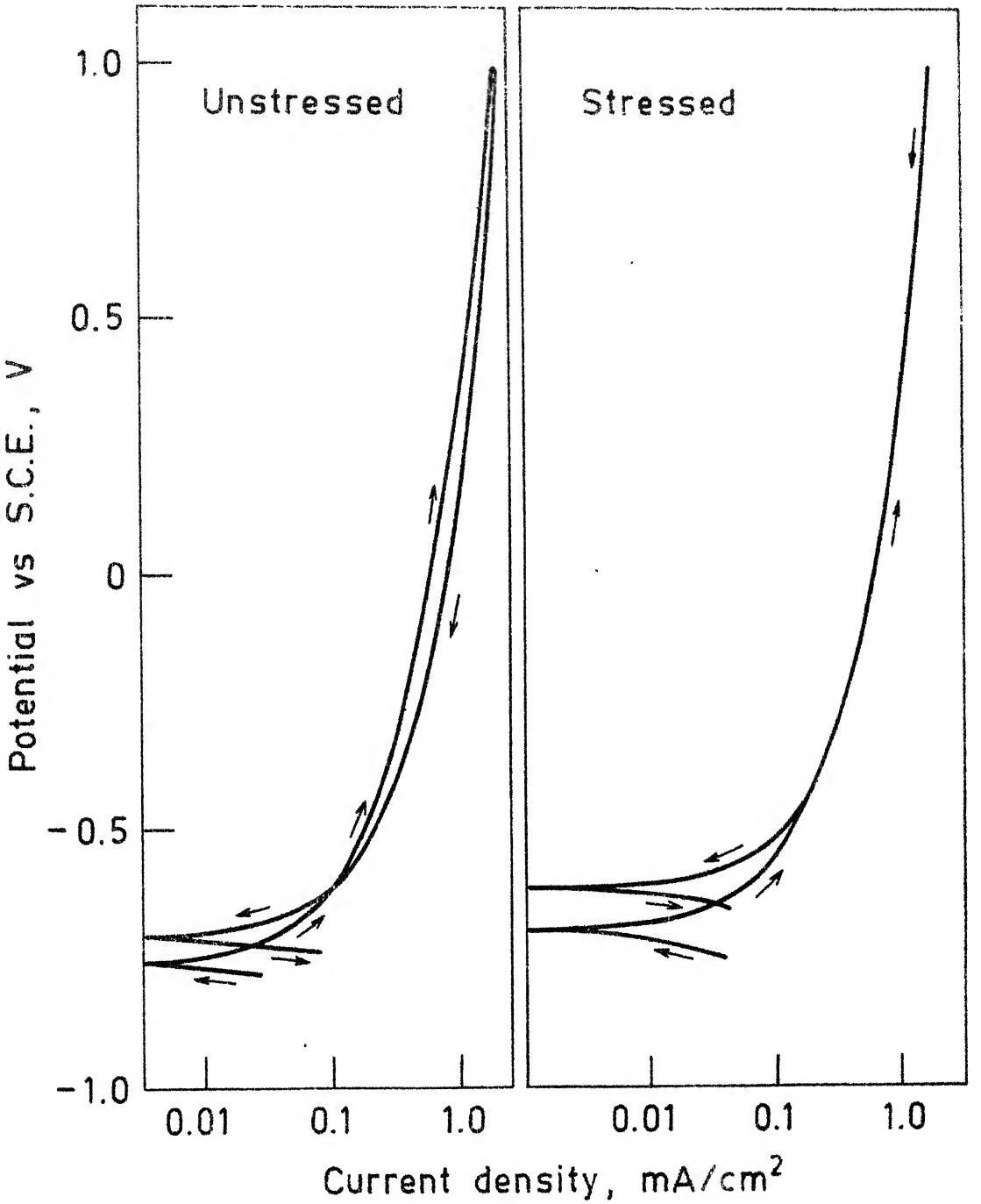

Fig. 4.6. Anodic polarization curves for unstressed and stressed prestressing steel (as received) wires in sat. H_2S solution.

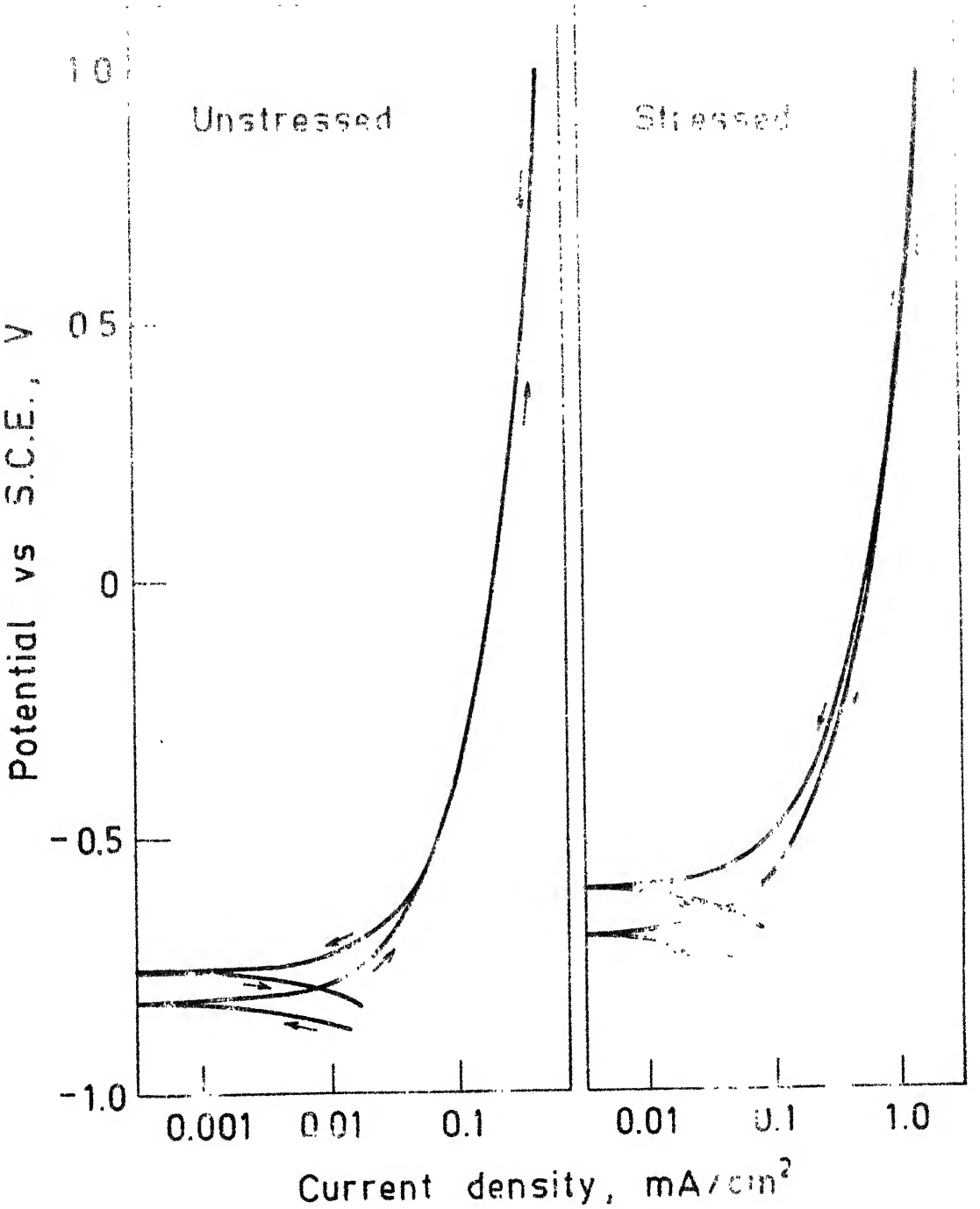

Fig 4.7. Anodic polarization curves for unstressed and stressed prestressing steel (annealed) wires in sat. H_2S solution.

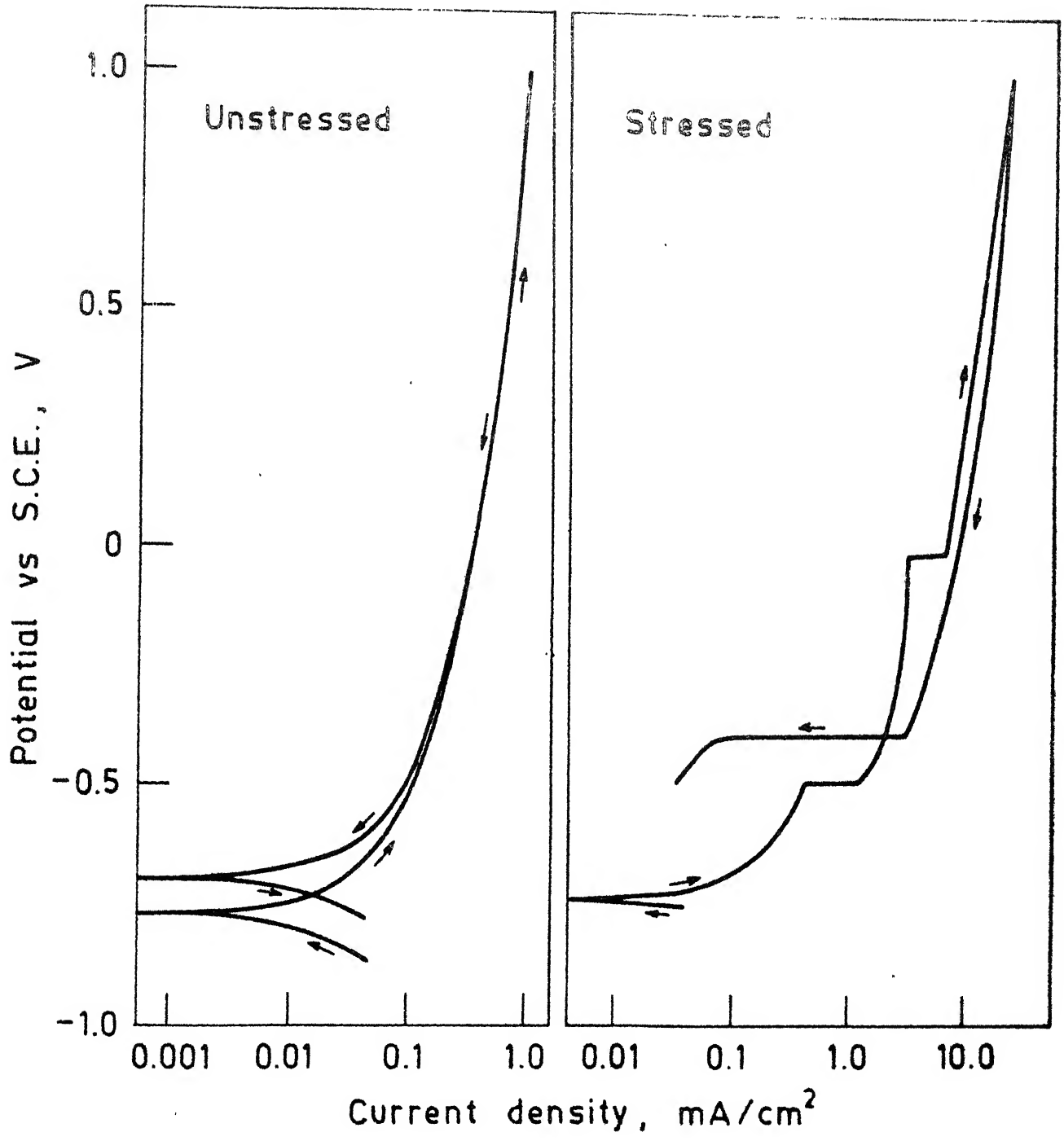

Fig. 4.8. Anodic polarization curves for unstressed and stressed prestressing steel (IT 350 °C) wires in sat. H_2S solution.

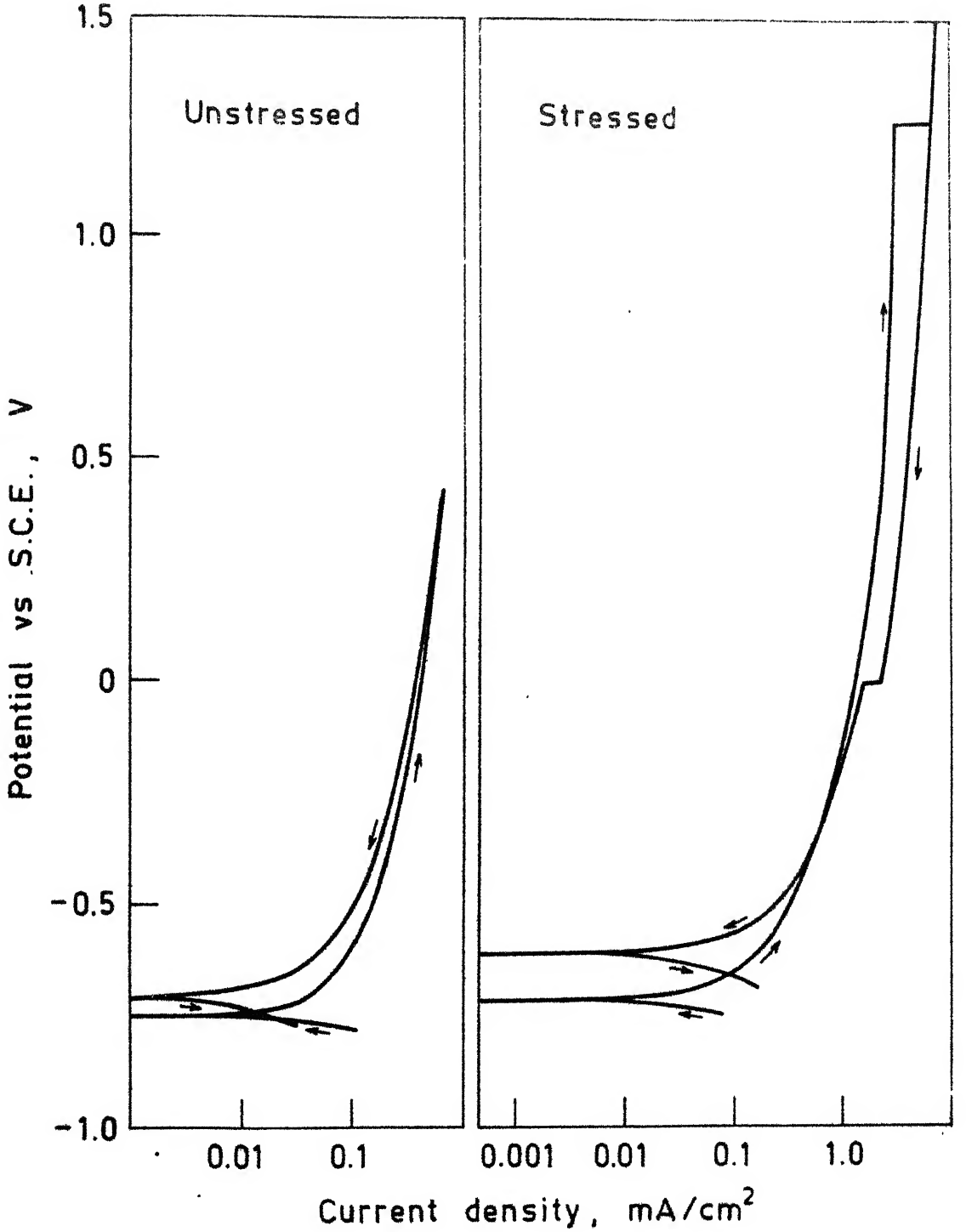

Fig. 4.9. Anodic polarization curves for unstressed and stressed prestressing steel (IT 425°C) wires in sat. H_2S solution.

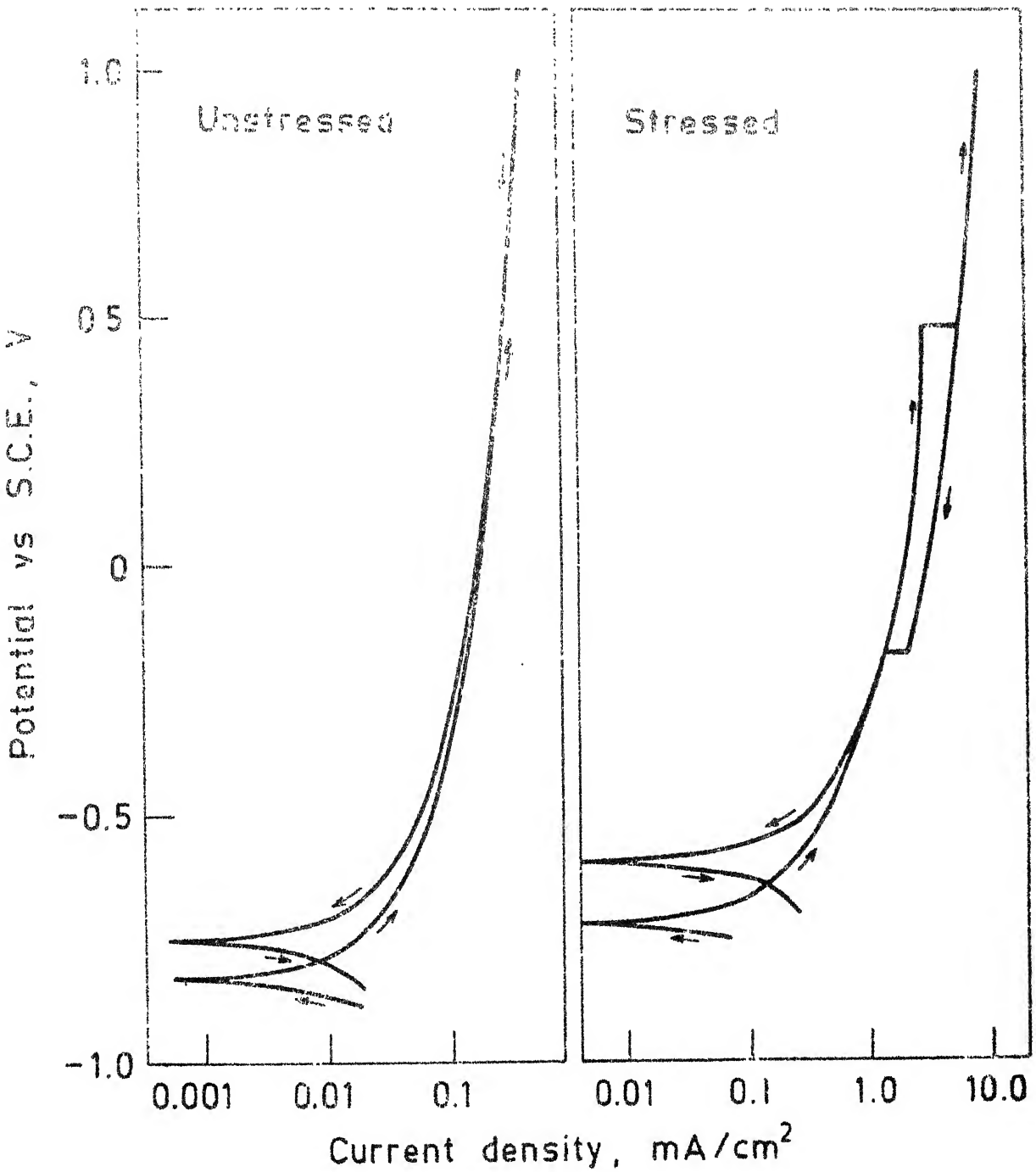

Fig. 4.10. Anodic polarization curves for unstressed and stressed prestressing steel (IT 500°C) wires in sat. H_2S solution.

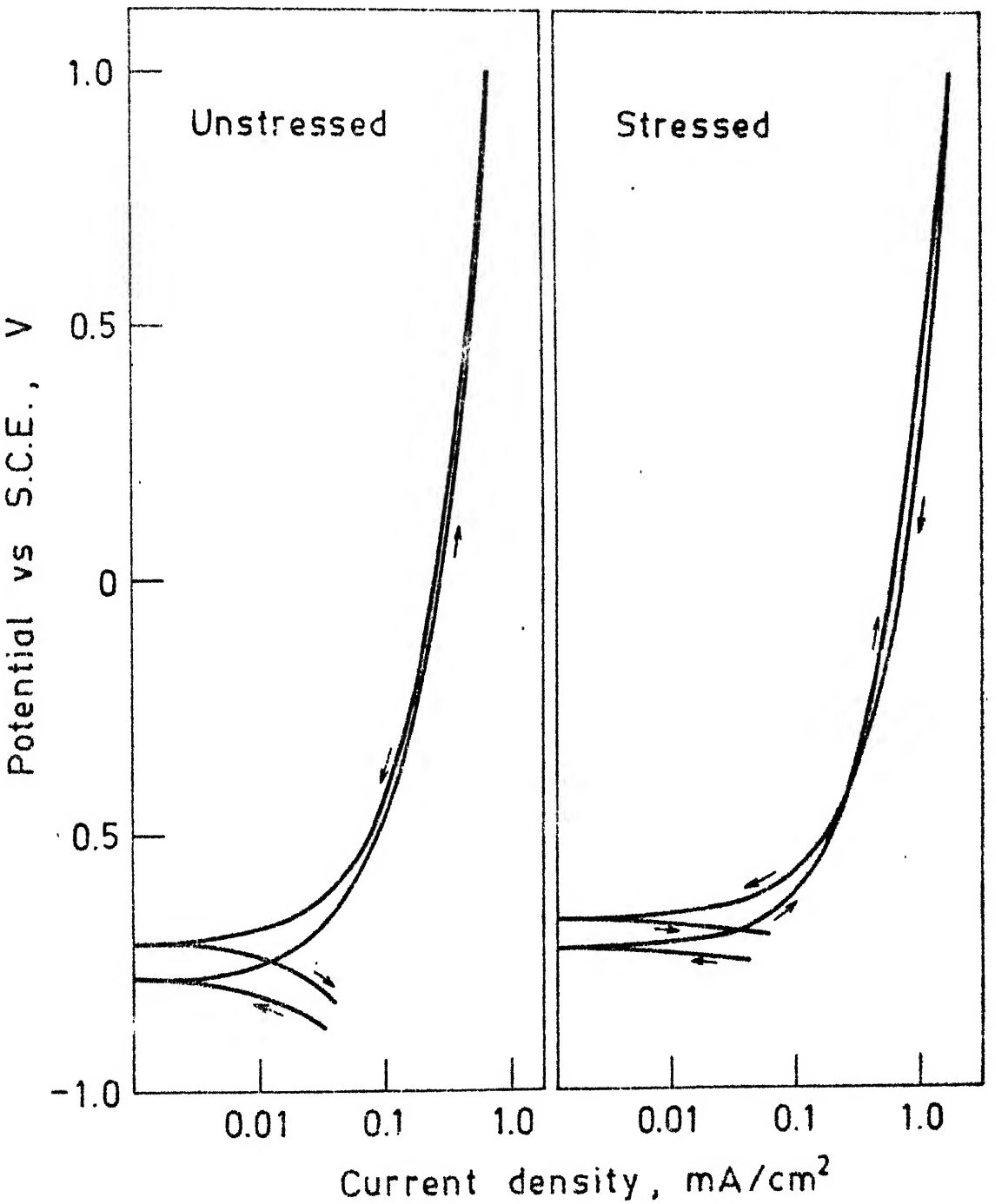

Fig. 4.11. Anodic polarization curves for unstressed and stressed prestressing steel (IT 575°C) wires in sat. H_2S solution.

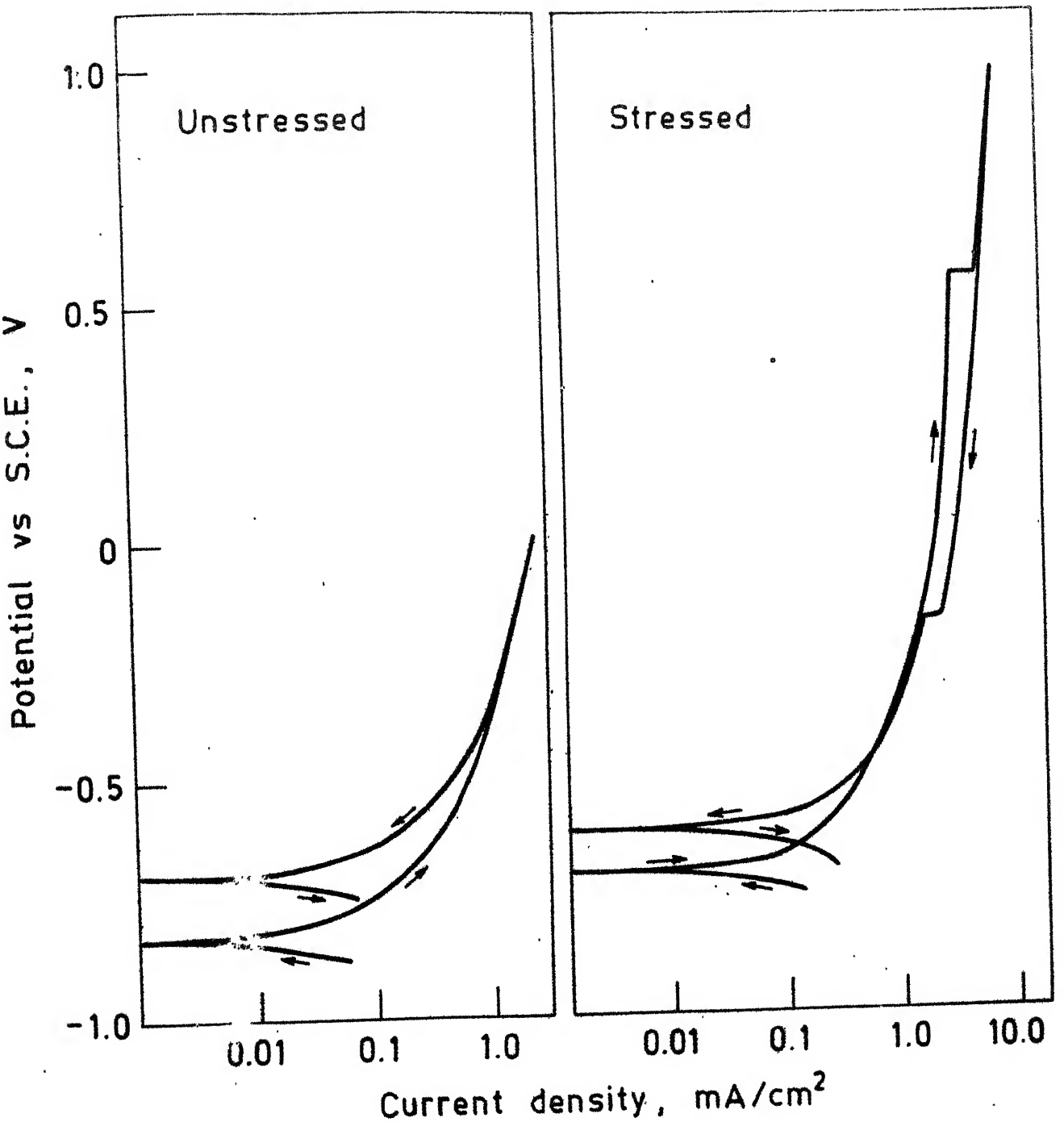

Fig. 4.12. Anodic polarization curves for unstressed and stressed prestressing steel (IT 670°C) wires in sat. H_2S solution.

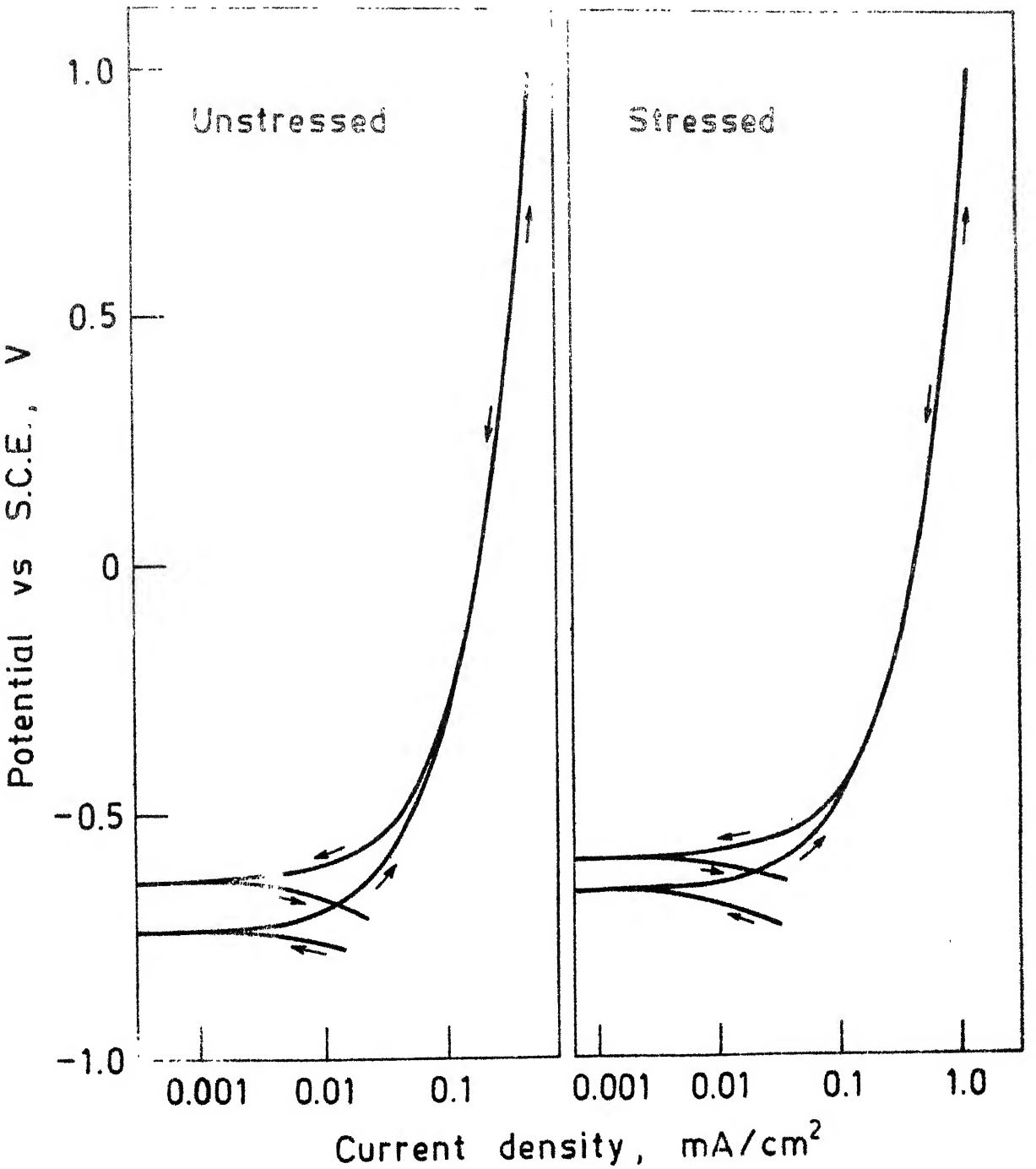

Fig. 4.13. Anodic polarization curves for unstressed and stressed prestressing steel (QT 200° C, 1 hr) wires in sat. H_2S solution.

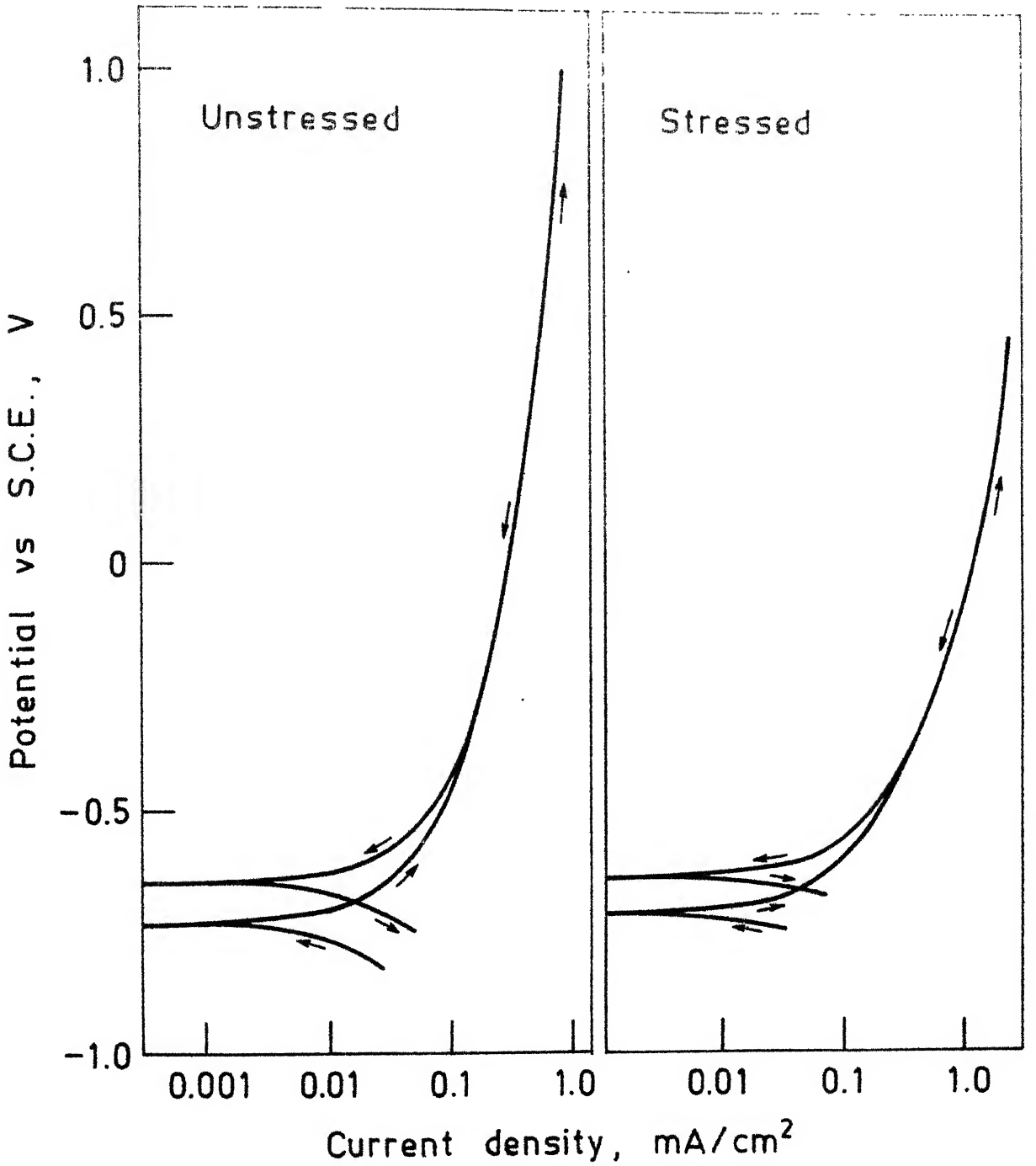

Fig. 4.14. Anodic polarization curves for unstressed and stressed prestressing steel (QT 300° C, 1 hr) wires in sat. H_2S solution.

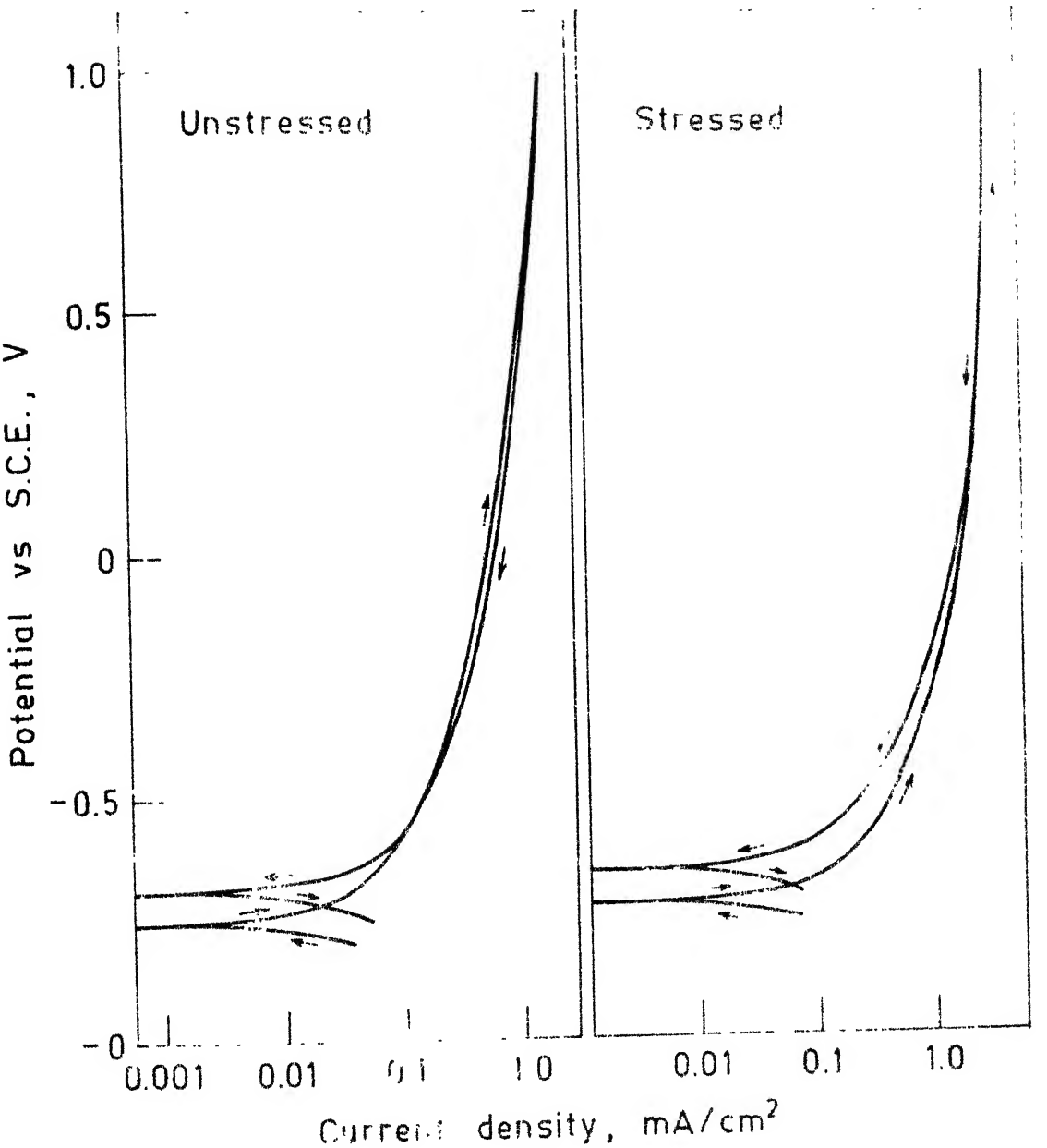

Fig. 4.15. Anodic polarization curves for unstressed and stressed prestressing steel (QT 400° C, 1 hr) wires in sat. H_2S solution.

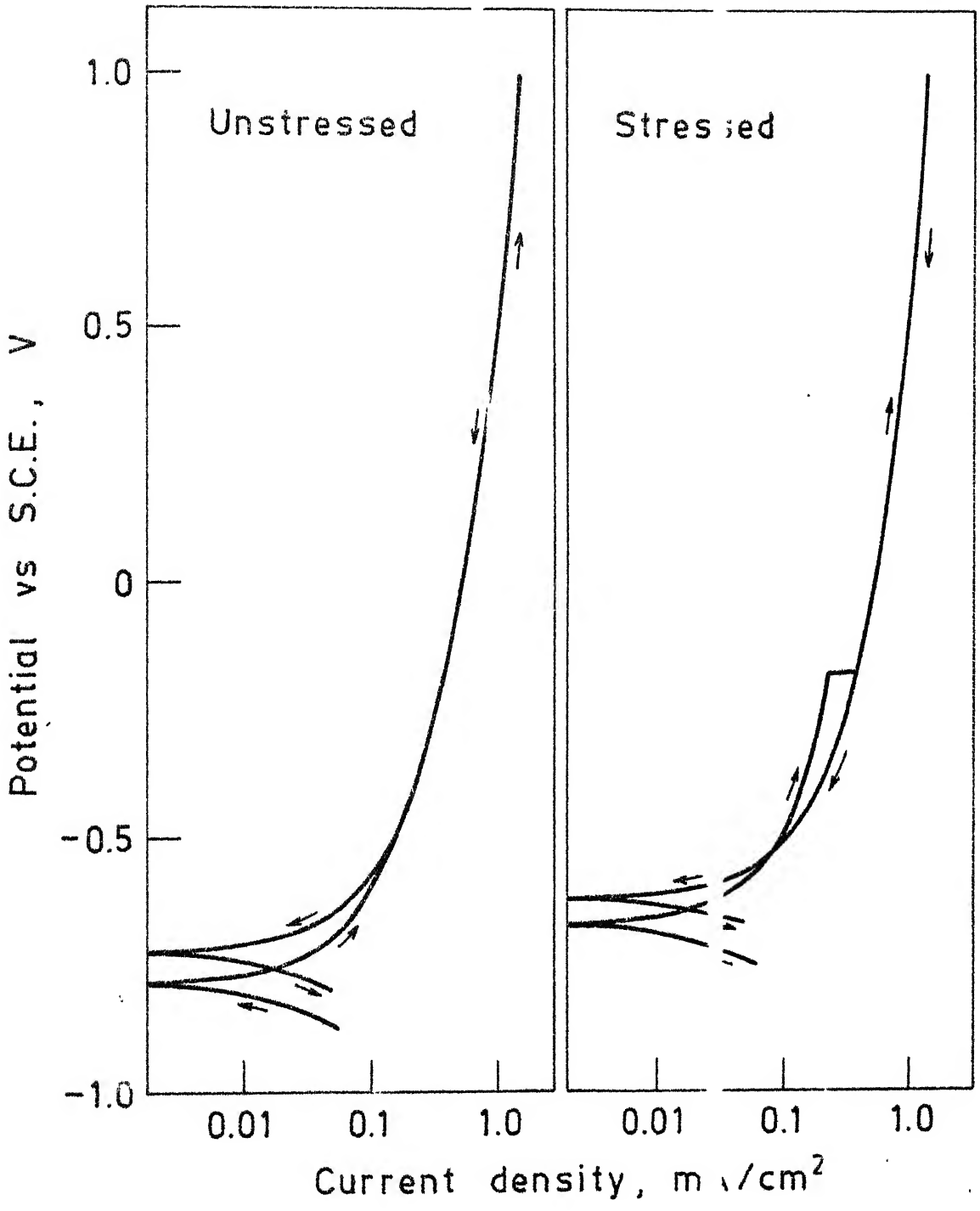

Fig. 4.16. Anodic polarization curves for unstressed and siressed prestressing teel (QT 500°C, 1 hr) wires in sat. H_2S so ution.

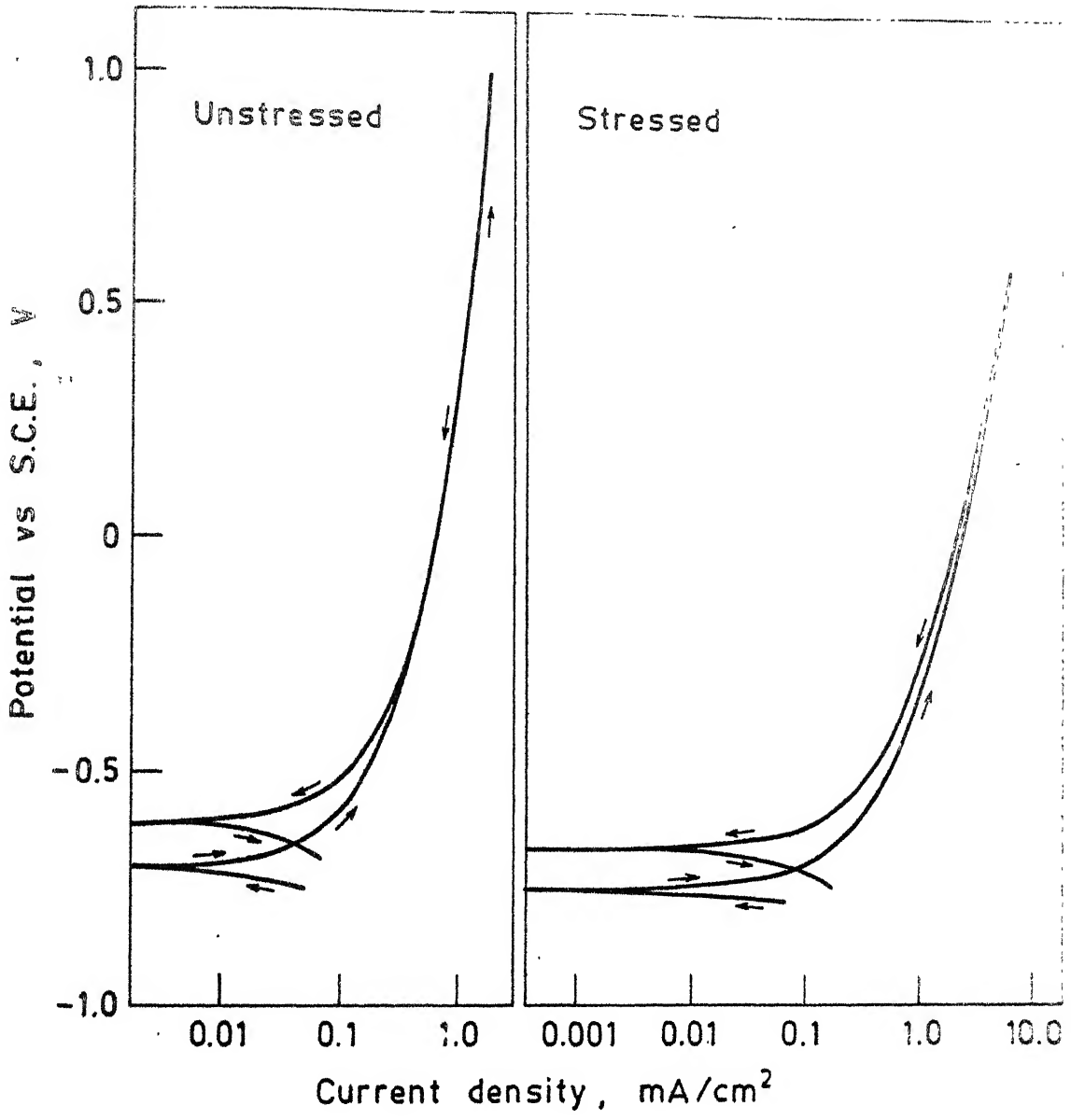

Fig. 4.17. Anodic polarization curves for unstressed and stressed prestressing steel (QT 600°C, 1 hr) wires in sat. H_2S solution.

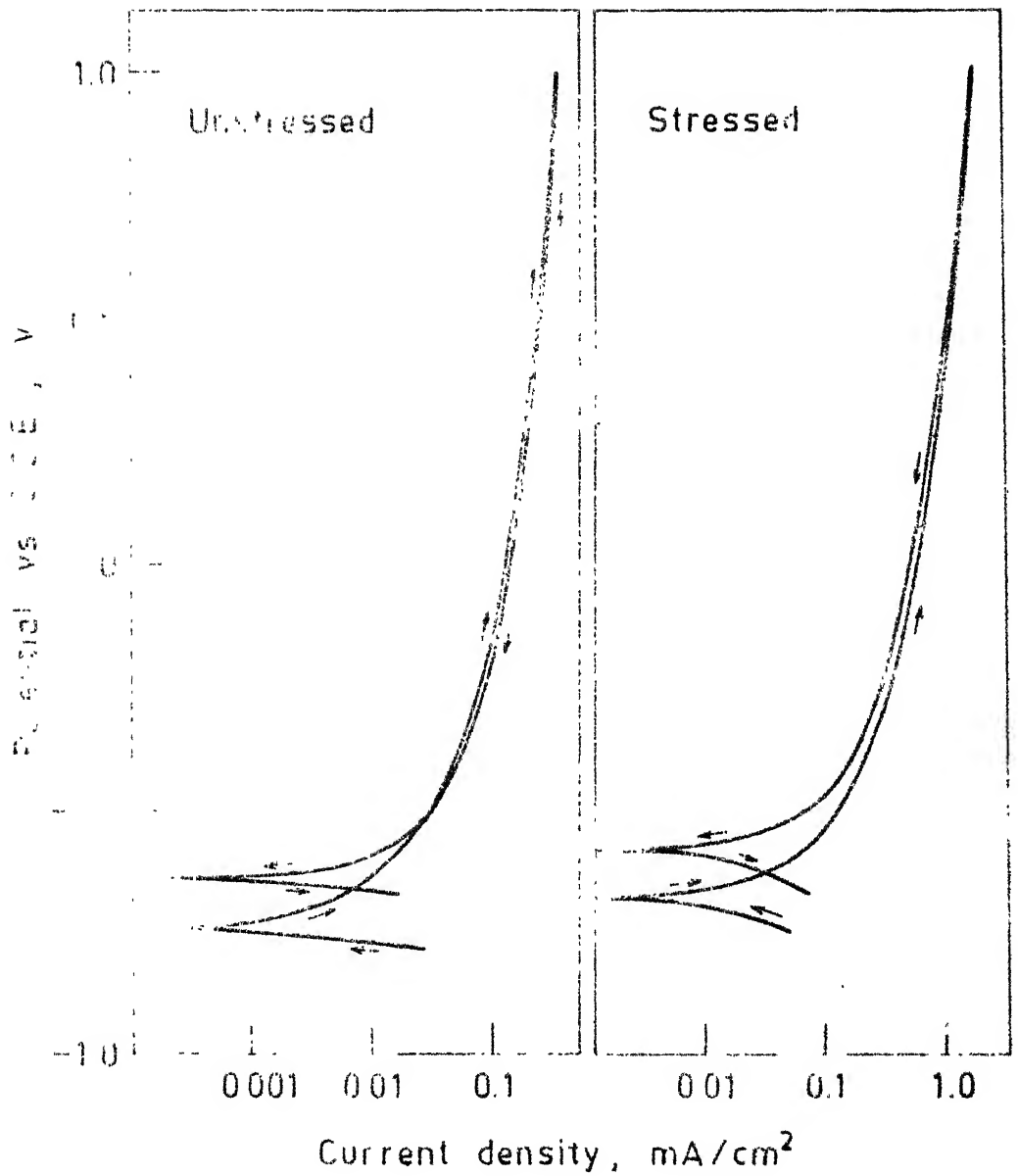

Fig. 4.18 Anodic polarization curves for unstressed and stressed prestressing steel (QT 200°C, 4 hr) wires in sat. H_2S solution.

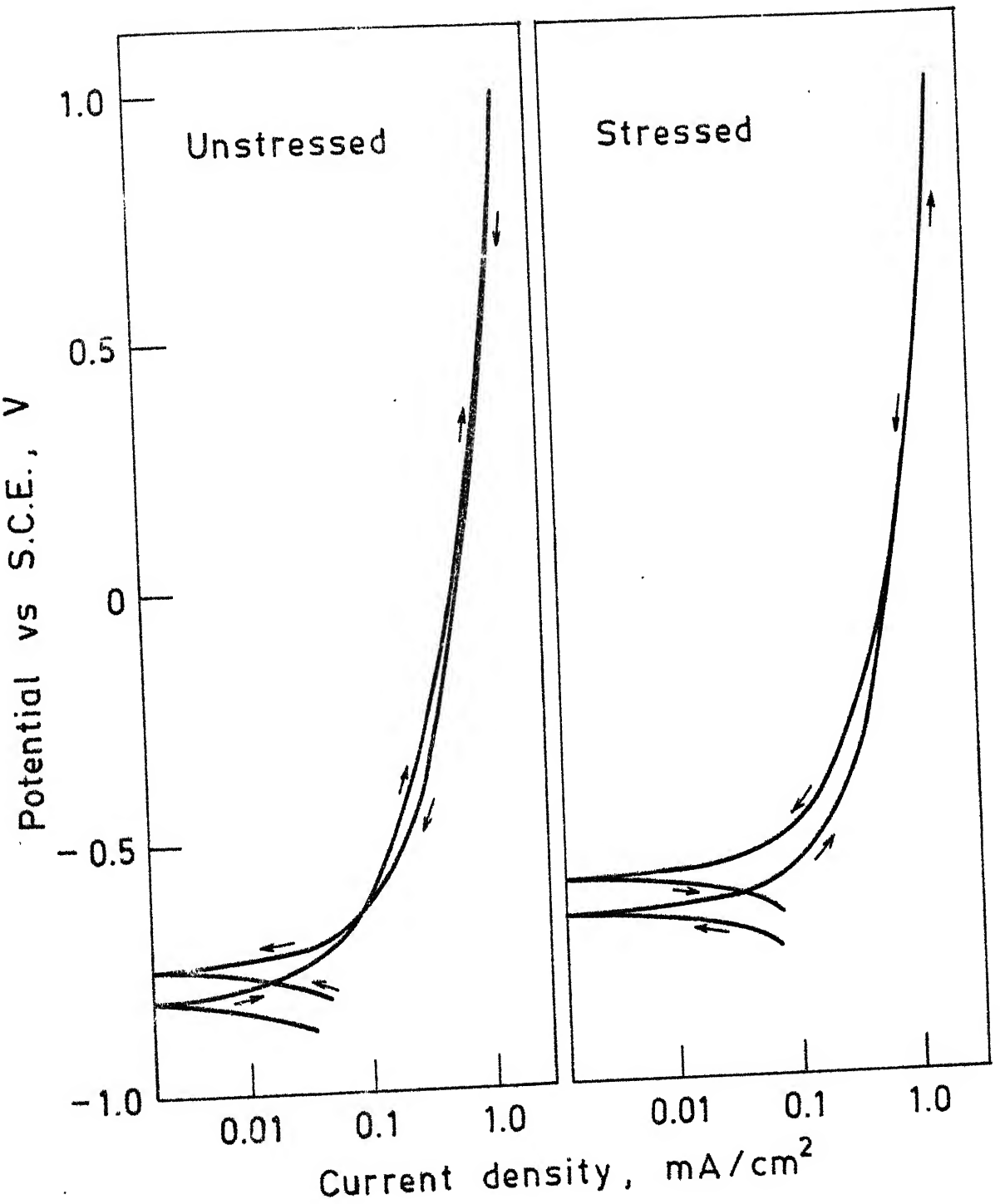

Fig. 4.19. Anodic polarization curves for unstressed and stressed prestressing steel (QT 300° C, 4 hr) wires in sat. H_2S solution.

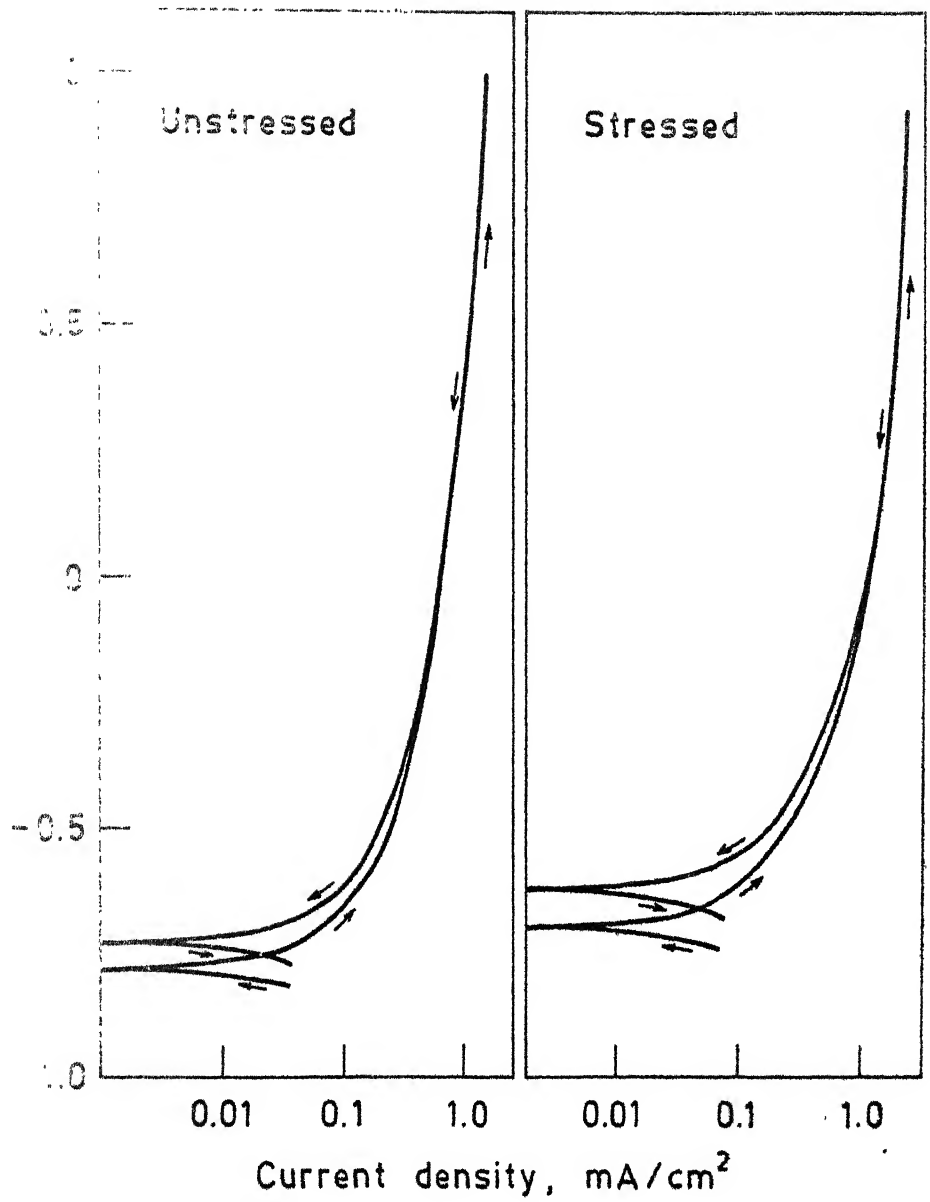

Fig 4.20. Anodic polarization curves for unstressed and stressed prestressing steel (QT 400°C, 4 hr) wires in sat. H_2S solution.

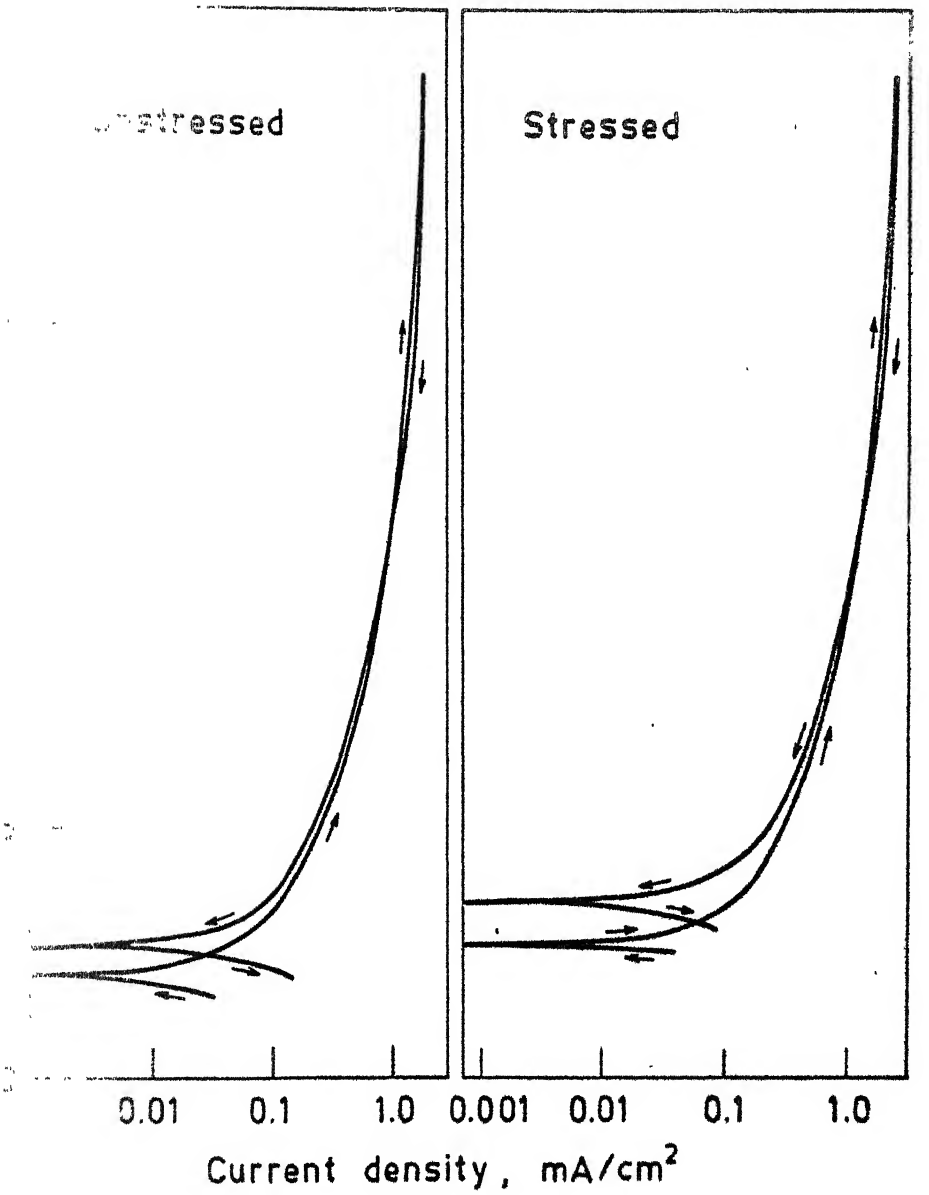

Anodic polarization curves for unstressed and stressed prestressing steel (QT 500°C, 4 hr) wires in sat. H_2S solution.

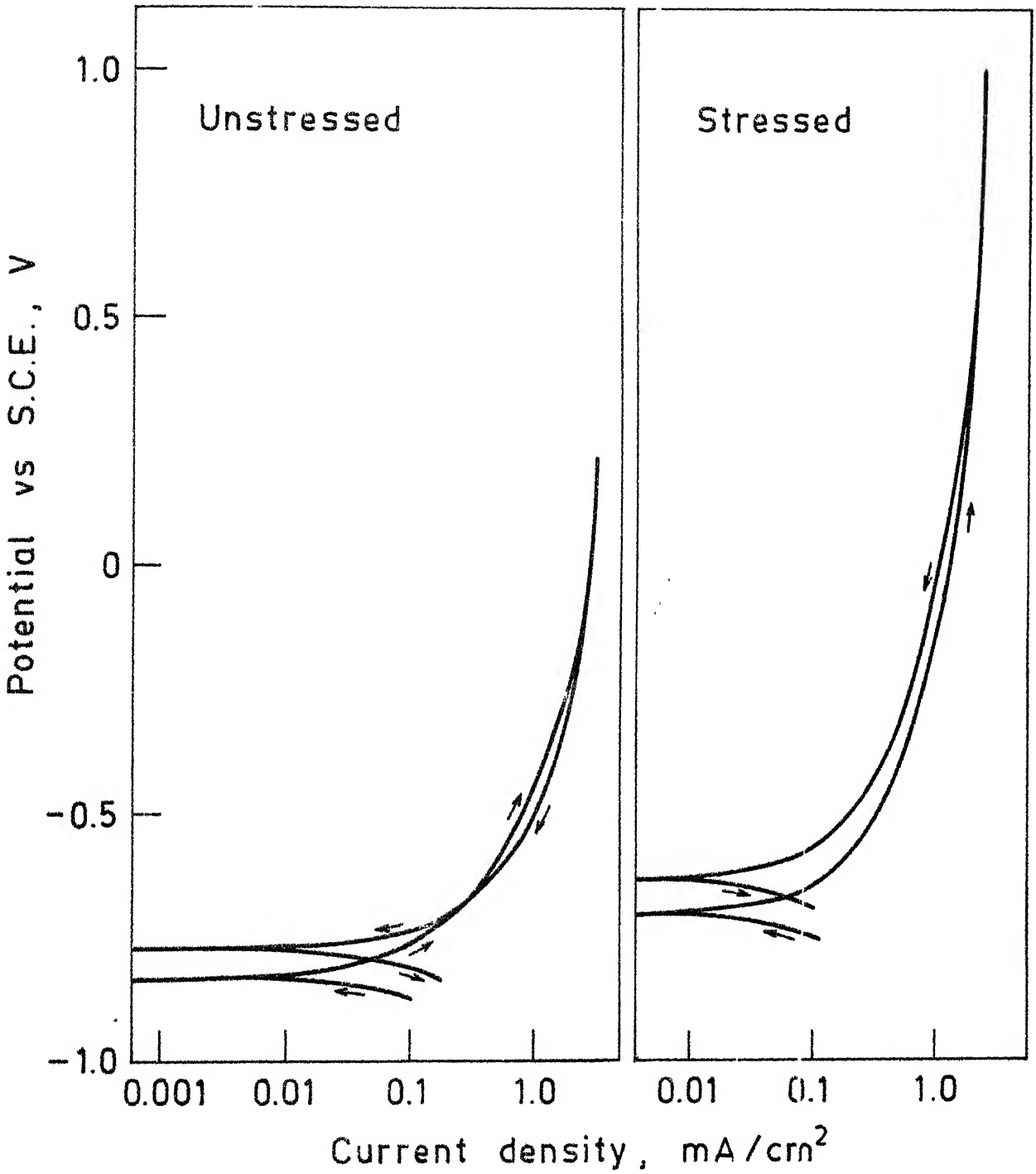

Fig. 4.22. Anodic polarization curves for unstressed and stressed prestressing steel (QT 600° C, 4 hr) wires in sat. H_2S solution.

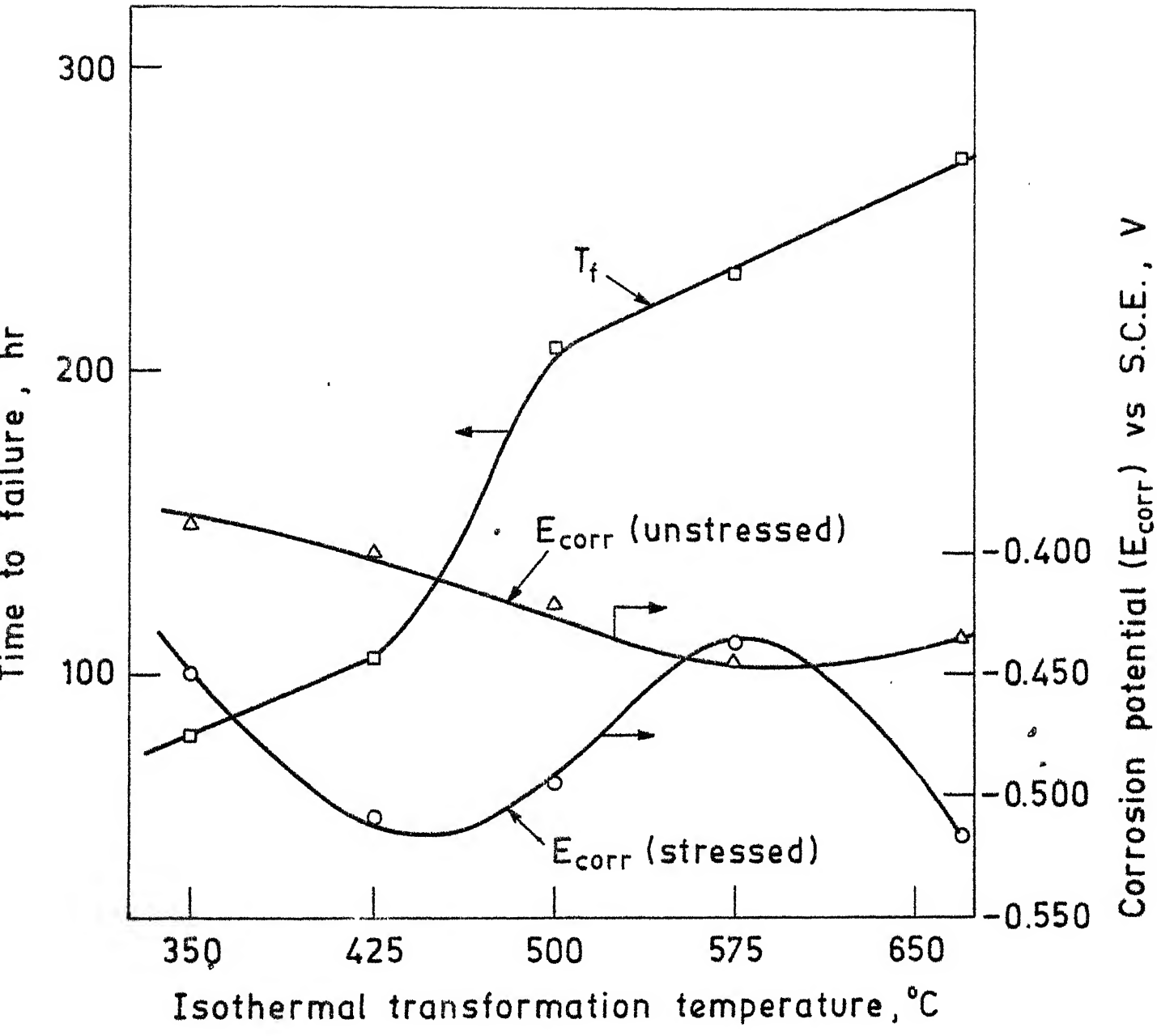

. 4.23. Effect of isothermal transformation temperature on time to failure (T_f) and corrosion potential (E_{corr}) of unstressed and stressed prestressing steel wires exposed to 50 % $Ca(NO_3)_2$ + 5 % NH_4NO_3 solution at 100 °C.

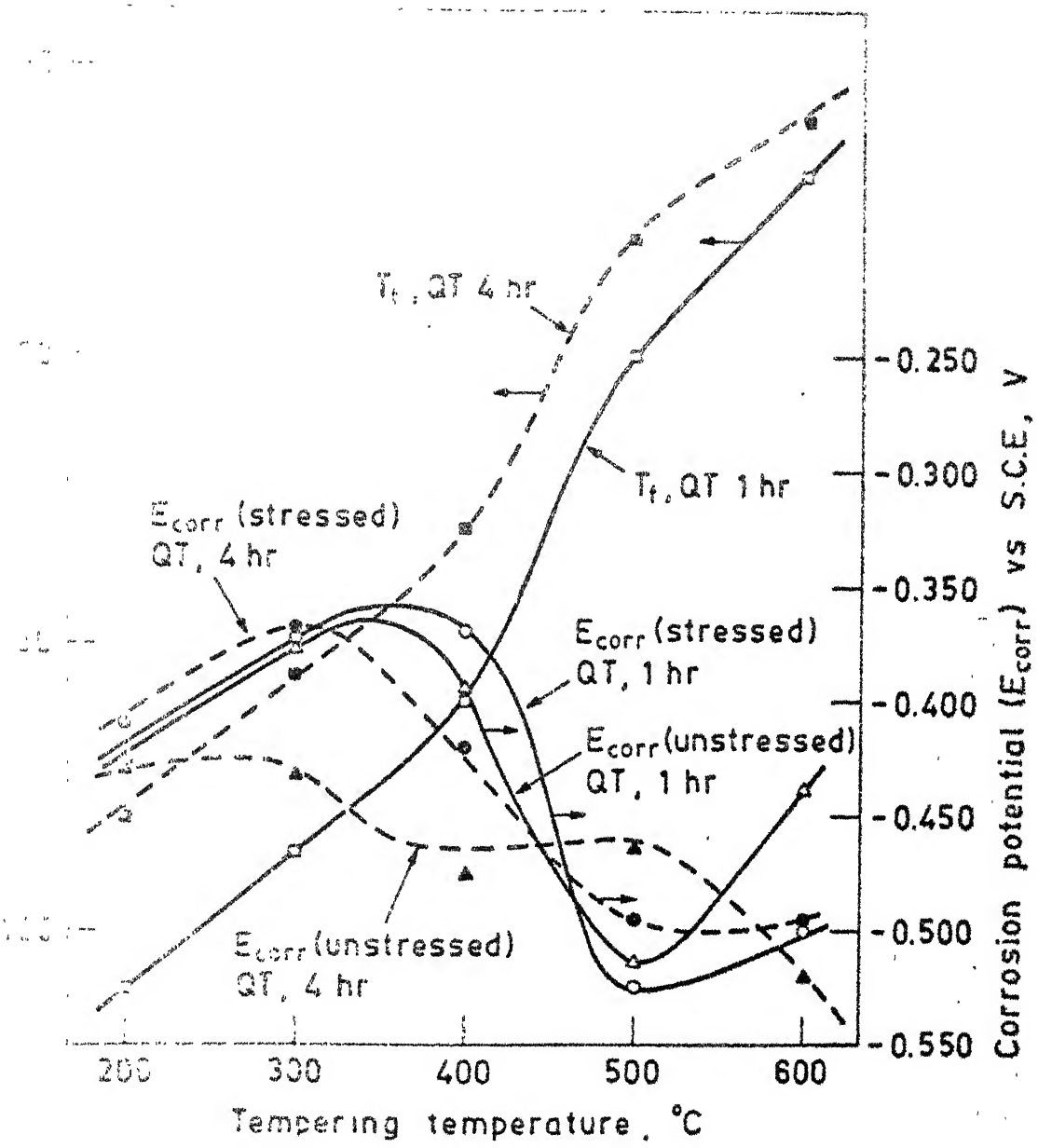

Effect of tempering temperature and time on time to failure (T_f) and corrosion potential (E_{corr}) of unstressed and stressed prestressing steel wires exposed to 50 % $Ca(NO_3)_2$ + 5 % NH_4NO_3 solution at 100 °C.

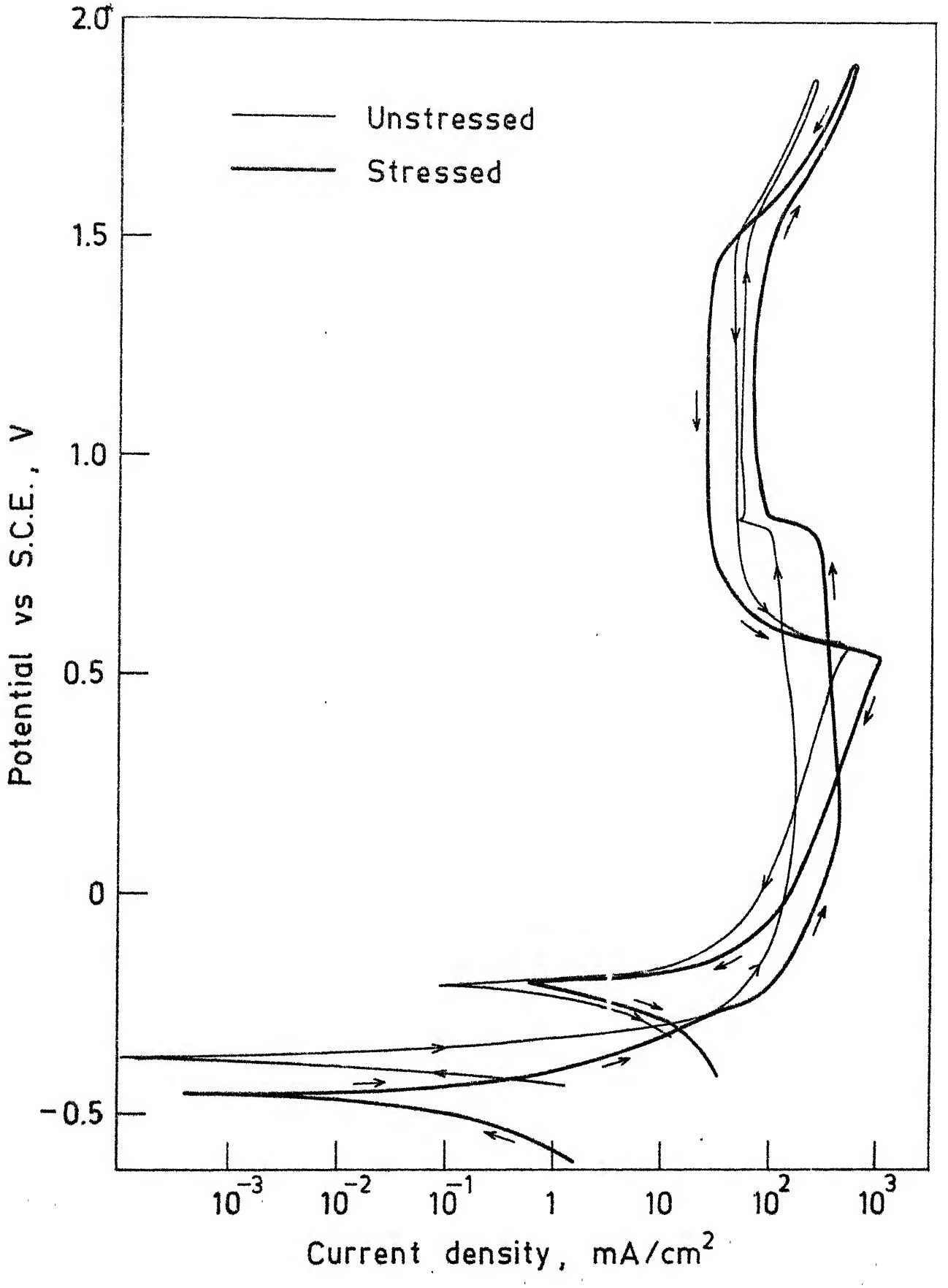

Fig. 4.25. Anodic polarization curves for unstressed and prestressing steel (as received) wires $Ca(NO_3)_2$ + 5 % NH_4NO_3 solution.

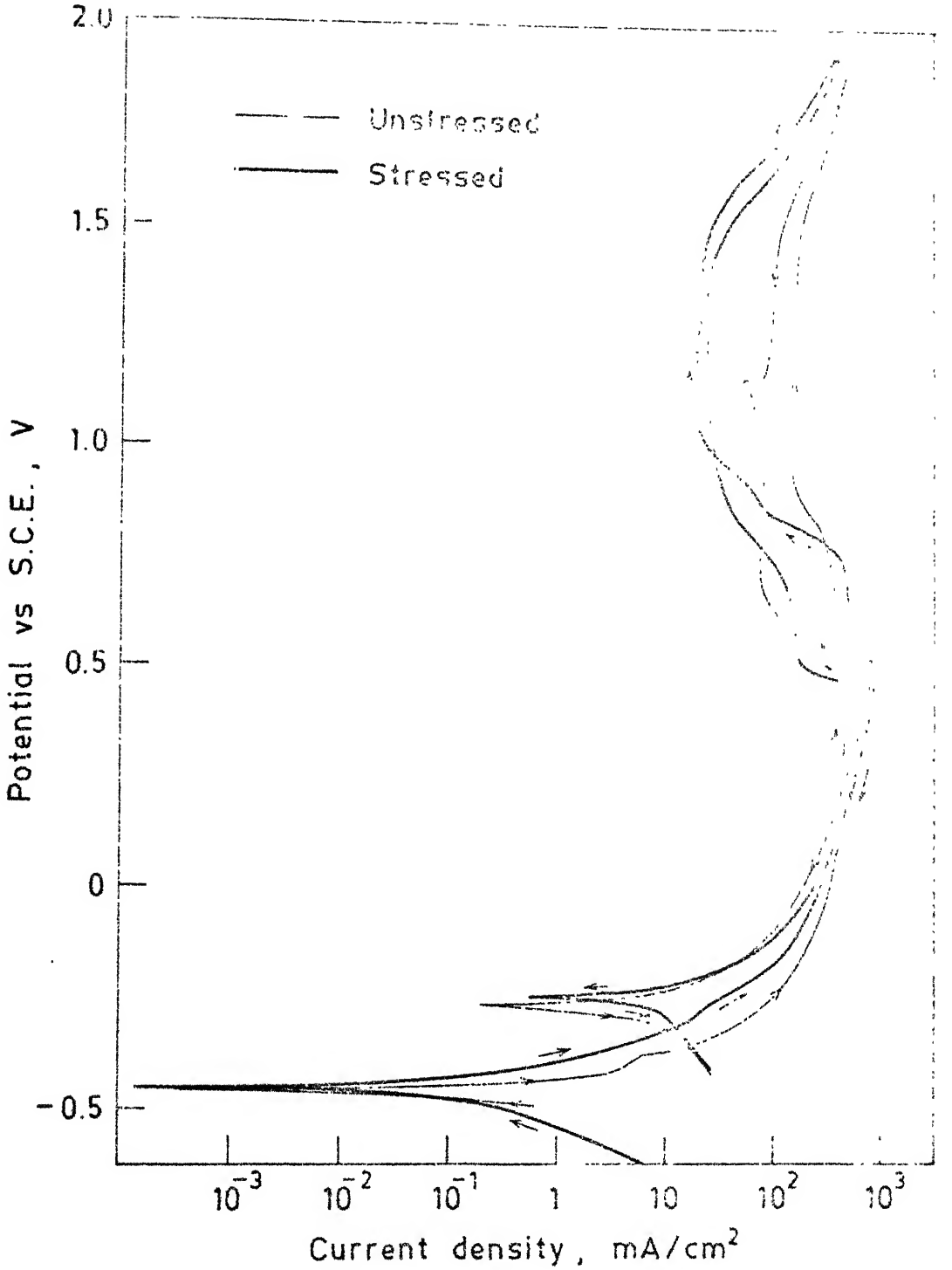

Fig. 4.26. Anodic polarization curves for unstressed and stressed prestressing steel (annealed) wires in 50 % $Ca(NO_3)_2$ + 5 % NH_4NO_3 solution.

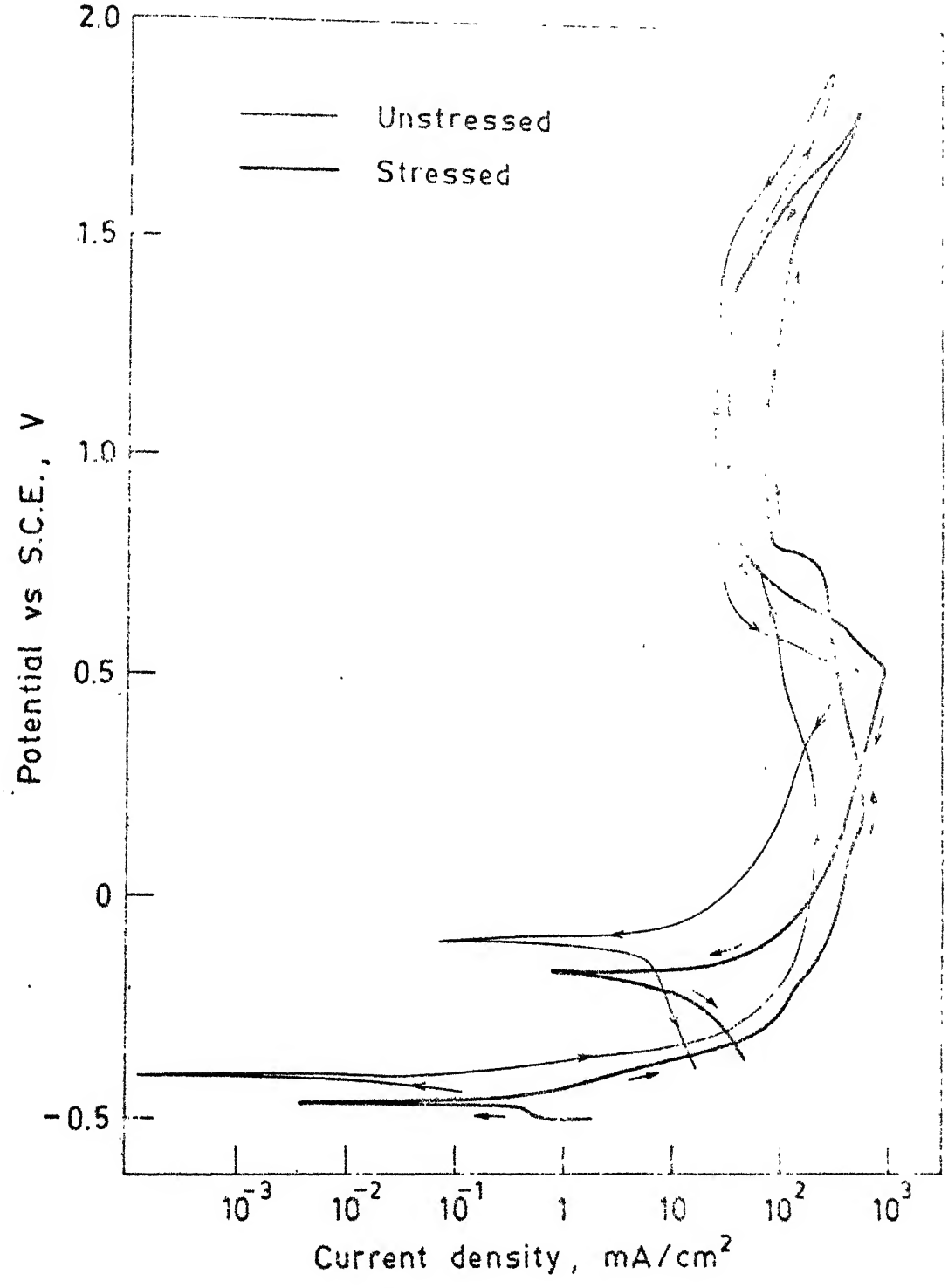

Fig. 4.27. Anodic polarization curves for unstressed and stressed prestressing steel (IT 350°C) wires in 50 % $Ca(NO_3)_2$ + 5 % NH_4NO_3 solution.

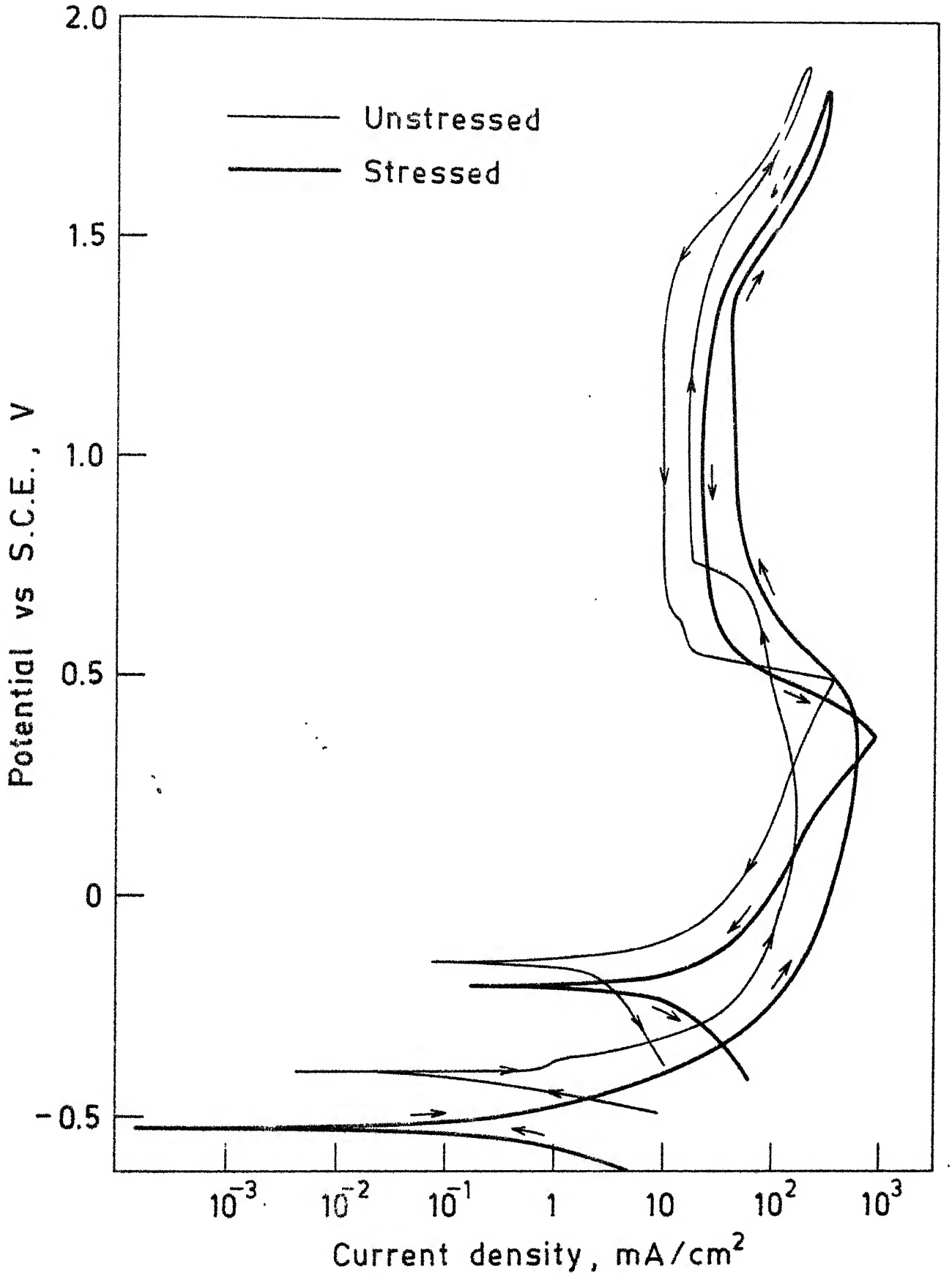

Fig. 4.28. Anodic polarization curves for unstressed and stressed prestressing steel (IT 425°C) wires in 50 % $Ca(NO_3)_2$ + 5 % NH_4NO_3 solution.

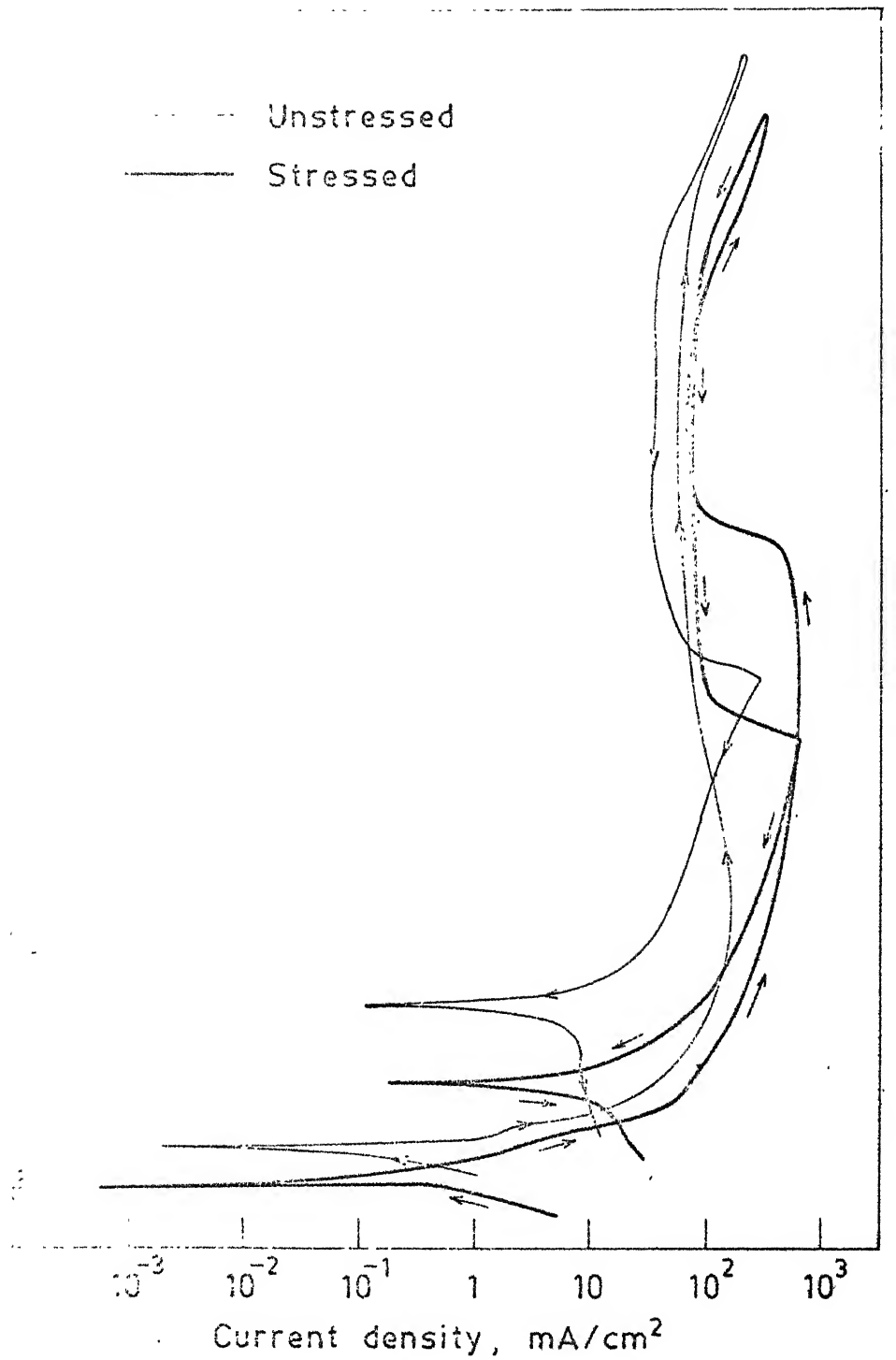

Anodic polarization curves for unstressed and stressed prestressing steel (IT 500°C) wires in 50 % $Ca(NO_3)_2$ + 5 % NH_4NO_3 solution.

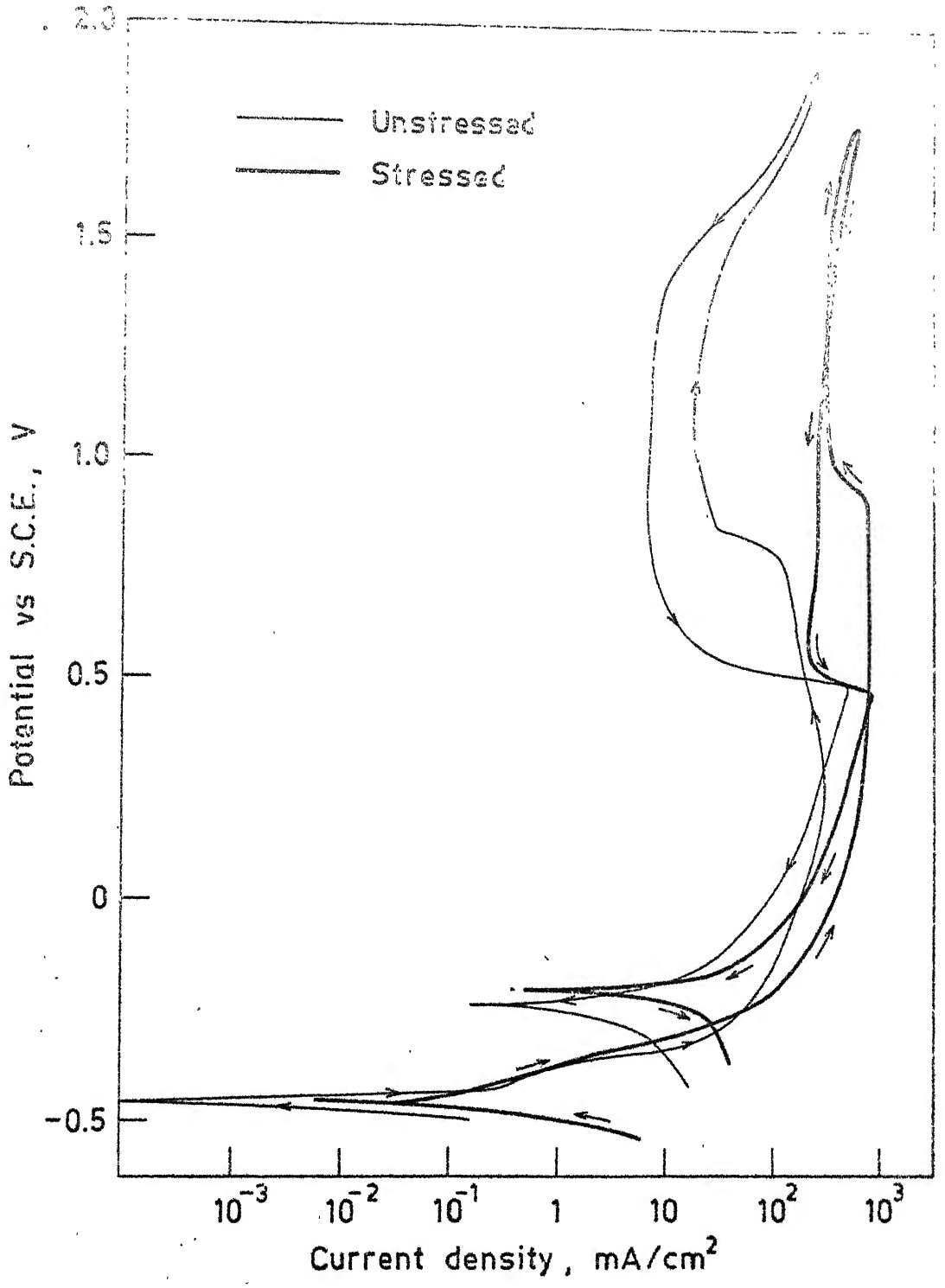

Fig. 4.30. Anodic polarization curves for unstressed and stressed prestressing steel (IT 575°C) wires in 50 % $Ca(NO_3)_2$ + 5 % NH_4NO_3 solution.

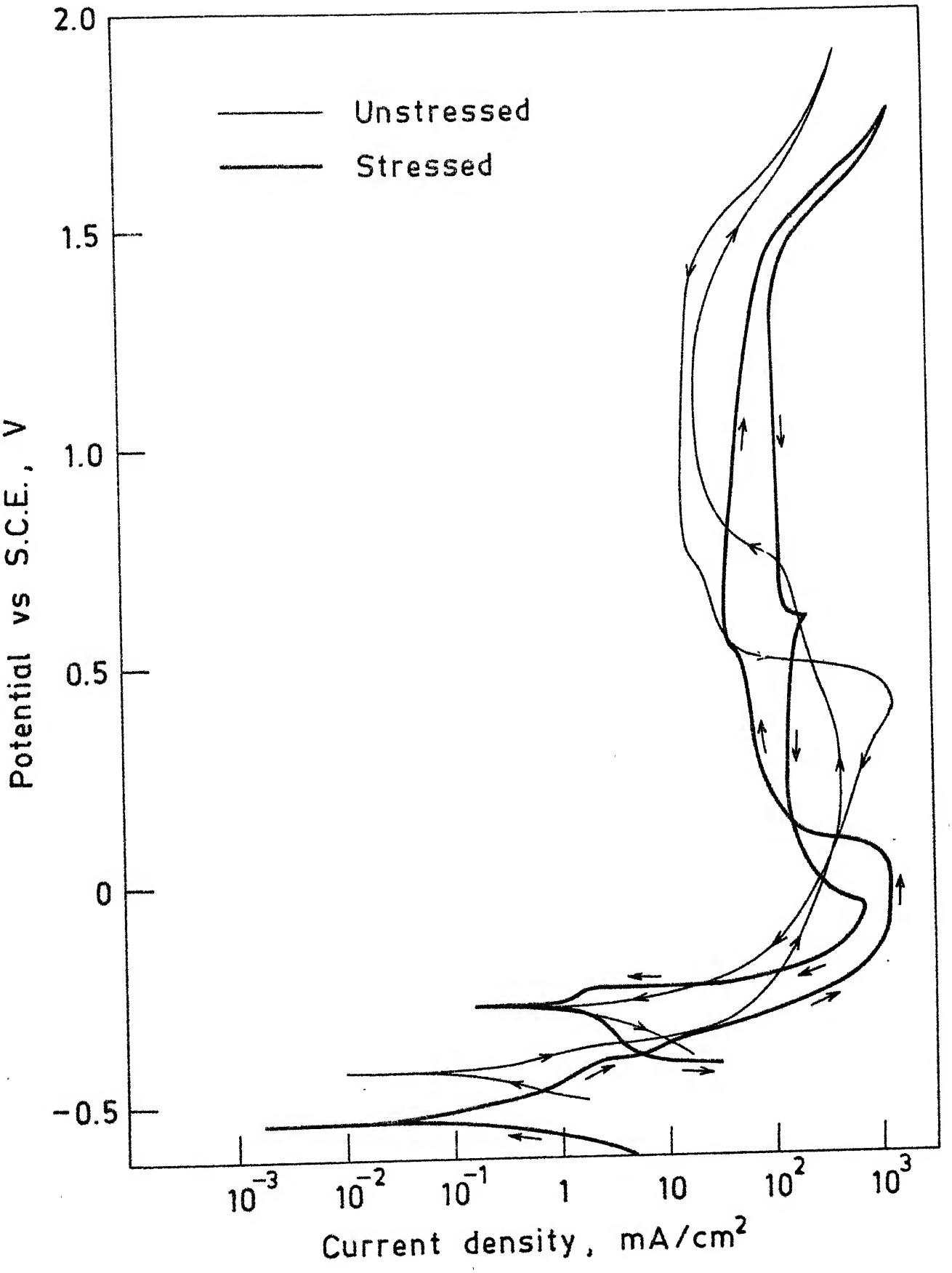

Fig. 4.31. Anodic polarization curves for unstressed and stressed prestressing steel (IT 670° C) wires in 50 % $Ca(NO_3)_2$ + 5 % NH_4NO_3 solution.

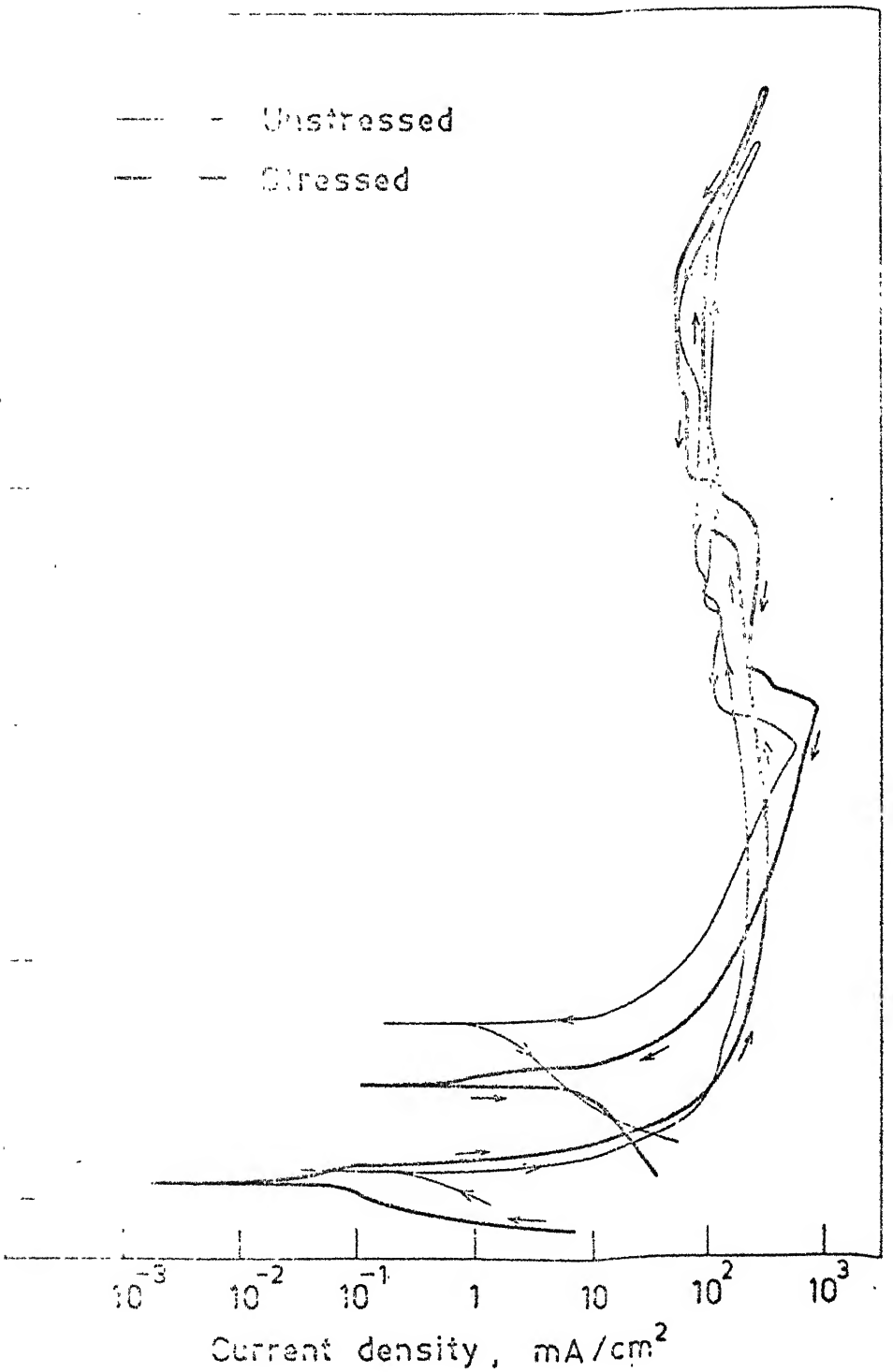

Anodic polarization curves for unstressed and stressed prestressing steel (QT 200°C, 1 hr) wires in 60 % $Ca(NO_3)_2$ + 5 % NH_4NO_3 solution.

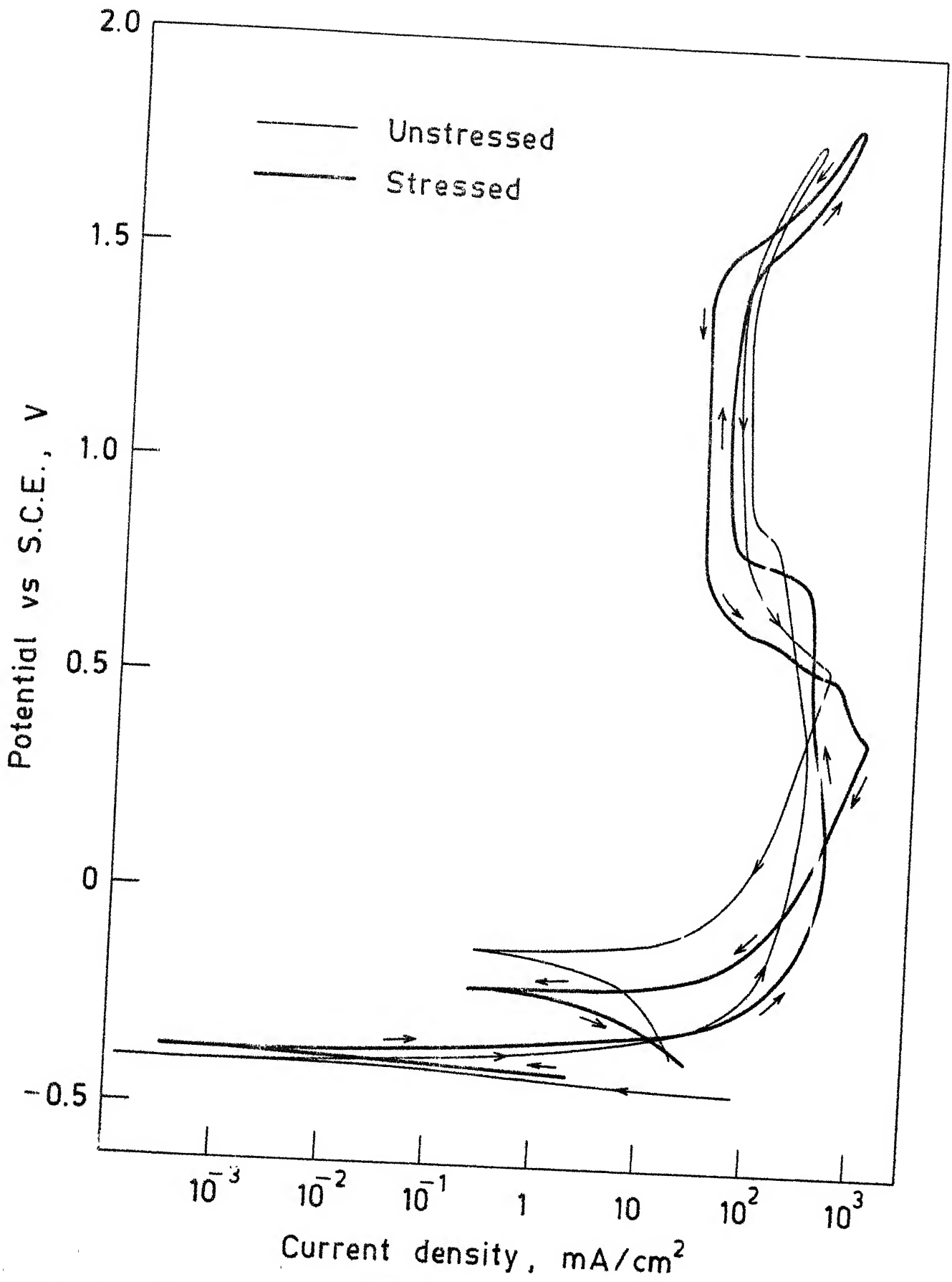

ig. 4.33. Anodic polarization curves for unstressed and stressed prestressing steel (QT 300°C, 1 hr) wires in 50 % $Ca(NO_3)_2$ + 5 % NH_4NO_3 solution.

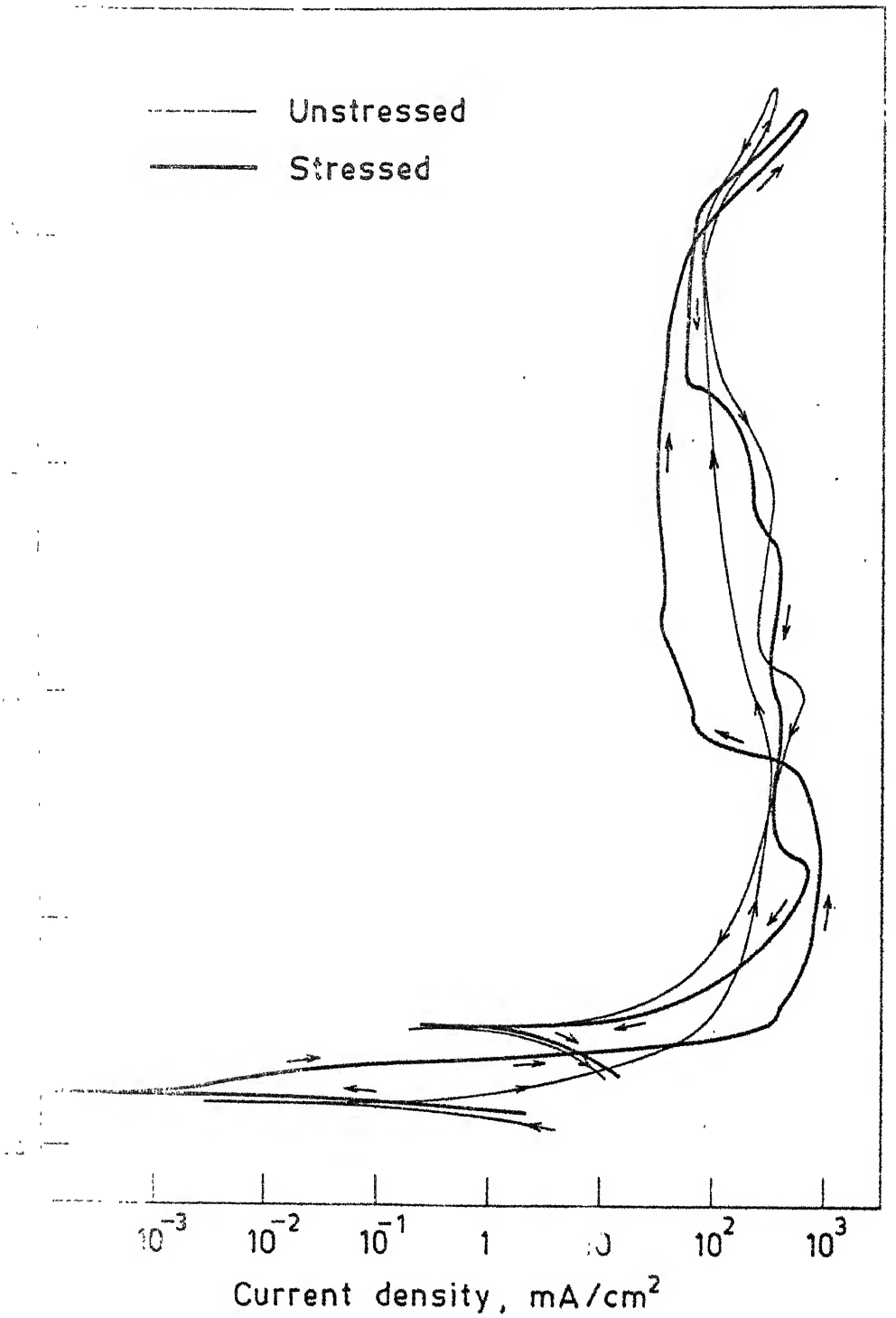

Anodic polarization curves for unstressed and stressed prestressing steel (QT 400° C, 1 hr) wires in 50 % $Ca(NO_3)_2$ + 5 % NH_4NO_3 solution.

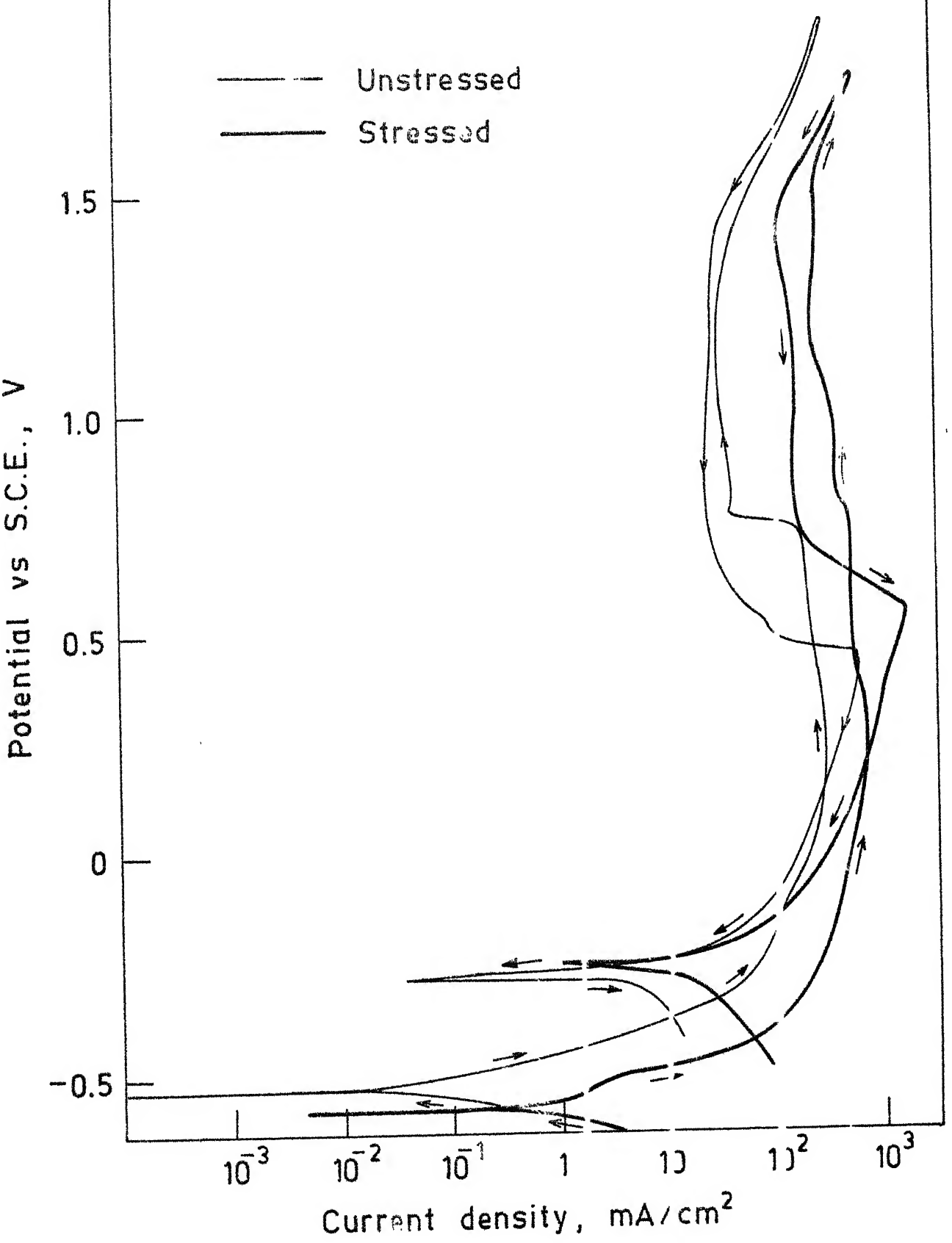

Fig. 4.35. Anodic polarization curves for unstressed and stressed prestressing steel (Q: 500° C, 1 hr) wires in 50 % $Ca(NO_3)_2 + NH_4NO_3$ solution.

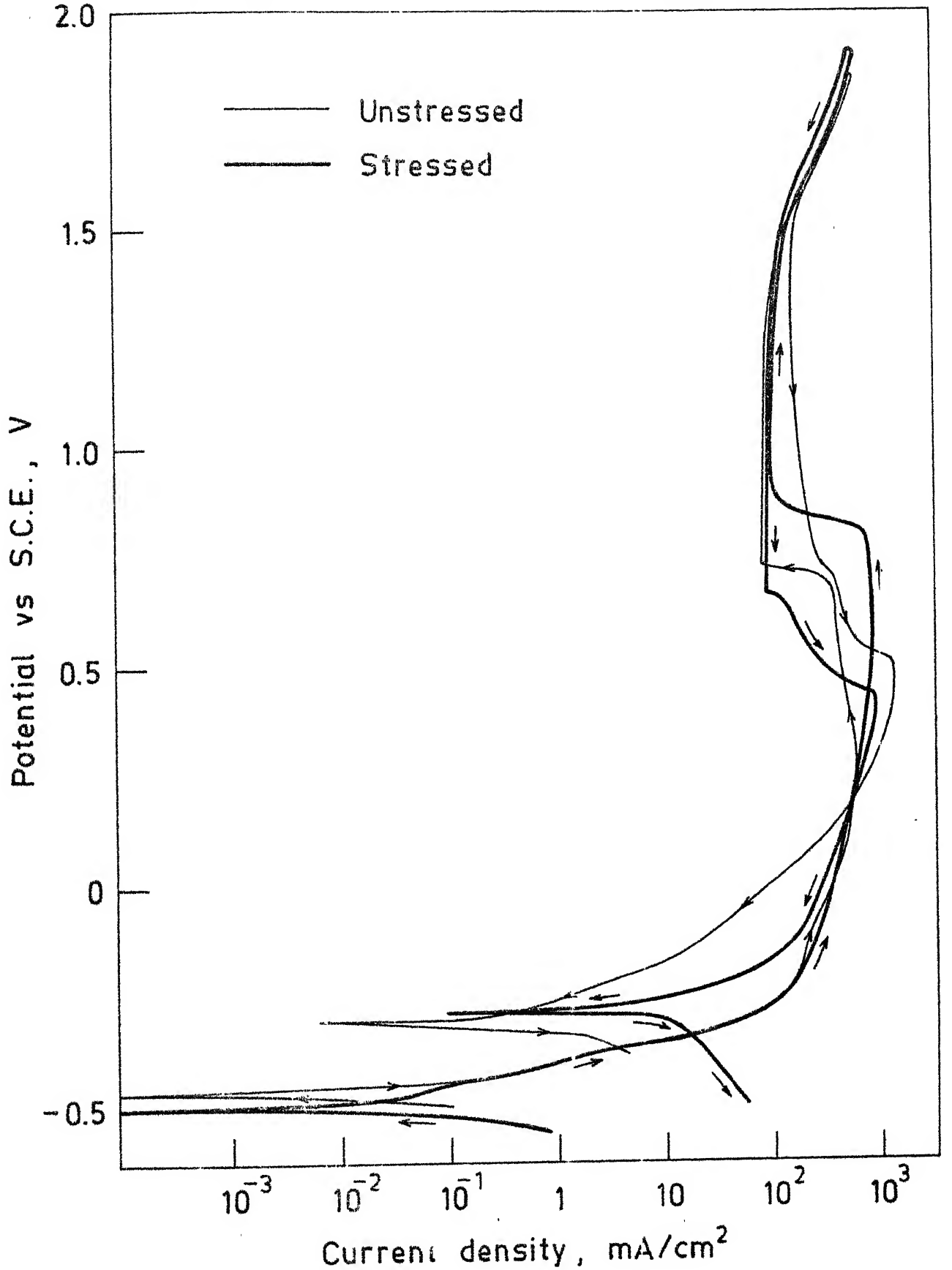

g. 4.36. Anodic polarization curves for unstressed and stressed prestressing steel (QT 600° C, 1 hr) wires in 50 % $Ca(NO_3)_2$ + 5 % NH_4NO_3 solution.

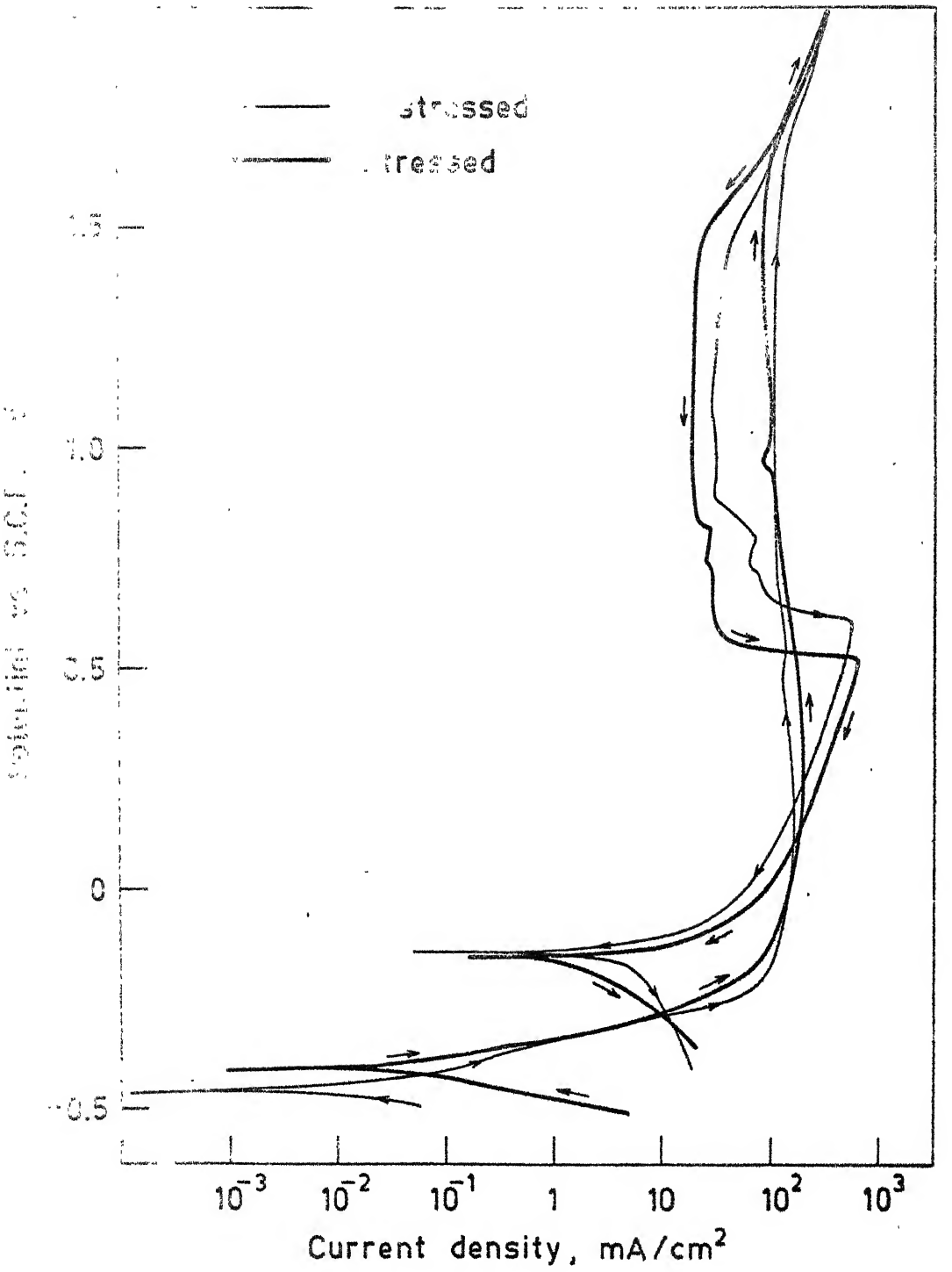

Fig. 4.37. Anodic polarization curves for unstressed and stressed prestressing steel (QT 200°C, 4 hr) wires in 50 % $Ca(NO_3)_2$ + 5 % NH_4NO_3 solution.

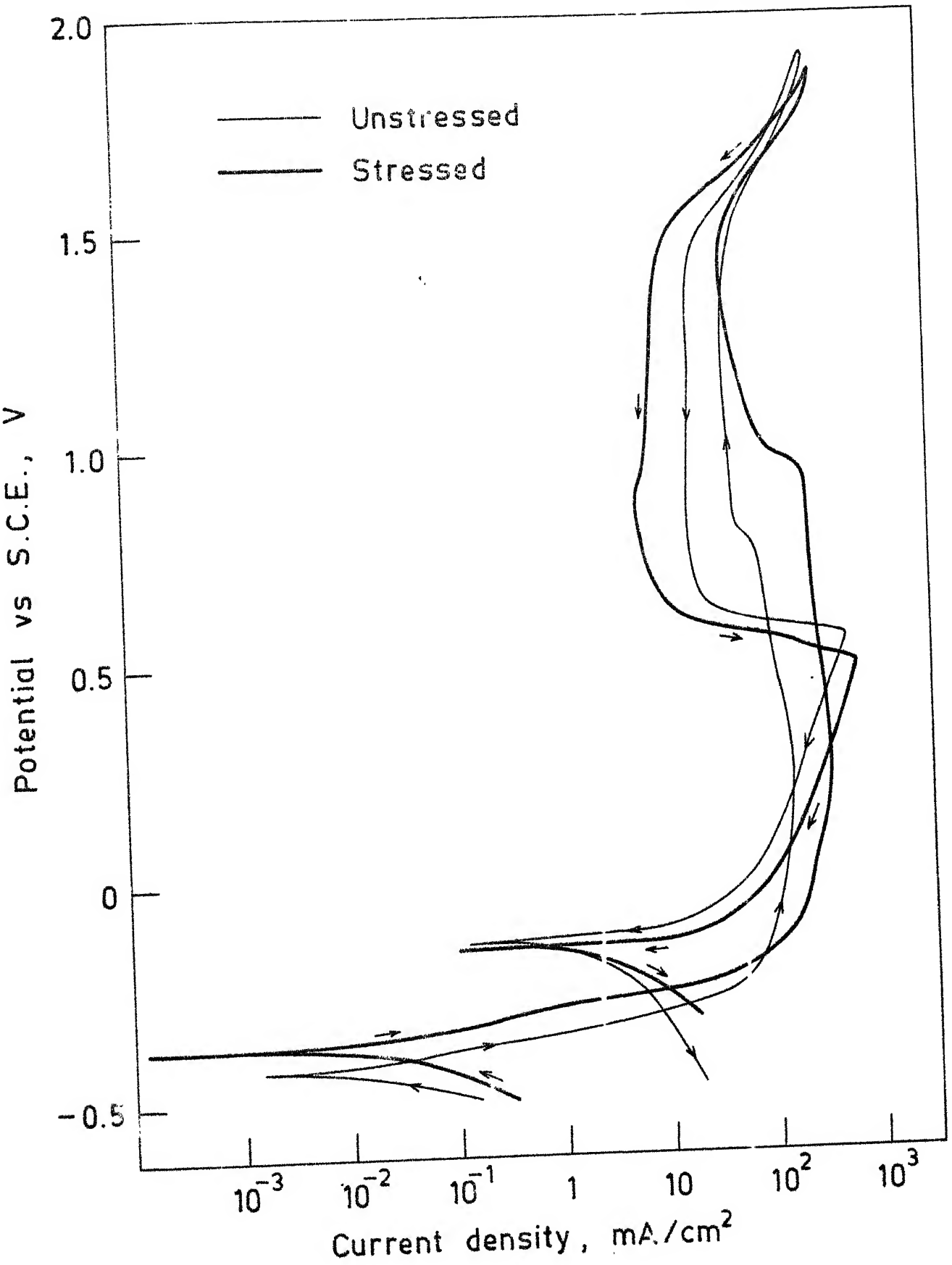

Fig. 4.38. Anodic polarization curves for unstressed and stressed prestressing steel (QT 300°C, 4 hr) wires in 50 % $Ca(NO_3)_2$ + 5 % NH_4NO_3 solution.

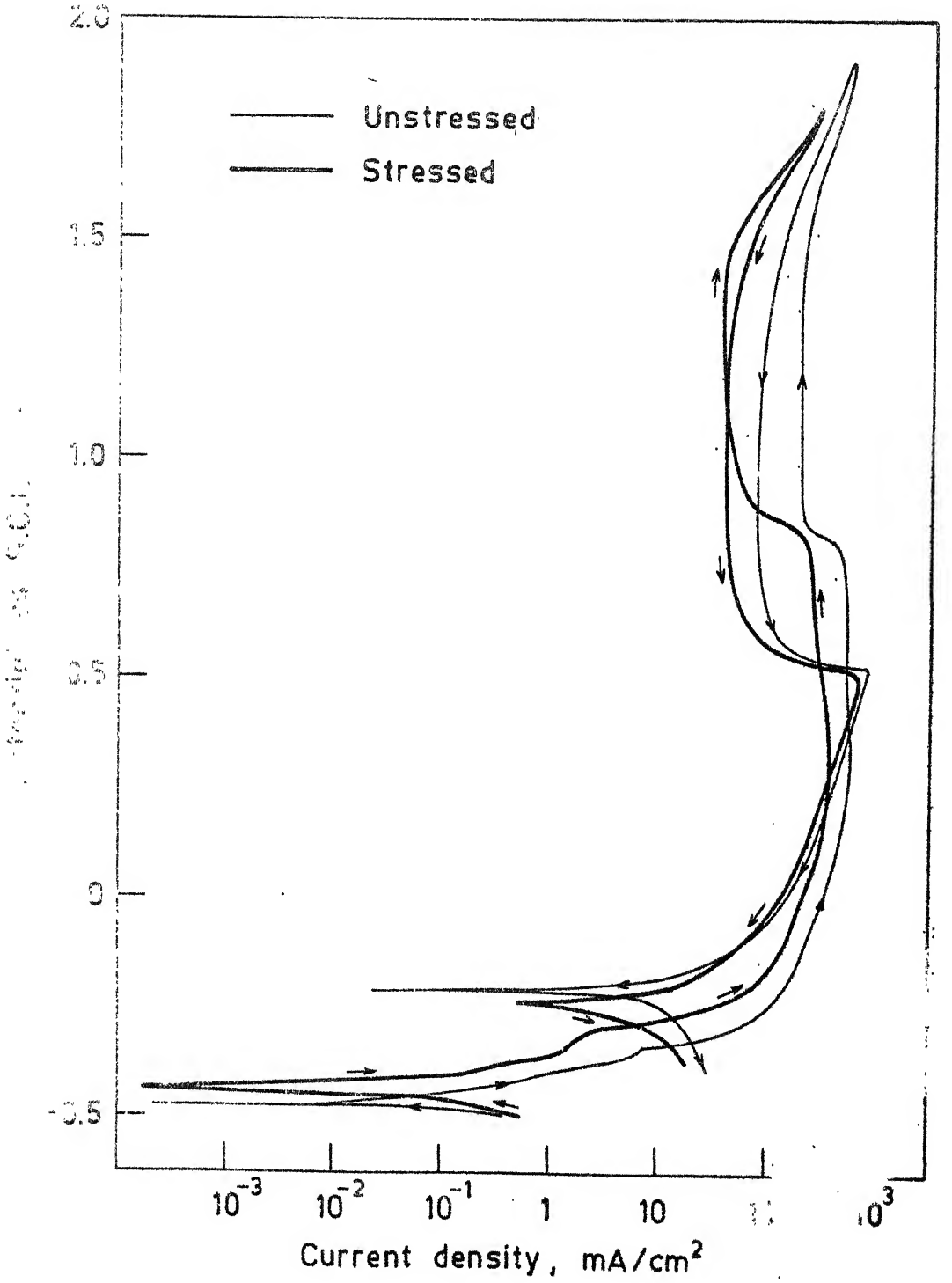

Fig. 4.39. Anodic polarization curves for u[illegible]ssed and stressed prestressing steel (QT [illegible]C, 4 hr) wires in 50 % $Ca(NO_3)_2$ + 5 % NH_4NO_3 solution.

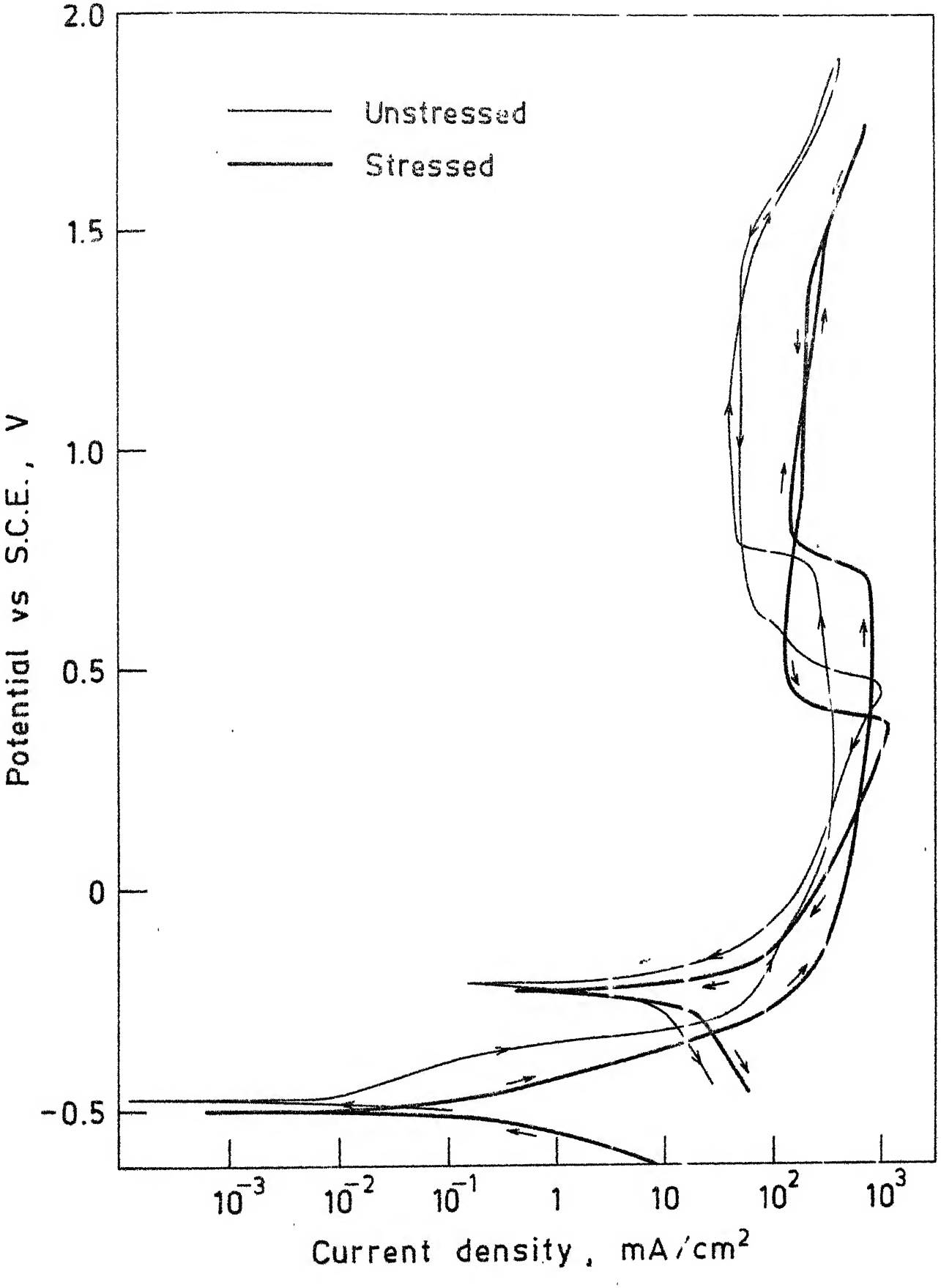

g. 4.40. Anodic polarization curves for unstressed and stressed prestressing steel (QT 500°C, 4 hr) wires in 50 % $Ca(NO_3)_2$ + 5 % NH_4NO_3 solution.

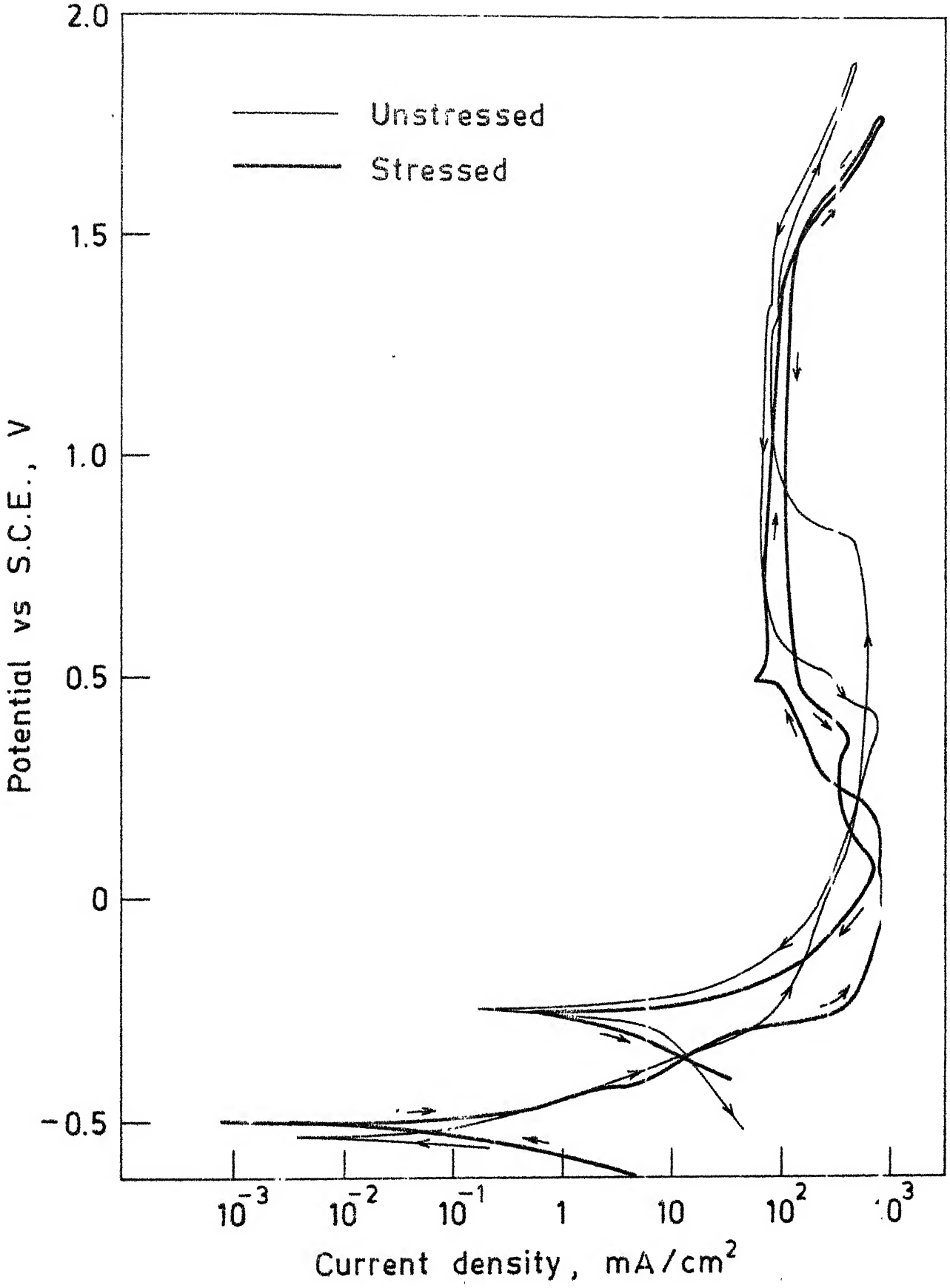

g. 4.41. Anodic polarization curves for unstressed and stressed prestressed steel (QT 600°C, 4 hr) wires in 50 % $Ca(NO_3)_2$ + 5 % NH_4NO_3 solution.

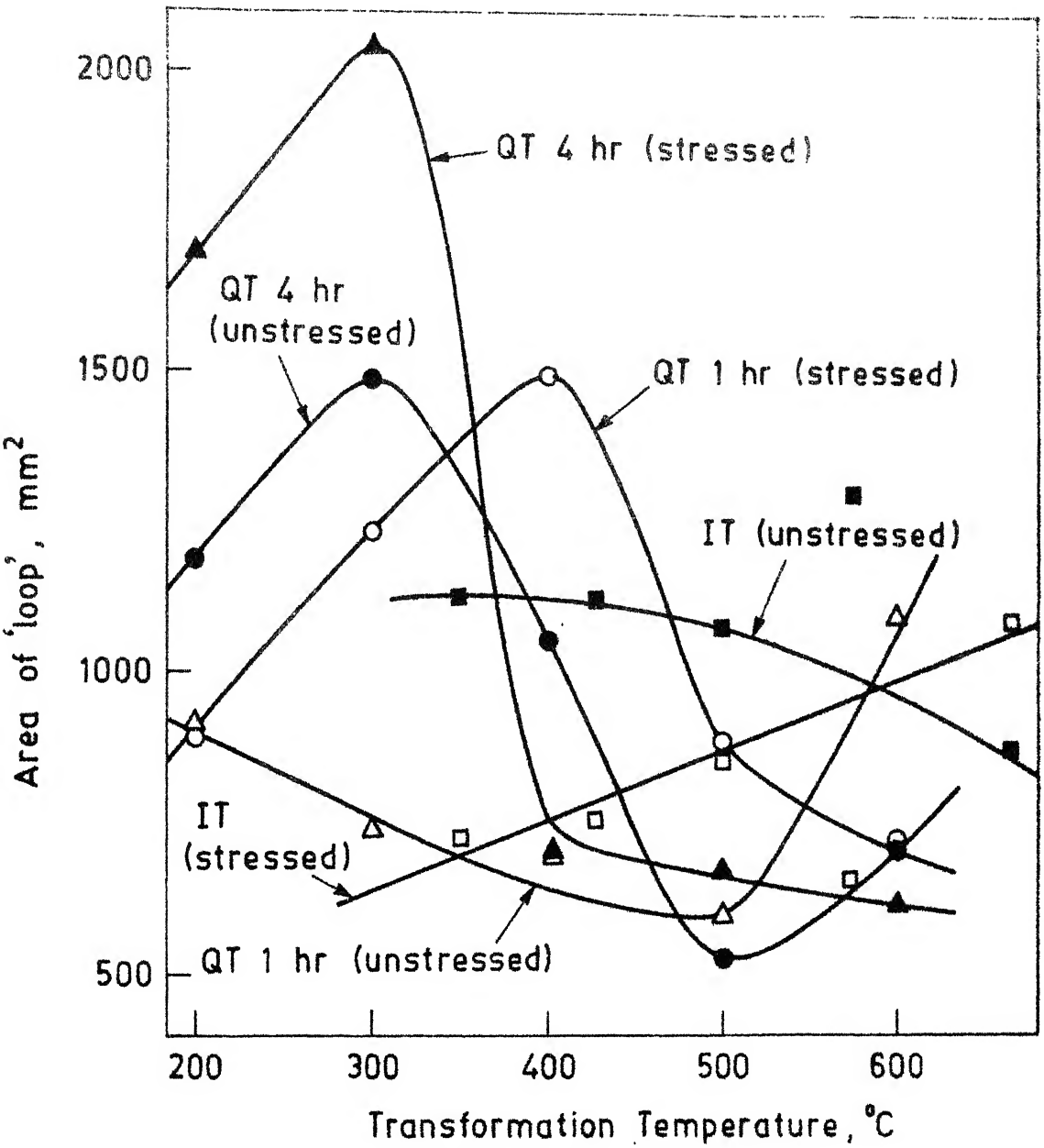

Fig. 4.42. Effect of transformation temperature on the area of the anodic loop for prestressing steel wires in unstressed and stressed conditions in 50 % $Ca(NO_3)_2$ + 5 % NH_4NO_3 solution at 100 °C.

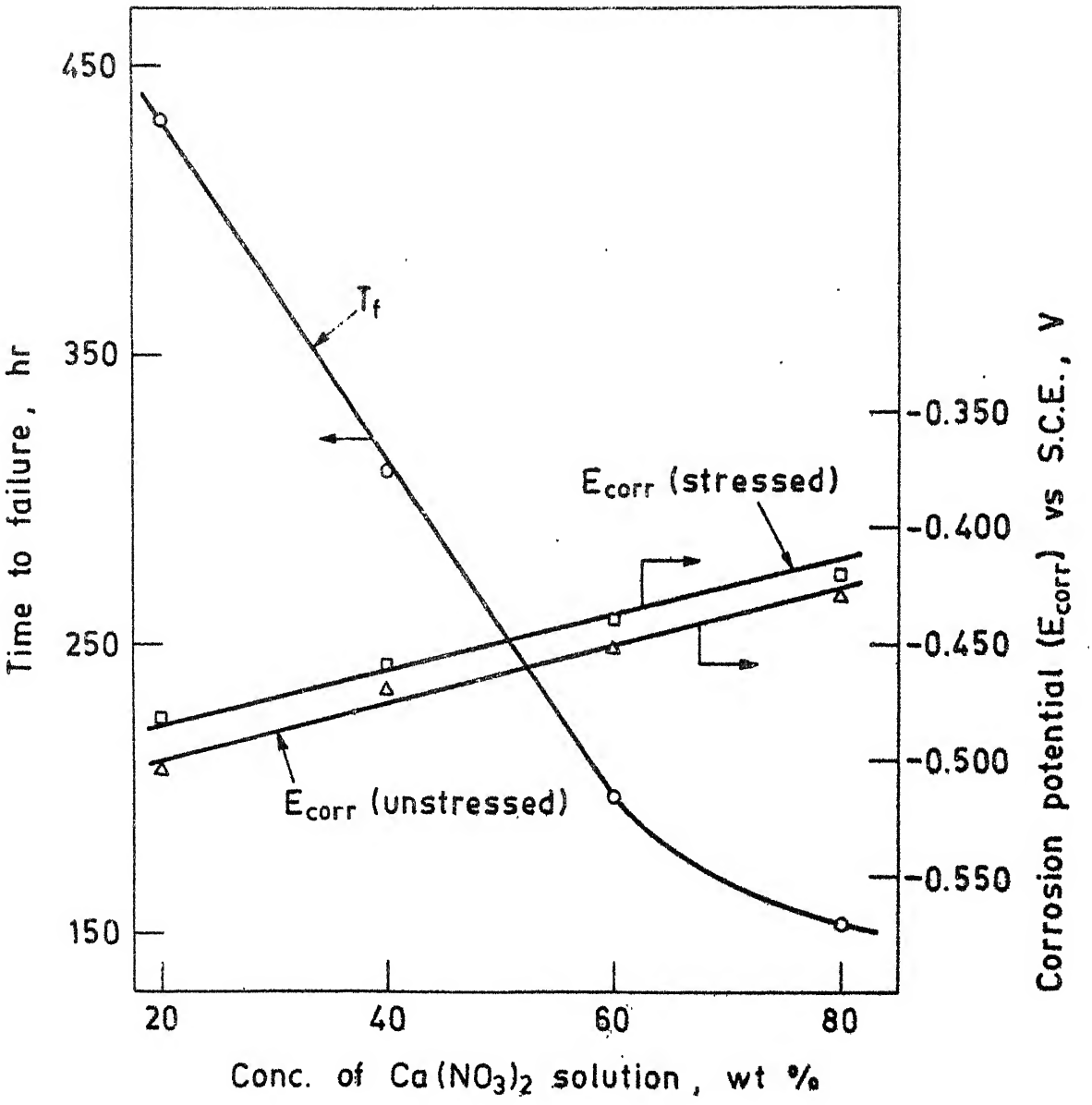

Fig 4.43 Effect of $Ca(NO_3)_2$ concentration on time to failure (T_f), E_{corr} (unstressed) and E_{corr} (stressed) of as received prestressing steel wires at 100 °C.

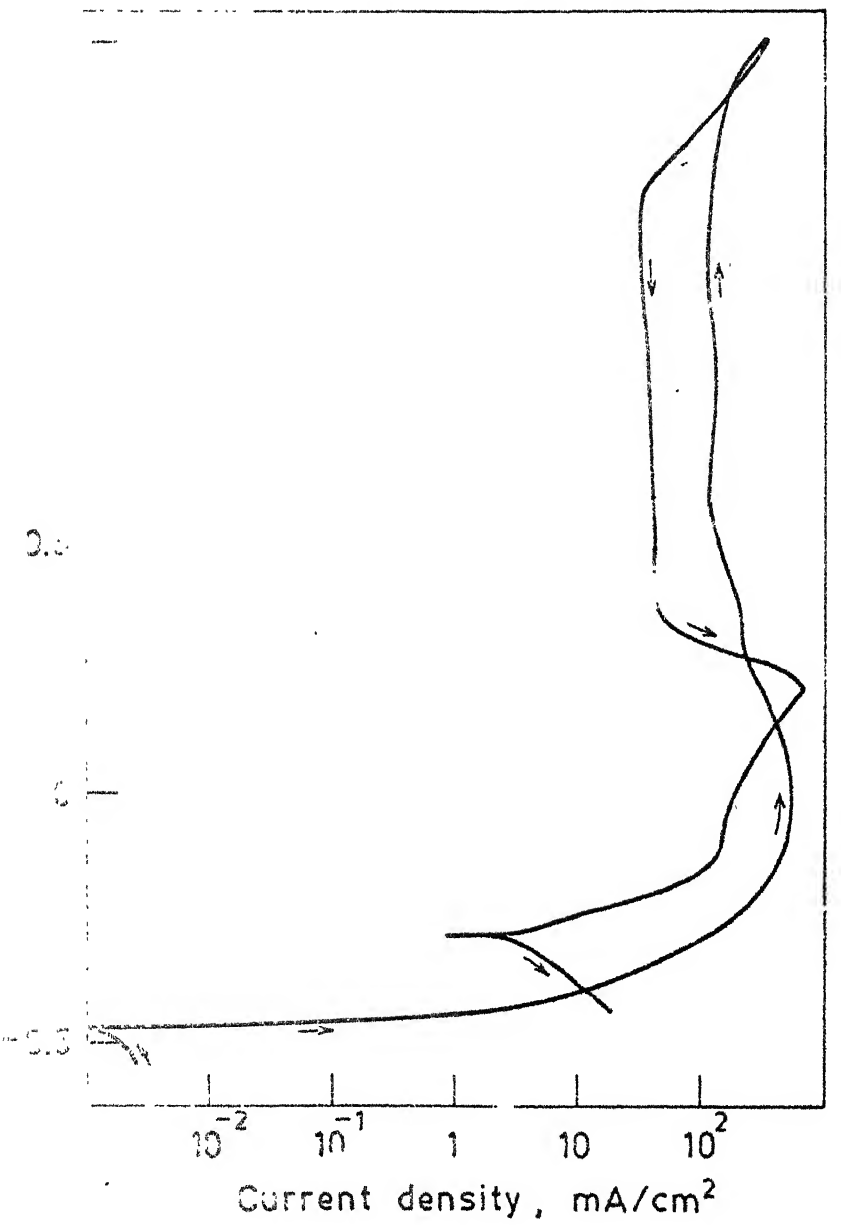

...nodic polarization curve for unstressed ...s received prestressing steel wire in ...0 % $Ca(NO_3)_2$ solution at 100° C.

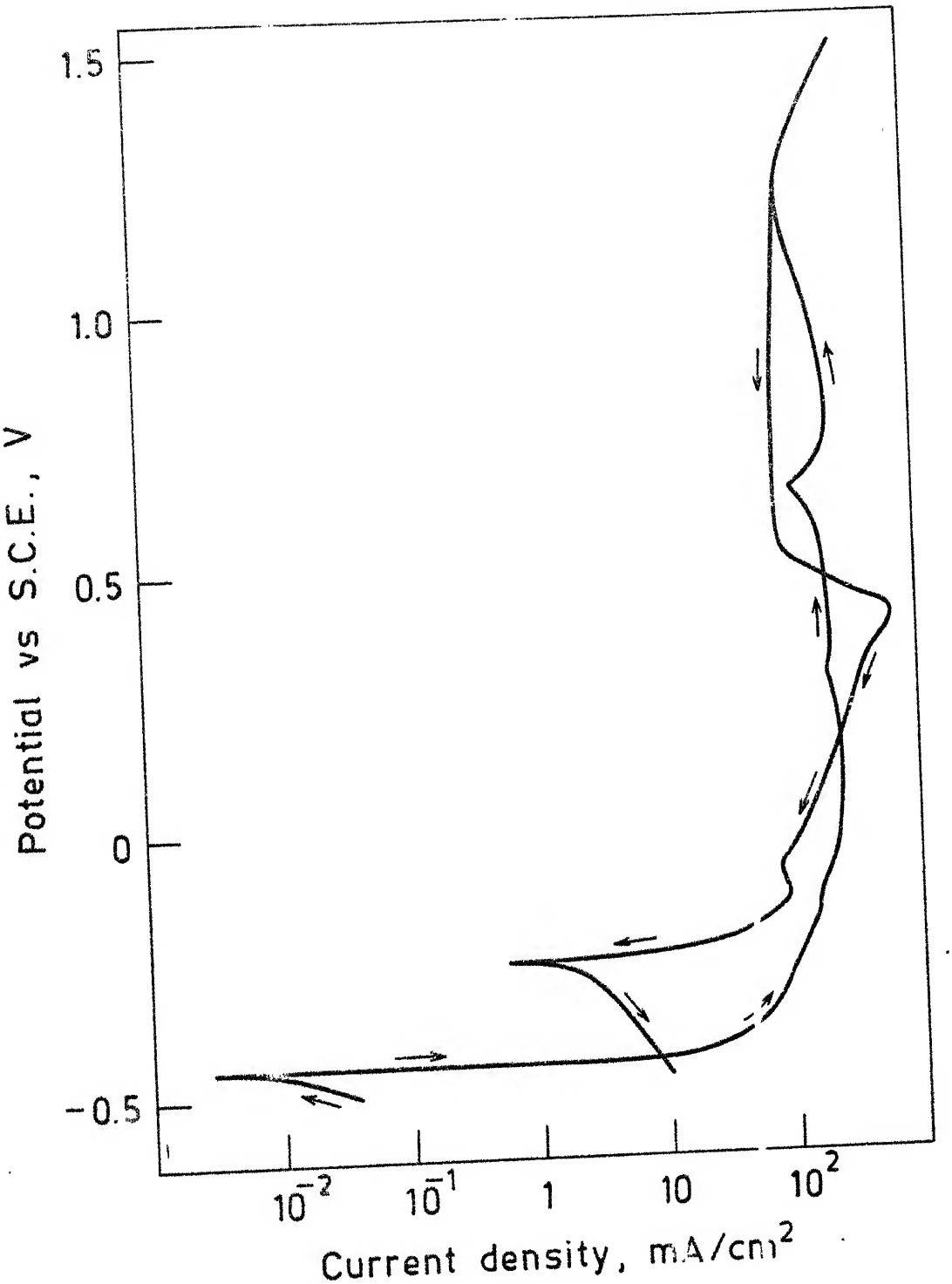

Fig. 4.45. Anodic polarization curve for stressed as received prestressing steel wire in 40 % $Ca(NO_3)_2$ solution at 100° C.

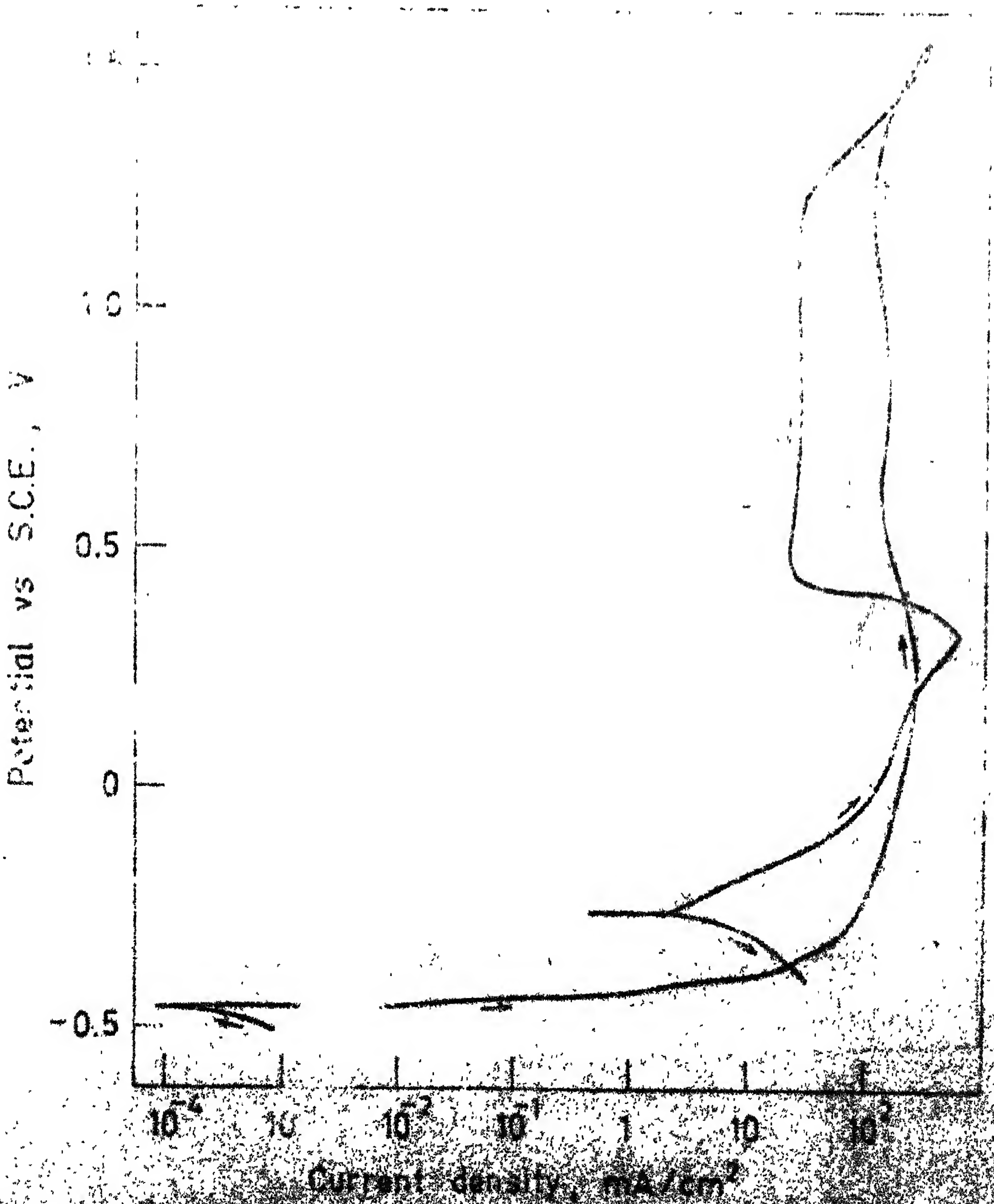

4.48 Anodic polarization curve for unstressed as received prestressing steel wire in 60 % $Ca(NO_3)_2$ solution at 100° C

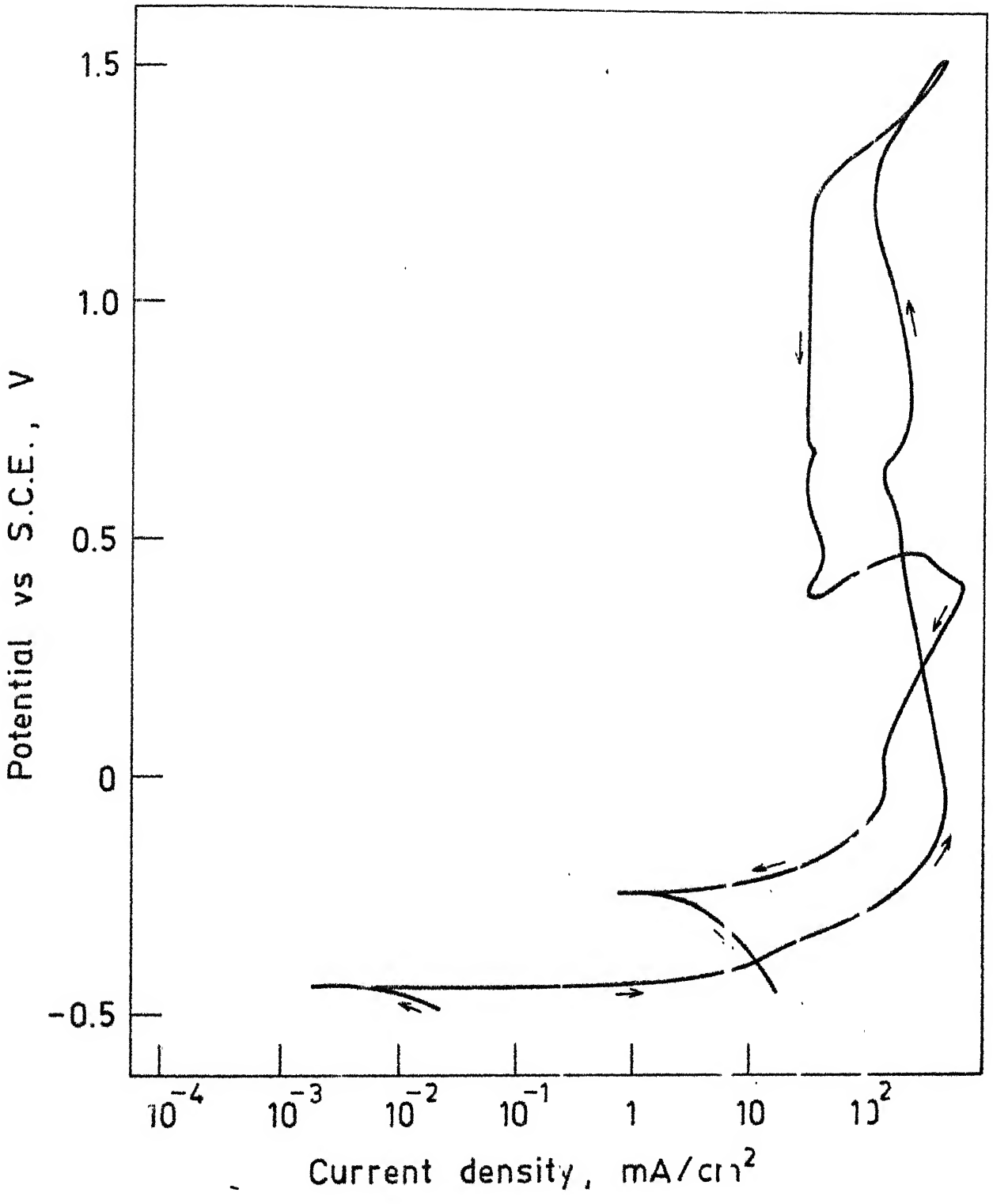

ig. 4.47. Anodic polarization curve for stressed as received prestressing steel wire in 60 % $Ca(NO_3)_2$ solution at 100°C.

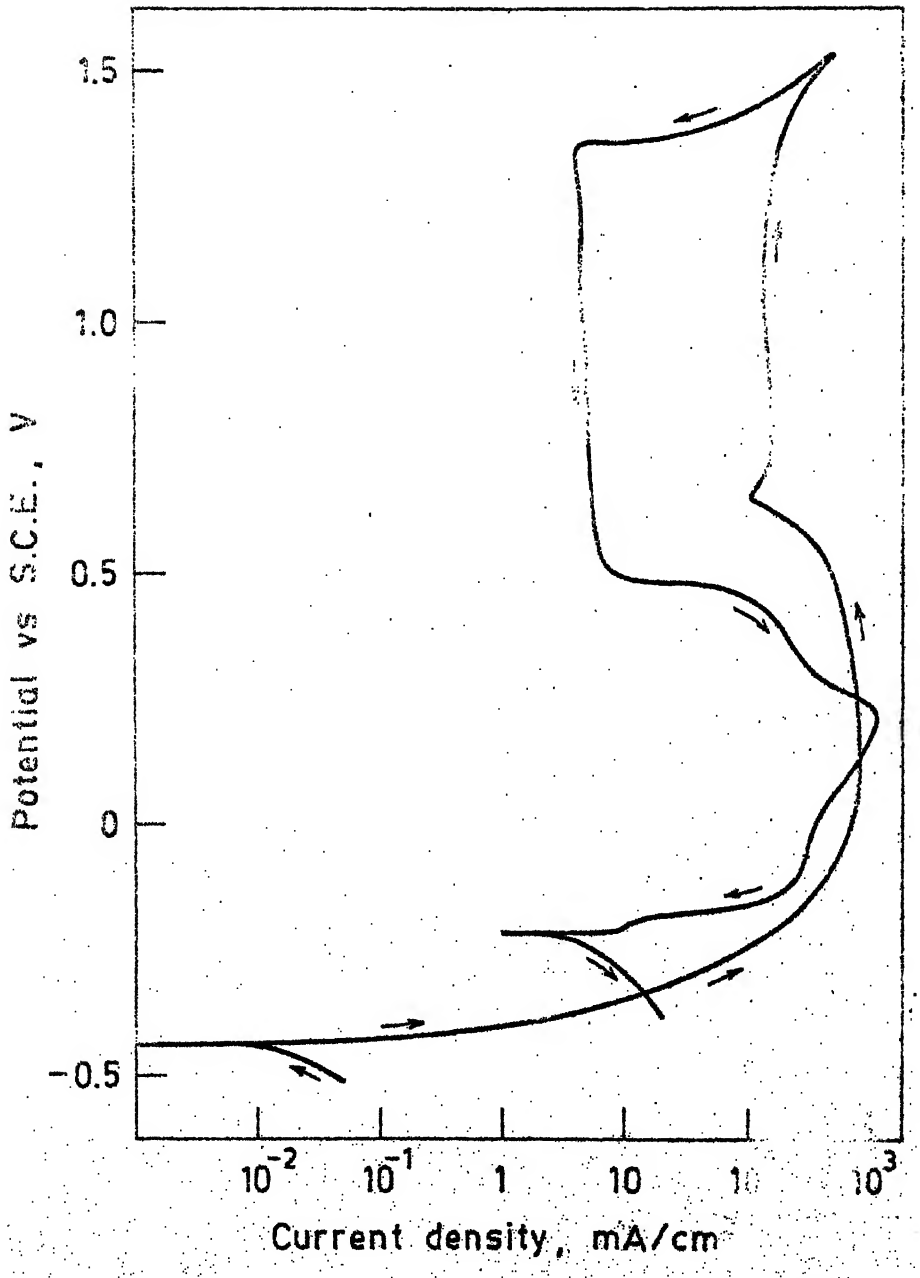

Fig. 4.48. Anodic polarization curve for ... essed as received prestressing steel ... in 80 % $Ca(NO_3)_2$ solution at 100°

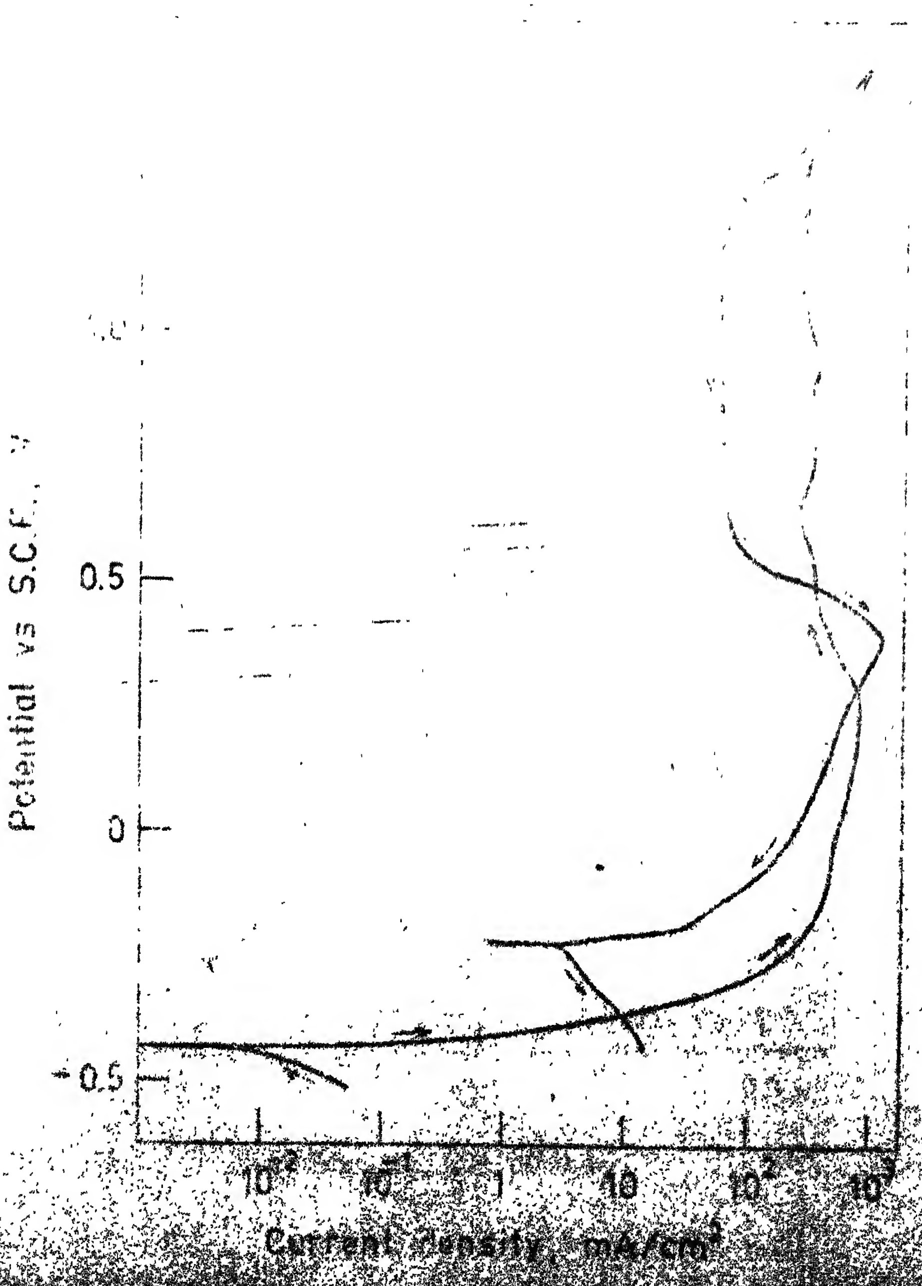

FIG. A-40 Anodic polarization curve for stress relieved prestressing steel [illegible]

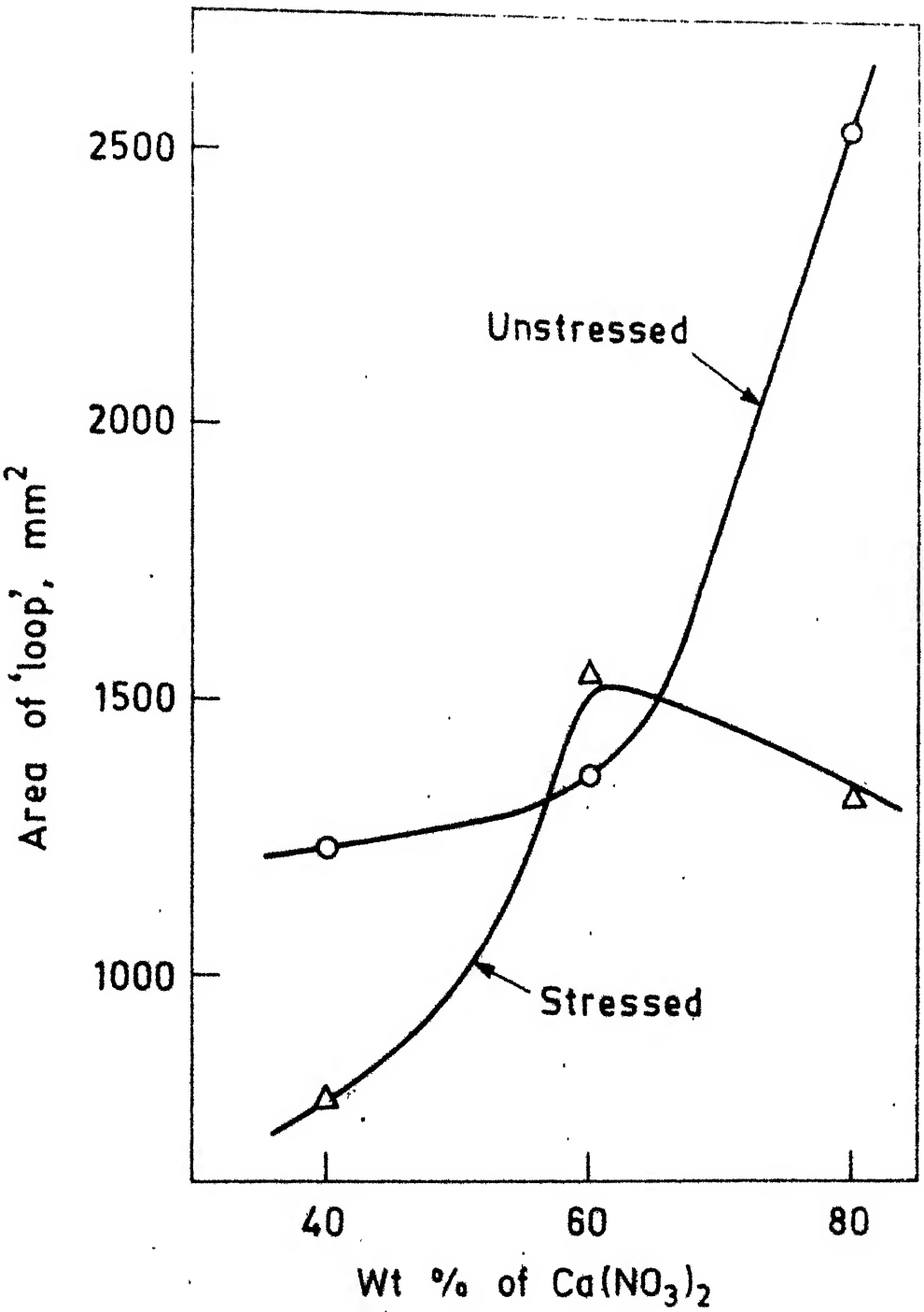

Fig. 4.50. Effect of $Ca(NO_3)_2$ concentration on the area of the anodic loop for As Received prestressing steel wires in untressed and stressed conditions at 100 °C.

LONGITUDINAL SECTION 1500 X

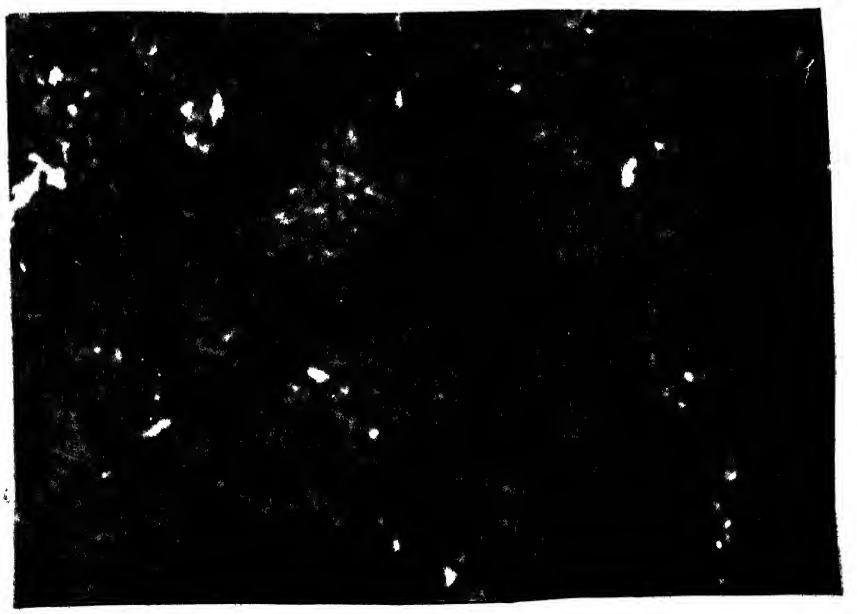

TRANSVERSE SECTION 1500 X

Fig. 4.51 Optical micrographs of As Received wire.

Fig. 4.52 Optical micrograph of Annealed wire at 1500 X.

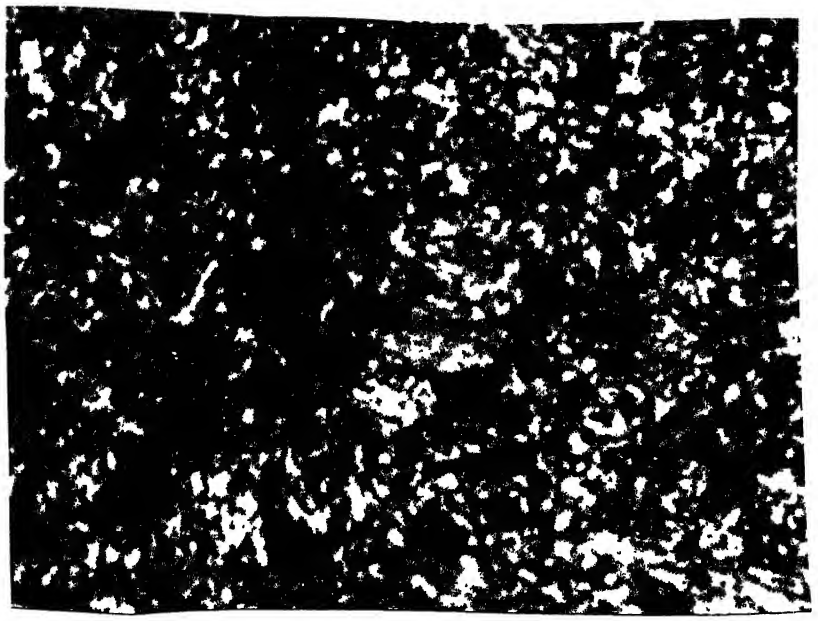

Fig. 4.53 Optical micrograph of Isothermally Transformed wire at 350°C. 1500 X

Fig. 4.54 Optical micrograph of Isothermally Transformed wire at 425°C. 1500 X.

Fig. 4.55 Optical micrograph of Isothermally Transformed wire at 575°C. 1500 X.

Fig. 4.56 Optical micrograph of Isothermally Transformed wire at 670°C. 1500 X.

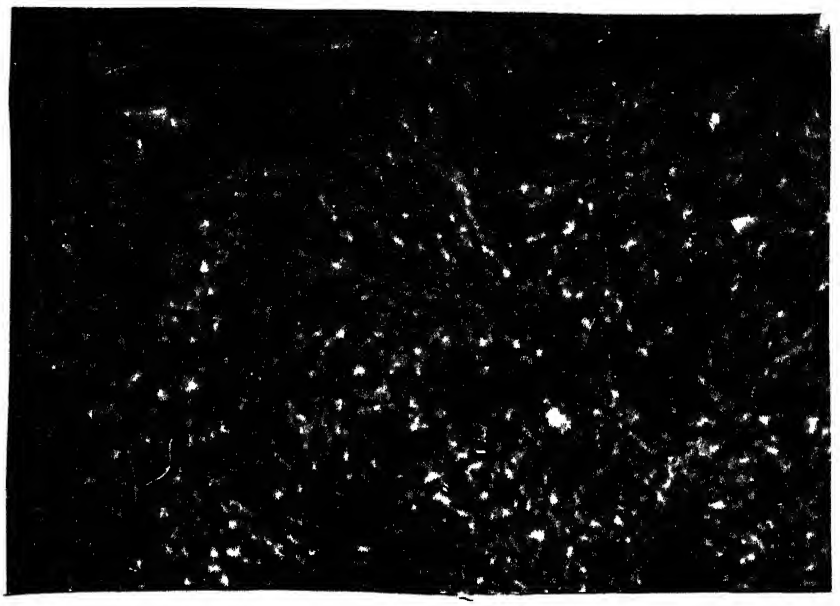

Fig. 4.57 Optical micrograph of Quenched & Tempered wire for 1 hour at 200°C. 1500 X.

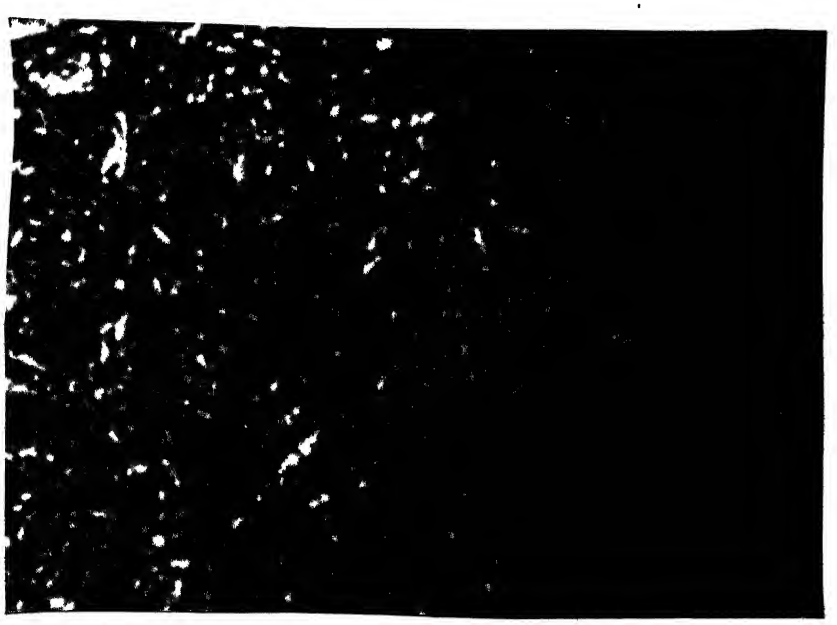

Fig. 4.58 Optical micrograph of Quenched & Tempered wire for 1 hour at 300°C. 1500 X.

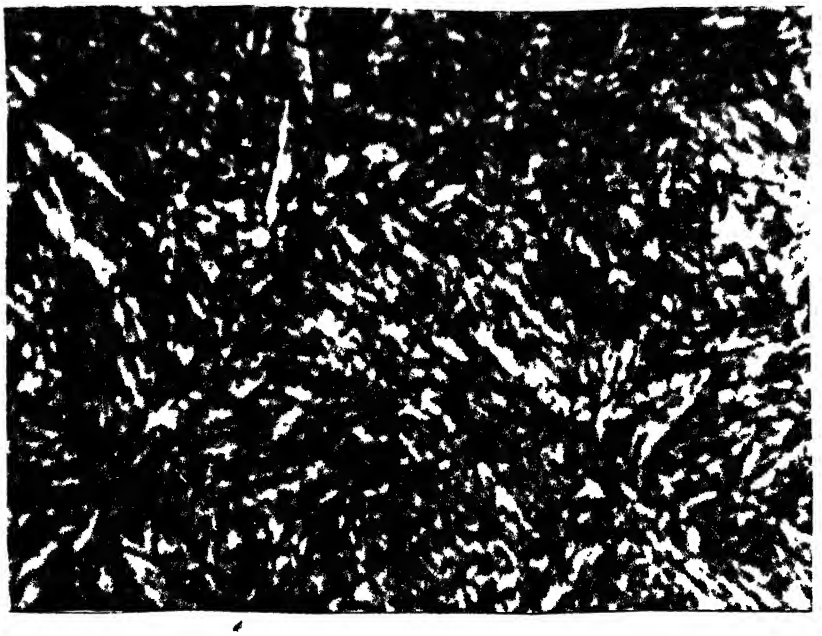

Fig. 4.59 Optical micrograph of Quenched & Tempered wire for 1 hour at 400°C. 1500 X.

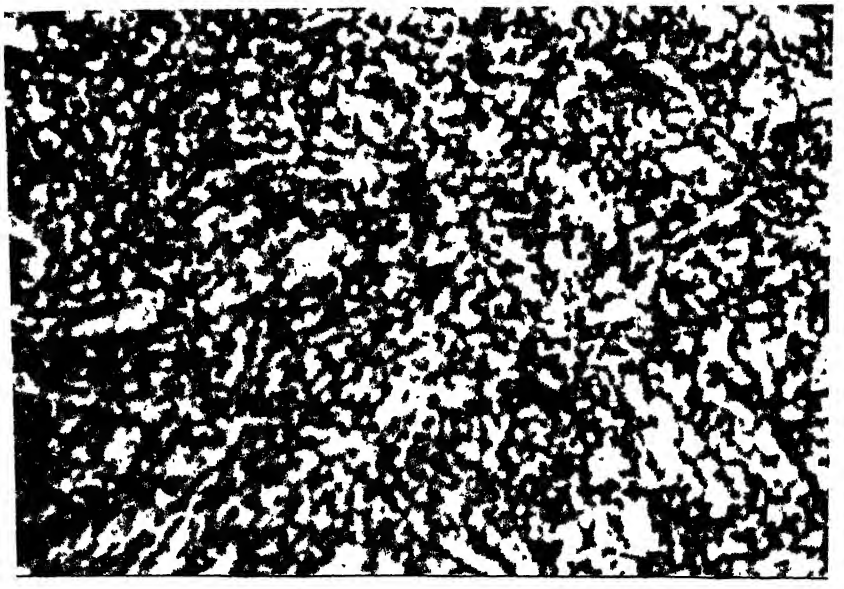

Fig. 4.60 Optical micrograph of Quenched & Tempered wire for 1 hour at 500°C. 1500 X.

Fig. 4.61 Optical micrograph of Quenched & Tempered wire for 1 hour at 600°C. 1500 X.

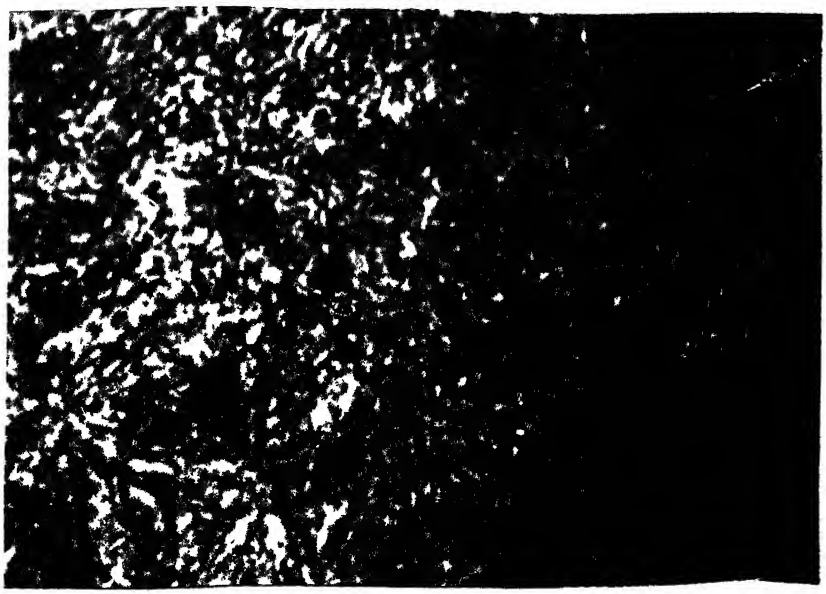

Fig. 4.62 Optical micrograph of Quenched & Tempered wire for 4 hours at 200°C. 1500 X.

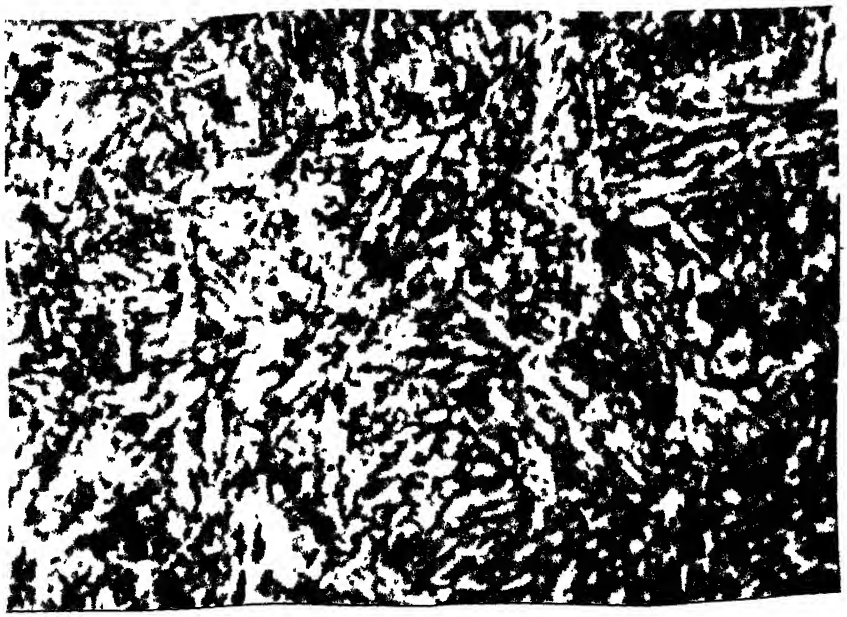

Fig. 4.63 Optical micrograph of Quenched & Tempered wire for 4 hours at 300°C. 1500 X.

Fig. 4.64 Optical micrograph of Quenched & Tempered wire for 4 hours at 400°C. 1500 X.

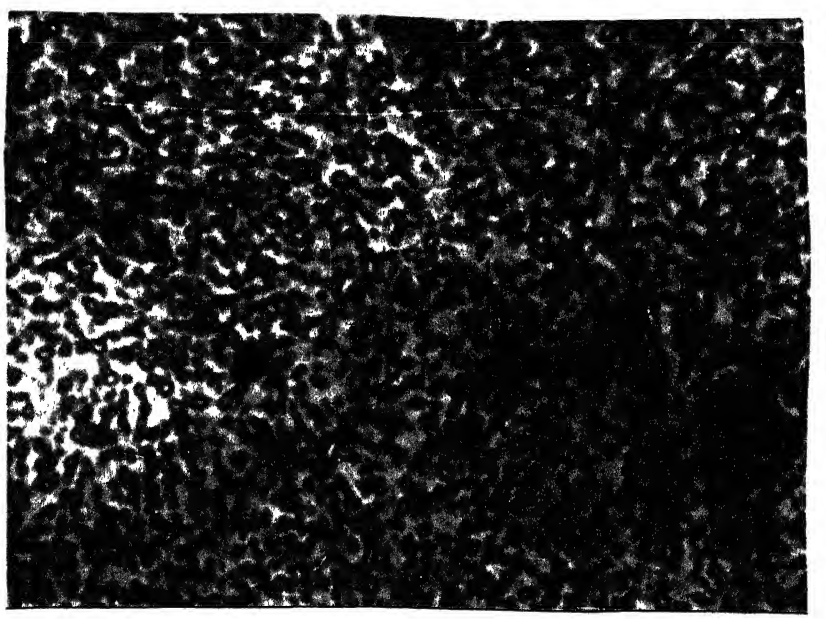

Fig. 4.65 Optical micrograph of Quenched & Tempered wire for 4 hours at 600°C. 1500 X.

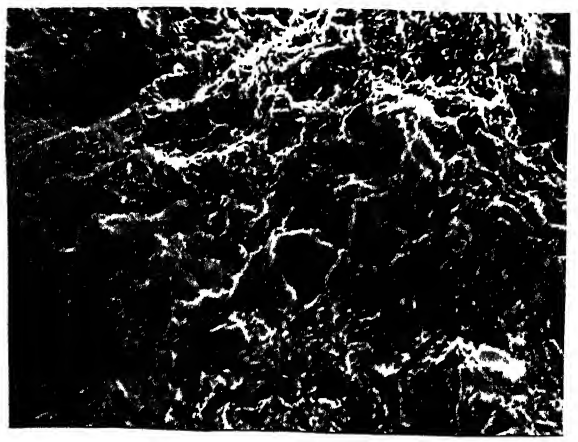

Fig. 4.66 (a) 520 X.

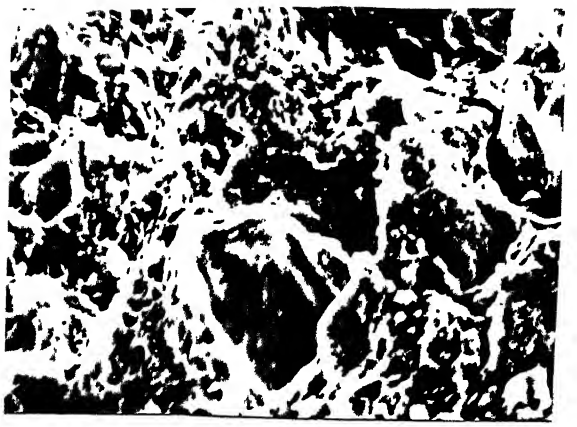

Fig. 4.66 (b) 1120 X.

Fig. 4.66 (c) 1950 X.

Fig. 4.66 Scanning electron fractograph of the As Received wire tested in air.

Fig. 4.67 (a) 325 X.

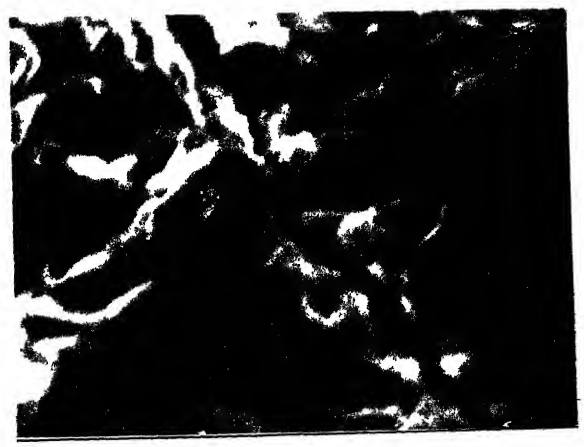

Fig. 4.67 (b) 3380 X.

Fig. 4.67 Scanning electron fractograph of the As Received wire tested in 80% $Ca(NO_3)_2$ at 100°C.

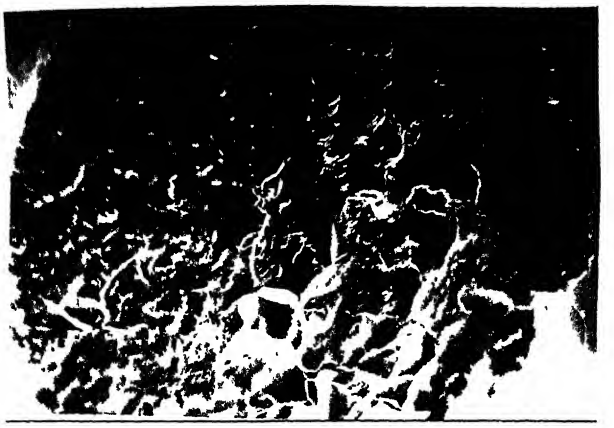

Fig. 4.68 Scanning electron fractograph of the Quenched & Tempered wire for 1 hour at 300°C, tested in 50% $Ca(NO_3)_2$ + 5% NH_4NO_3 solution at 100°C. 40 X.

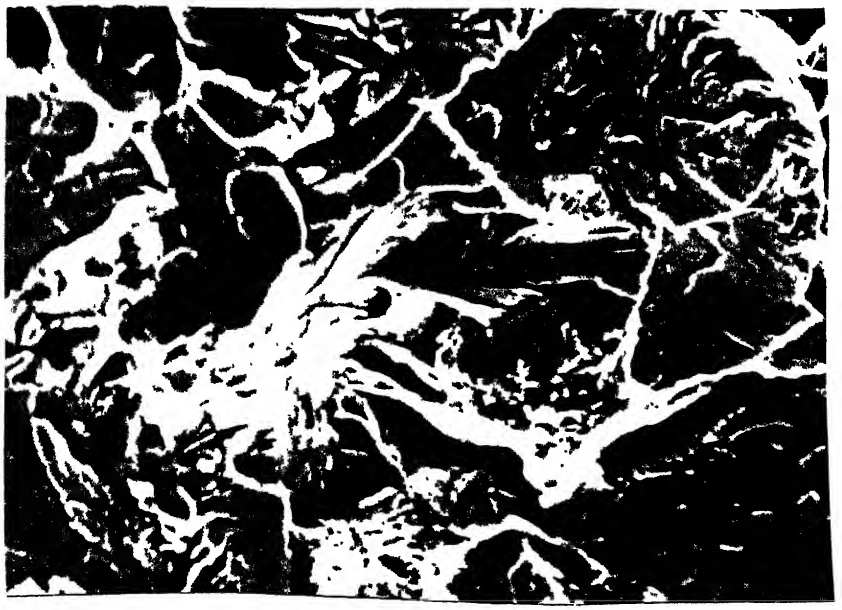

Fig. 4.69 Scanning electron fractograph of the Annealed wire tested in saturated H_2S at room temperature. 1100 X.

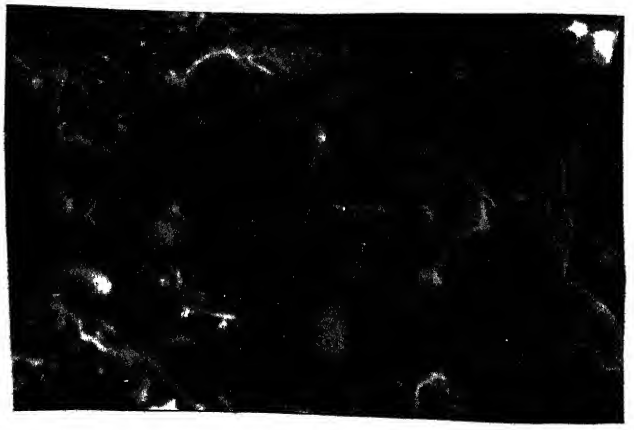

Fig. 4.70 Scanning electron fractograph of the Quenched & Tempered wire for 1 hour at 500°C. 1100 X.

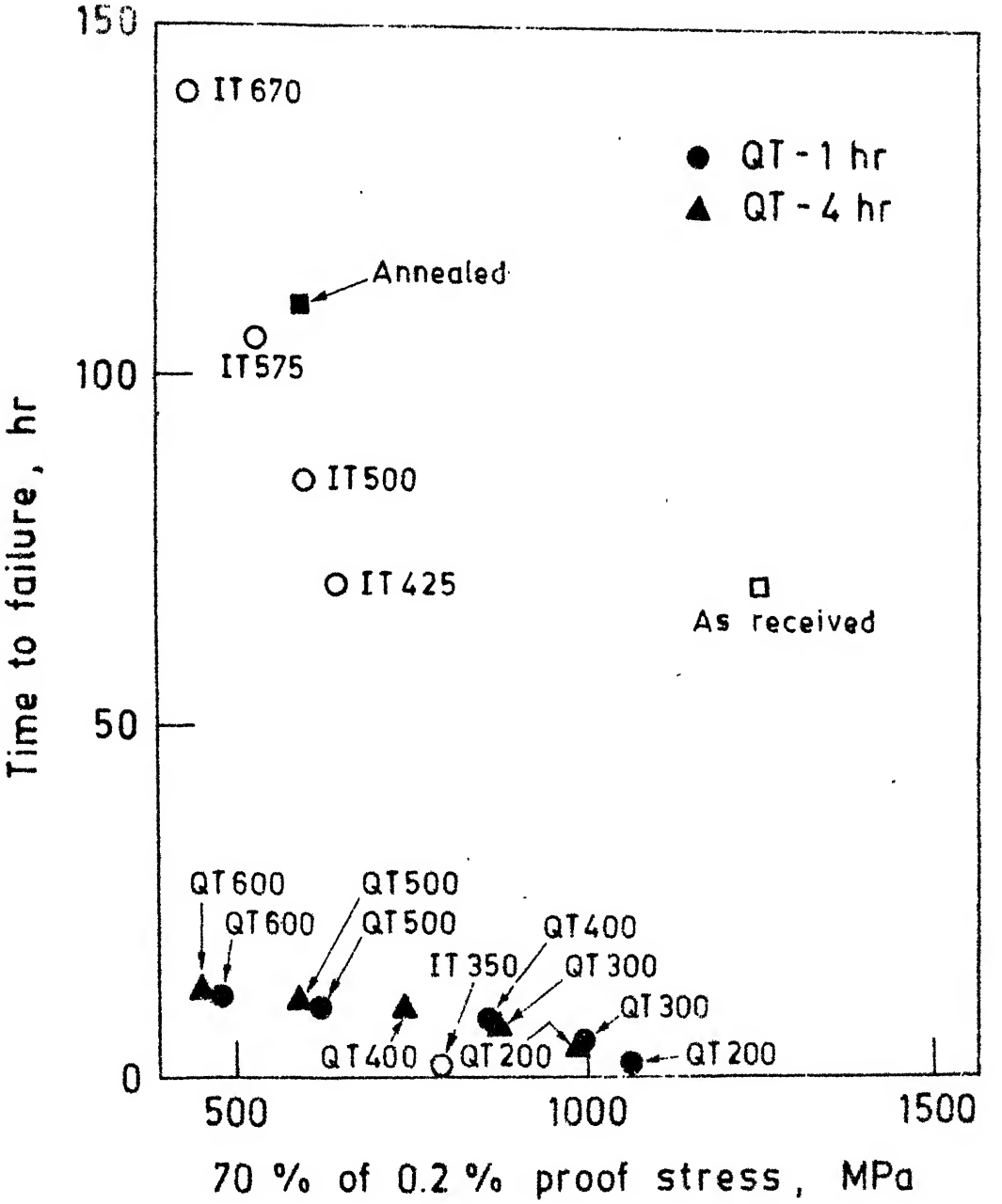

Fig. 4.71. Effect of stress level on time to failure in sat. H_2S solution at room temperature.

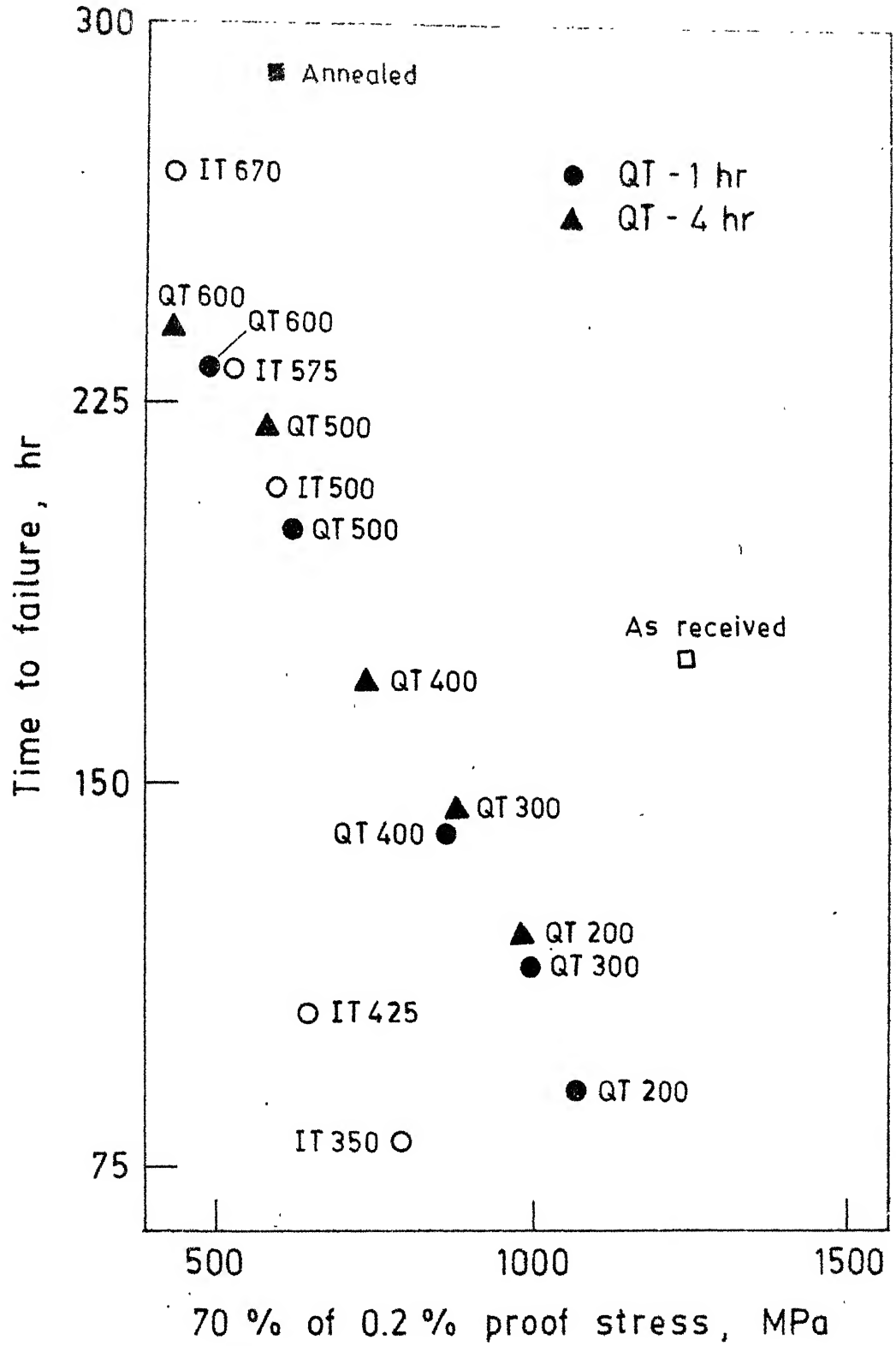

Fig. 4.72. Effect of stress level on time to failure in 50 % $Ca(NO_3)_2$ + 5 % NH_4NO_3 solution at 100 °C.

TABLE 4.1

Mechanical Properties of prestressing steel wires in As Received, Annealed, Quenched & Tempered and Isothermally Transformed conditions.

Heat Treatment	U.T.S.		Fracture Stress		0.2%Proof Stress		% Elongation	% Reduction in Area	Rockwell hardness (Rc)
	kg/mm^2	MPa	kg/mm^2	MPa	kg/mm^2	MPa			
As Recd.	195.14	1913.67	155.54	1525.33	181.72	1782.06	13.36	23.40	45.00
Annealed	97.99	960.95	93.67	918.59	86.46	847.88	31.75	28.50	16.00
QT 200°C, 1 Hr.	191.25	1875.52	185.72	1821.29	156.12	1531.01	8.00	16.24	55.00
QT 300°C, 1 Hr.	172.97	1696.26	170.16	1668.70	146.23	1434.03	9.60	17.50	40.75
QT 400°C, 1 Hr.	147.34	1444.91	145.84	1430.20	125.98	1235.44	10.52	19.62	33.00
QT 500°C, 1 Hr.	110.30	1081.67	106.06	1040.09	90.04	882.99	11.04	22.42	27.25
QT 600°C, 1 Hr.	87.67	859.75	77.77	762.66	70.02	686.66	12.50	25.62	19.75
QT 200°C, 4 Hrs.	173.45	1700.96	164.96	1617.70	144.16	1413.73	17.60	20.00	48.50
QT 300°C, 4 Hrs.	159.32	1562.40	150.07	1471.68	127.31	1248.48	20.16	23.46	33.00
QT 400°C, 4 Hrs.	134.18	1315.86	130.42	1278.98	108.15	1060.59	22.52	27.72	31.00
QT 500°C, 4 Hrs.	97.57	956.83	90.50	887.50	85.28	836.31	24.00	29.49	21.75
QT 600°C, 4 Hrs.	79.14	780.32	72.12	707.26	62.97	617.52	25.36	32.14	15.75
IT 350°C, 15 Min.	141.41	1386.76	101.81	998.41	115.95	1137.08	28.12	53.42	40.00
IT 425°C, 5 Min.	118.50	1162.08	97.40	955.17	94.15	923.30	28.25	42.16	31.25
IT 500°C, 30 Sec.	125.85	1234.16	93.33	915.25	87.67	859.75	28.50	34.54	28.75
IT 575°C, 1 Min.	115.95	1137.08	96.16	943.00	77.77	762.66	28.75	40.13	22.50
IT 670°C, 10 Min.	93.33	915.25	89.09	873.67	63.63	624.00	35.00	46.24	14.00

TABLE 4.2

Corrosion potential and Time to failure of As Received, Annealed, Isothermally transformed and Quenched & tempered of prestressing steel wires in saturated H_2S solution at Room Temperature and 50% $Ca(NO_3)_2$+5% NH_4NO_3 solution at 100°C.

Heat Treatment	Saturated H_2S at Room Temperature			50% $Ca(NO_3)_2$+5% NH_4NO_3 at 100°C		
	Time to Failure (Stressed to 70% of 0.2% Proof Stress) Hrs.	Corrosion Potential Stressed Volts vs. S.C.E.	Unstressed	Time to Failure (Stressed to 70% of 0.2% Proof Stress) Hrs.	Corrosion Potential Stressed Volts vs. S.C.E.	Unstressed
As Recd.	70.00	- 0.684	- 0.710	175.00	- 0.434	- 0.370
Annealed	110.00	- 0.680	- 0.750	290.00	- 0.462	- 0.460
IT 350°C, 15 Min.	1.50	- 0.715	- 0.703	80.00	- 0.450	- 0.390
IT 425°C, 5 Min.	70.00	- 0.705	- 0.720	105.00	- 0.508	- 0.400
IT 500°C, 30 Sec.	85.00	- 0.698	- 0.740	208.00	- 0.495	- 0.422
IT 575°C, 1 Min.	105.00	- 0.690	- 0.742	232.00	- 0.437	- 0.445
IT 670°C, 10 Min.	140.00	- 0.670	- 0.753	270.00	- 0.516	- 0.435
QT 200°C, 1 Hr.	1.92	- 0.700	- 0.740	90.00	- 0.422	- 0.425
QT 300°C, 1 Hr.	5.00	- 0.675	- 0.684	114.00	- 0.372	- 0.375
QT 400°C, 1 Hr.	7.92	- 0.685	- 0.700	140.00	- 0.370	- 0.394
QT 500°C, 1 Hr.	9.17	- 0.688	- 0.714	200.00	- 0.525	- 0.513
QT 600°C, 1 Hr.	11.08	- 0.707	- 0.721	232.00	- 0.500	- 0.440
QT 200°C, 4 Hrs.	4.25	- 0.690	- 0.705	120.00	- 0.410	- 0.430
QT 300°C, 4 Hrs.	7.50	- 0.691	- 0.700	145.00	- 0.370	- 0.432
QT 400°C, 4 Hrs.	9.17	- 0.709	- 0.698	170.00	- 0.420	- 0.474
QT 500°C, 4 Hrs.	10.67	- 0.715	- 0.710	220.00	- 0.495	- 0.465
QT 600°C, 4 Hrs.	12.00	- 0.694	- 0.725	240.00	- 0.498	- 0.520

TABLE 4.3

Corrosion potential, Primary passive potential, Critical current density, Current in passive state, Passive range and Corrosion current of As Received, Annealed, Isothermally Transformed and Quenched & tempered wires in unstressed condition in 50% $Ca(NO_3)_2$ + 5% NH_4NO_3 solution at 100°C.

Heat Treatment	Corrosion Potential (E_{Corr}) Volts Vs. S.C.E.		Primary Passive Potential, (E_{pp}) Volts Vs. S.C.E.		Critical Current Density (i_{Crit}) mA/cm^2		Current in Passive state (i_{cp}), mA/cm^2		Passivation range Volts Vs. S.C.E.		Corrosion current (i_{corr}) mA/cm^2
	Forward Scan	Reverse Scan	Forward Scan	Reverse Scan	Forward Scan	Reverse Scan	Forward Scan	Reverse Scan	Forward Scan	Reverse Scan	
As Recd.	-0.370	-0.213	0.312	0.562	200	500	50	40	0.850 to 1.5	1.5 to 0.687	.001
Annealed	-0.460	-0.275	0.375	0.500	560	890	160	80	0.850 to 1.5	1.375 to 0.625	.707
IT 350°C, 15 Min.	-0.390	-0.100	0.187	0.525	220	560	50	25	0.875 to 1.375	1.437 to 0.750	.063
IT 425°C, 5 Min.	-0.400	-0.145	0.250	0.487	180	400	20	10	0.762 to 1.200	1.375 to 0.750	.707
IT 500°C, 30 Sec.	-0.422	-0.100	0.200	0.585	160	310	65	35	0.625 to 1.500	1.500 to 0.762	.794
IT 575°C, 1 Min.	-0.445	-0.245	0.250	0.487	310	560	20	63	1.025 to 1.125	1.250 to 0.750	.070
IT 670°C, 10 Min.	-0.435	-0.320	0.250	0.387	500	800	22	15	0.937 to 1.250	1.312 to 0.750	.022
QT 200°C, 1 Hr.	-0.425	-0.124	0.250	0.450	224	631	112	90	0.775 to 1.5	1.250 to 0.812	.790
QT 300°C, 1 Hr.	-0.375	-0.120	0.375	0.537	280	500	70	56	0.900 to 1.437	1.437 to 0.762	.017
QT 400°C, 1 Hr.	-0.394	-0.225	0.375	0.500	315	560	100	100	0.937 to 1.500	1.500 to 1.200	.350
QT 500°C, 1 Hr.	-0.513	-0.270	0.250	0.462	320	630	35	25	0.775 to 1.275	1.375 to 0.750	.140
QT 600°C, 1 Hr.	-0.440	-0.296	0.250	0.500	630	890	100	160	0.725 to 1.375	1.500 to 0.950	.056
QT 200°C, 4 Hrs.	-0.430	-0.134	0.187	0.612	160	560	100	30	0.625 to 1.625	1.437 to 0.875	.025
QT 300°C, 4 Hrs.	-0.432	-0.136	0.250	0.550	150	500	40	20	0.812 to 1.375	1.375 to 0.750	.017
QT 400°C, 4 Hrs.	-0.474	-0.187	0.375	0.525	560	890	200	90	0.850 to 1.387	1.312 to 0.625	.039
QT 500°C, 4 Hrs.	-0.465	-0.200	0.250	0.425	350	1000	45	55	0.787 to 1.062	1.437 to 0.750	.002
QT 600°C, 4 Hrs.	-0.520	-0.240	0.500	0.437	560	900	90	70	1.000 to 1.437	1.500 to 0.625	.083

TABLE 4.4

Corrosion potential, Primary passive potential, Critical current density, Current in passive state, Passive range and corrosion current of As Received, Annealed, Isothermallytransformed and Quenched & tempered wires in stressed condition in 50% $Ca(NO_3)_2$ + 5% NH_4NO_3 solution at 100°C.

Heat Treatment	Corrosion Potential (E_{Corr}) Volts Vs. S.C.E.		Primary Passive Potential, (E_{pp}) Volts Vs. S.C.E.		Critical Current Density (i_{Crit}) mA/cm^2		Current in Passive state (i_{cp}), mA/cm^2		Passivation range Volts Vs. S.C.E.		Corrosion current (i_{corr}) mA/cm^2
	Forward Scan	Reverse Scan	Forward Scan	Reverse Scan	Forward Scan	Reverse Scan	Forward Scan	Reverse Scan	Forward Scan	Reverse Scan	
As Recd.	-0.434	-0.225	0.312	0.537	446	1120	80	25	0.875 to 1.440	1.440 to 0.750	.028
Annealed	-0.462	-0.245	0.687	0.450	500	890	20	30	1.000 to 1.312	1.500 to 0.950	.095
IT 350°C,15 Min.	-0.450	-0.172	0.250	0.512	560	1000	65	30	0.612 to 1.125	1.375 to 0.850	.446
IT 425°C, 5 Min.	-0.508	-0.196	0.250	0.437	630	1000	50	25	0.812 to 1.375	1.250 to 0.687	.126
IT 500°C,30 Sec.	-0.495	-0.270	0.500	0.350	530	700	70	70	0.937 to 1.250	1.250 to 0.625	.100
IT 575°C, 1 Min.	-0.437	-0.184	0.312	0.462	790	890	300	250	1.000 to 1.375	1.125 to 0.750	.009
IT 670°C,10 Min.	-0.516	-0.273	0.000	-0.062	1120	700	120	64	0.625 to 1.437	0.832 to 0.562	.074
QT 200°C, 1 Hr.	-0.422	-0.260	0.062	0.462	310	980	110	80	0.912 to 1.500	1.500 to 0.950	.100
QT 300°C, 1 Hr.	-0.372	-0.208	0.125	0.387	500	1100	45	30	0.875 to 1.375	1.437 to 0.750	.096
QT 400°C, 1 Hr.	-0.370	-0.220	0.125	0.125	890	700	30	60	0.600 to 1.125	1.500 to 1.175	.001
QT 500°C, 1 Hr.	-0.525	-0.260	0.250	0.562	630	950	250	160	1.187 to 1.500	1.500 to 0.750	.930
QT 600°C, 1 Hr.	-0.500	-0.280	0.625	0.437	830	970	100	100	0.875 to 1.437	1.437 to 0.662	.031
QT 200°C, 4 Hrs.	-0.410	-0.146	0.250	0.525	180	700	100	20	0.750 to 1.625	1.500 to 0.600	.044
QT 300°C, 4 Hrs.	-0.370	-0.140	0.250	0.500	360	800	40	70	1.250 to 1.500	1.375 to 0.687	.012
QT 400°C, 4 Hrs.	-0.420	-0.194	0.250	0.525	380	900	40	40	1.000to 1.312	1.500 to 0.625	.050
QT 500°C, 4 Hrs.	-0.495	-0.221	0.500	0.375	890	1110	140	125	0.812 to 0.875	0.930 to 0.475	.079
QT 600°C, 4 Hrs.	-0.498	-0.223	0.125	-0.062	920	750	70	130	0.500 to 1.250	1.437 to 0.557	.14

TABLE 4.5

Potential at the point of intersection of forward and reverse anodic polarization curves for As Received, Annealed, Isothermally Transformed, and Quenched&tempered prestressing steel wires in unstressed and stressed conditions in 50% $Ca(NO_3)_2$ + 5% NH_4NO_3 at 100°C.

Heat Treatment	Potential at Intersection, V					
	Untressed			Stressed		
	1st	2nd	3rd	1st	2nd	3rd
As Recd.	0.637	0.187	- 0.300	0.575	0.275	- 0.312
Annealed	0.537	0.312	- 0.375	0.475	0.062	- 0.312
IT 350°C,15 Min.	0.587	0.350	- 0.337	0.637	0.275	- 0.335
IT 425°C, 5 Min.	0.520	0.287	- 0.337	0.400	0.312	- 0.350
IT 500°C,30 Sec.	0.637	0.362	- 0.350	0.350	-	- 0.362
IT 575°C, 1 Min.	0.512	0.300	- 0.337	0.475	-	- 0.275
IT 670°C,10 Min.	0.500	0.000	- 0.375	0.125	-	- 0.412
QT 200°C, 1 hr.	0.512	0.250	- 0.375	0.562	0.150	- 0.375
QT 300°C, 1 hr.	0.637	0.387	- 0.312	0.550	0.150	- 0.312
QT 400°C, 1 hr.	-	0.187	- 0.312	0.362	-	- 0.250
QT 500°C, 1 hr.	0.475	0.150	- 0.375	0.637	0.212	- 0.412
QT 600°C, 1 hr.	-	0.187	- 0.375	0.312	0.187	- 0.350
QT 200°C, 4 hrs.	0.650	0.187	- 0.287	0.537	0.125	- 0.287
QT 300°C, 4 hrs.	0.587	0.187	- 0.312	0.525	0.275	- 0.250
QT 400°C, 4 hrs.	0.537	0.375	- 0.324	0.537	0.275	- 0.300
QT 500°C, 4 hrs.	0.500	0.135	- 0.312	0.387	0.162	- 0.337
QT 600°C, 4 hrs.	0.412	0.225	- 0.350	0.250	-	- 0.361

TABLE 4.6

Current density at the point of intersection of forward and reverse anodic polarization curves for As Received, Annealed, Isothermally transformed and Quenched & tempered prestressing steel wires in unstressed and stressed condition in 50% $Ca(NO_3)_2$ + 5% NH_4NO_3 at 100°C.

Heat Treatments	Current density at intersection, mA/cm^2					
	Unstressed			Stressed		
	1st	2nd	3rd	1st	2nd	3rd
As Recd.	125.90	158.5	10.00	354.0	446.7	15.85
Annealed	501.20	562.3	17.78	501.2	316.2	10.00
IT 350°C, 15 Min.	89.13	158.5	12.59	281.8	562.3	39.81
IT 425°C, 5 Min.	89.13	158.5	7.93	562.3	631.0	31.62
IT 500°C, 30 Sec.	70.79	125.9	10.00	707.9	-	17.78
IT 575°C, 1 Min.	112.20	281.8	7.94	707.9	-	25.12
IT 670°C, 10 Min.	251.20	316.2	5.62	177.8	-	3.16
QT 200°C, 1 hr.	177.80	223.9	31.60	223.9	316.2	223.90
QT 300°C, 1 hr.	199.50	281.8	15.80	316.2	891.3	10.00
QT 400°C, 1 hr.	-	316.2	12.59	398.1	-	5.62
QT 500°C, 1 hr.	251.20	281.8	7.90	562.3	707.9	56.23
QT 600°C, 1 hr.	-	562.3	3.10	794.3	446.7	17.78
QT 200°C, 4 hrs.	125.90	158.5	10.00	177.8	177.8	10.00
QT 300°C, 4 hrs.	95.50	159.4	7.94	281.8	316.2	5.01
QT 400°C, 4 hrs.	631.00	562.3	19.95	316.2	398.1	6.30
QT 500°C, 4 hrs.	316.20	354.8	10.00	794.3	631.0	7.07
QT 600°C, 4 hrs.	631.00	501.2	12.59	354.8	-	12.59

TABLE 4.7

Corrosion potential, primary passive potential, critical current density, current in passive state, passive range, corrosion current and time to failure of As Received prestressing steel wires exposed to $Ca(NO_3)_2$ solution at 100°C.

Stress Condition	Conc. of $Ca(NC_3)_2$ solution, wt%	Corrosion Potential (E_{corr}) Volts Vs. S.C.E.		Primary Passive Potential (E_{pp}) Volts Vs. S.C.E.		Critical Current Density (i_{crit}) mA/cm^2		Current in Passive State, (i_{cp}) mA/cm^2		Passive range, Volts Vs. S.C.E.		Corrosion Current (i_{corr}), mA/cm^2	Time to Failure Hrs.
		Forward Scan	Reverse Scan	Forward Scan	Reverse Scan	Forward Scan	Reverse Scan	Forward Scan	Reverse Scan	Forward Scan	Reverse Scan		
Unstressed	20	-0.506	*	*	*	*	*	*	*	*	*	*	N.F.
	40	-0.470	-0.287	-0.062	0.212	500	700	125	45	0.562 to 1.250	1.115 to 0.325	0.007	N.F.
	60	-0.451	-0.262	-0.250	0.312	280	660	110	20	0.500 to 1.250	1.125 to 0.437	0.001	N.F.
	80	-0.428	-0.212	0.125	0.225	890	1120	140	6	0.650 to 1.250	1.350 to 0.500	0.100	N.F.
Stressed 70% of 0.2% proof. stress	20	-0.482	*	*	*	*	*	*	*	*	*	*	430
	40	-0.458	-0.250	0.125	0.402	230	660	**	90	**	1.125 to 0.525	0.056	310
	60	-0.440	-0.237	-0.062	0.412	500	700	**	30	**	1.187 to 0.562	0.699	198
	80	-0.420	-0.225	0.250	0.400	800	1250	**	56	**	1.187 to 0.600	0.720	154

* Polarization is not done due to potentiostat showed over loading.
** No passive state in forward scan.
N.F. No failure.

TABLE 4.8

Potential & Current density at the point of intersection of forward and reverse anodic polarization curves for As Received prestressing steel wires in unstressed and stressed conditions in $Ca(NO_3)_2$ solution at 100°C.

Wt% of $Ca(NO_3)_2$	Potential at intersection, V						Current density at interaction mA/cm^2					
	Unstressed			Stressed			Unstressed			Stressed		
	1st	2nd	3rd	1st	2nd	3rd	1st	2nd	3rd	1st	2nd	3rd
40	0.275	0.137	-0.387	0.475	0.175	-0.412	223.9	398.1	12.59	199.5	234.4	7.90
60	0.400	0.212	-0.362	0.475	0.250	-0.387	229.1	251.2	22.39	199.5	316.2	12.59
80	0.250	0.125	-0.337	0.500	0.287	-0.362	794.3	794.3	25.12	354.8	794.3	10.00

CHAPTER-V

CONCLUSIONS

1. Prestressing steel wire in As Received, Annealed, Isothermally transformed and quenched & tempered conditions was susceptible to stress corrosion cracking in mediums examined.

2. Quenched and tempered wires in general are more susceptible than annealed and isothermally transformed wires. As Received wire had intermediate susceptibility.

3. Anodic polarization behaviour of prestressing steel wires was effected by the nature of the heat treatment given to it. However, the change was not very systematic.

4. There was not much corelation between the anodic polarization behaviour of prestressing steel wire and its susceptibility to stress corrosion cracking except that in some case a change in slope in time to failure curves was associated with minimum difference in $E_{corr.}$ in unstressed and stressed conditions.

16. H. LIBERT & A. HACHE; 8th Colloquim of Metallurgy, Cadarache (Commissariat a l'Energie Atomique) June 1964, Translation by CEGB Information Services, Grindall House, 25 Newgate St., London.

17. P.S. THEOCARIS; Inst. J. Mech. Sci., 1967, Vol. 9, pp. 195-204.

18. St. KAZFASZ & M. CZERNIK; Colloquim of the RILEM Commission at Wexham Springs, June 1965.

19. E. HERZOG; 3rd Metallurgical Symposium on Corrosion, pp. 217-239, North Holland Publishing Co. Amsterdam, 1960.

20. R.A. DAVIES; Corrosion, 1963, No. 2, Vol. 19, pp. 44-45.

21. M. HERZOG; Discussion to paper by H. Libert & A. Hache, 8th Metallurgy Symposium on Corrosion, Cardarach, (Commissariat a l'Energie Atomique), June 1964, Translation by CEGB information Services, Grindall House, 25 Newgate St., London.

22. K.F. McGUINN & J.R. GRIFFITHS, Proc. Tewpsbury Symposium, C.S. Osboin & R.C. Goffin, Univ. of Melbourne, 1974, pp. 274-285.

23. HOWARD & J. GODFREY; Corrosion, 1961, No. 4, Vol. 17, pp.24-25.

24. N.S. RENGASWAMY & K.S. RAJAGOPALAN, Indian Concrete Journal, 1977, No. 10, Vol. 51, pp. 301.

25. N.S. RENGASWAMY & K.S. RAJAGOPALAM, Indian Concrete Journal, 1977, No. 11, Vol. 51, pp. 342.

26. TREADAWAY, K.W.J., Brit. Corrosion J., 1971, No. 3, Vol. 6(2), pp. 66-72.

27. JORG EICKEMEYER, Corrosion Science, 1978, Vol. 18, pp. 397-400.

28. R.N. PARKINS, M. ELICES, V. SANCHEZ-GALVEZ & L. CABALLERO, Corrosion Science, 1982, Vol. 22, No. 5, pp. 379-405.

29. G.V. KARPENKO & I.I. VAILENKO, "Cracking of steels in nitrate solutions", Chapter 8 of Stress Corrosion Cracking of Steels, edited by A. Aladzem, D. Sc., 1979, pp. 103-121.

30. W. RADEKER, STAHL U. EISEN, 1953, 73, pp. 485.

31. G. SHVARTS & M. KRISTAL', Korroziya Khimichskoi Apparatury, Mashgiz, Moscow 1958

32. E. HERZOG, Corrosion Anticorr, 1954, No. 2, pp. 3.

33. PARKINS, R.N.,"Stress Corrosion Cracking of Mild Steel", Chapter 10 of Stress Corrosion Cracking and Embrittlement, edited by W.D. Robertson, John Wiley & Sons, New York, 1965, pp. 140-157.

34. POLLARD, R.E., Symposium on Stress Corrosion Cracking of Metals, ASTM-AIME, 1944, pp. 437-452.

35. H. BOHNI, Werkstoffe U. Korrosion, 1975, No. 3, Vol. 26, pp. 199-207.

36. PEPENAR, MARIA SOLACOLU & D. TEODORESCU, Metallurgia (Bucharest), 1978, No. 3, Vol. 30, pp. 155-161.

37. J. FRASER, G. ELDREDGE & R. TRESEDER, Corrosion, 1958, Vol.14.

38. J. FRASER & G. ELDREDGE, Corrosion, 1958, Vol. 14, pp. 524.

39. F. NAUMANN, STAHL U. EISEN, 1967, Vol. 87, pp. 147.

40. A. SCHUETZ & W. ROBERTS, Corrosion, 1957, Vol. 13, pp. 437.

ME-1983-M-KUM-EFF